A LINEAR MODAL COMBINATION PROCEDURE FOR STRUCTURAL DYNAMICS

A THESIS SUBMITTED TO
THE GRADUATE SCHOOL OF NATURAL AND APPLIED SCIENCES
OF
MIDDLE EAST TECHNICAL UNIVERSITY

BY

SADUN TANIŞER

IN PARTIAL FULFILLMENT OF THE REQUIREMENTS
FOR
THE DEGREE OF MASTER OF SCIENCE
IN
CIVIL ENGINEERING

JULY 2013

Approval of the thesis:

A LINEAR MODAL COMBINATION PROCEDURE FOR STRUCTURAL DYNAMICS

submitted by **SADUN TANIŞER** in partial fulfillment of the requirements for the degree of **Master of Science in Civil Engineering Department, Middle East Technical University** by

Prof. Dr. Canan Özgen _____
Dean, Graduate School of **Natural and Applied Sciences**

Prof. Dr. Ahmet Cevdet Yalçıner _____
Head of Department, **Civil Engineering**

Prof. Dr. Haluk Sucuoğlu _____
Supervisor, **Civil Engineering Dept., METU**

Examining Committee Members:

Prof. Dr. Polat Gülkan _____
Civil Engineering Dept., Çankaya University

Prof. Dr. Haluk Sucuoğlu _____
Civil Engineering Dept., METU

Prof. Dr. Sinan Akkar _____
Civil Engineering Dept., METU

Assoc. Prof. Dr. Murat Altuğ Erberik _____
Civil Engineering Dept., METU

Assoc. Prof. Dr. Yalın Arıcı _____
Civil Engineering Dept., METU

Date: 19.07.2013

I hereby declare that all information in this document has been obtained and presented in accordance with academic rules and ethical conduct. I also declare that, as required by these rules and conduct, I have fully cited and referenced all material and results that are not original to this work.

Name, Last name : SADUN TANIŞER

Signature :

ABSTRACT

A LINEAR MODAL COMBINATION PROCEDURE FOR STRUCTURAL DYNAMICS

Tanışer, Sadun

M.Sc., Department of Civil Engineering

Supervisor: Prof. Dr. Haluk Sucuoğlu

July 2013, 94 pages

Earthquake engineering practice utilizes different analysis procedures in the estimation of seismic demands on structures. These procedures are mainly divided into two groups as static and dynamic procedures. Dynamic procedures are more accurate than the static procedures since they include the entire history of any response parameter during the ground motion. Nevertheless, there are also approximate but much simpler static analysis procedures that overcome high computational demands and inherent difficulties of dynamic analysis such as tedious post-processing, and stability and convergence issues especially when the behavior is nonlinear.

A deterministic linear modal combination procedure is developed in this thesis as an alternative analysis tool to determine the maximum values of seismic response parameters of structures under earthquake ground motions. The proposed procedure is based on the linear combination of maximum modal responses which are obtained from single-degree-of-freedom modal analyses. In this procedure, modal scaling coefficients are determined when interstory drift ratio at each story attains its maximum value during dynamic response. Each maximum modal response is scaled with these coefficients and combined linearly. The modal scaling coefficients hold the directional information of each mode inside; thereby the direction of total maximum response is preserved. Alternative procedures combine the maximum modal responses with some statistical rules such as SRSS or CQC, which lead to the loss of accuracy and loss of directionality of

response. Since the contribution of each mode is linearly combined in the proposed procedure, it overcomes the major drawbacks of statistical combination rules.

The suggested procedure is tested on four different structures under three different ground motions. It has been shown that the procedure yields almost exact results for linear elastic response as compared to the statistical CQC method and it is a suitable analysis tool.

Keywords: Modal combination, modal scaling coefficient, higher mode effect, interstory drift ratio.

ÖZ

YAPI DİNAMİĞİ İÇİN DOĞRUSAL MOD BİRLEŞTİRME YÖNTEMİ

Tanışer, Sadun

Yüksek Lisans, İnşaat Mühendisliği Bölümü

Tez Yöneticisi: Prof. Dr. Haluk Sucuoğlu

Temmuz 2013, 94 sayfa

Deprem mühendisliği uygulaması, yapılar üzerindeki sismik taleplerin belirlenmesinde farklı dinamik analiz yöntemleri kullanır. Bu yöntemler, statik ve dinamik olarak iki ana gruba ayrılırlar. Dinamik yöntemler, yer hareketi sırasında herhangi bir tepki parametresinin tüm geçmişini içerdiği için statik yöntemlerden daha kesindir. Bununla birlikte, hesaba dayalı yüksek istemler ve özellikle davranış doğrusal değilken görülen karmaşık son işlem, stabilite ve yakınsama sorunları gibi dinamik analizin doğasında yer alan zorlukları aşan yaklaşık fakat basit statik analiz yöntemleri de vardır.

Bu tezde, alternatif bir statik analiz yöntemi olarak deprem yer hareketleri altında yapıların sismik davranış parametrelerinin maksimum değerlerini tahmin etmek için bir deterministik doğrusal mod birleştirme yöntemi geliştirilmiştir. Önerilen yöntem, modal tek serbestlik dereceli sistemlerin analizlerinden elde edilen maksimum modal tepkilerin doğrusal olarak birleştirilmesine dayanmaktadır. Bu yöntemde, her bir kattaki kat arası öteleme oranının maksimum değere ulaştığı anda modal ölçeklendirme katsayıları belirlenir. Her kattaki maksimum modal tepki, bu katsayılarla ölçeklendirilir ve doğrusal olarak birleştirilir. Modal ölçeklendirme katsayıları her bir modun yön bilgilerini içerir, dolayısıyla toplam maksimum tepkinin yönü korunur. Alternatif yöntemler maksimum modal tepkileri SRSS veya CQC gibi istatistiksel kurallar ile birleştirir ki bu, toplam tepkinin kesinliğinin ve yönlülüğünün kaybolmasına neden olur. Her bir modun katkısı doğrusal olarak birleştirildiği için bu yöntem, istatistiksel birleştirme kurallarının başlıca zayıflıklarını ortadan kaldırmaktadır.

Önerilen yöntem üç farklı yer hareketi kullanılarak dört farklı sistem üzerinde test edilmiştir. Doğrusal mod birleştirme yönteminin istatistiksel CQC yöntemiyle karşılaştırıldığında doğrusal elastik davranış için neredeyse hatasız sonuçlar verdiği gösterilmiştir ve bu nedenle uygun bir analiz yöntemi olarak önerilmektedir.

Anahtar Kelimeler: Mod birleştirme, mod ölçeklendirme katsayısı, yüksek mod etkisi, kat arası öteleme oranı.

To my family…

ACKNOWLEDGEMENTS

I would like to express my sincerest gratitude to my supervisor Prof. Dr. Haluk Sucuoğlu for his guidance and support throughout this study. Without his encouragement, great teaching and profound advices, this study would not be possible. It was a great chance and honor to work with him.

I am thankful to the Scientific and Technological Research Council of Turkey (TÜBİTAK) for granting its project assistant scholarship during my graduate studies.

I am also grateful to Bihlun Tamaylıgil for her support throughout my undergraduate and graduate studies.

My deepest thanks go to the most important two people in my life, my mother and my sister. In every decision I made, in success and failure, in my happiest and saddest days they supported me with their endless love and patience, for which it is impossible to show my gratitude enough. I feel blessed to have such a great family.

I would like to thank all my friends that worked and are currently working with me in K7-Z01 for their joyful friendship, their help and support. Especially, I am grateful to Kaan Kaatsız and F. Soner Alıcı. They became two important helping hands over the course of this study with their experience and effectual advices.

I am so grateful to Ali Rıza Yücel, S. Alp Yılmaz and Serdar Söğüt for their great friendship over the years. This long and tedious path that we all are on for years has been much more enjoyable with their supportive and joyful presence. Thank you fellows for your friendship that will last forever.

My very special thanks go to Berker Batur, Suzan Ceylan and K. Erdinç Tunçer, who become a family to me as well as being great friends. To them, your unconditional support and hearty presence that I always felt notably helped me achieve this goal. I am glad you are close to me.

TABLE OF CONTENTS

LIST OF TABLES

TABLES

LIST OF FIGURES

FIGURES

CHAPTER 1

INTRODUCTION

1.1 Problem Statement

Different analysis procedures can be employed in structural engineering for determining the dynamic forces acting on structures due to natural effects. Earthquake engineering particularly deals with the causes and results when those natural effects are the seismic actions resulting from earthquakes. Structural analysis procedures for predicting seismic actions on structures can be divided into four main groups: Nonlinear dynamic, nonlinear static, linear dynamic and linear static analysis procedures.

Dynamic analysis procedures, also known as time/response history analysis, are more rigorous compared to the static analysis procedures. In return, dynamic analysis requires high computational effort and it has several shortcomings such as stability and convergence, especially when the response is nonlinear. Dynamic analysis is generally used to generate benchmark results for developing and testing simplified procedures.

Static analysis procedures are divided into two subgroups, nonlinear static and linear static. Both nonlinear and linear static procedures are used to simulate the dynamic effects on structures with less computation and processing effort. In order to obtain more accurate results, a suitable number of vibration modes should be employed in both static procedures. For instance, a multi-mode pushover analysis and linear response spectrum analysis are used for nonlinear and linear static cases, respectively. However when combining the modal results, a significant drawback in these analysis procedures arises: statistical combination of modal responses.

Modal results are generally combined by using statistical methods in equivalent static mode superposition analysis procedures where the modal response maxima are obtained by response spectrum analysis. Generally, when the modal frequencies are well-separated, square root of the sum of the squares (SRSS) method is used. When the coupling between modal responses is significant, complete quadratic combination (CQC) is preferred as the more accurate combination method. However, both of these methods are purely statistical and when they are utilized in combining modal responses obtained

from response spectrum analysis, the actual time dependent characteristics of seismic response disappears. The sign (or direction) and the time of maximum response completely vanish due to a statistical combination.

In this study, a deterministic linear modal combination approach is proposed. This approach overcomes the aforementioned drawbacks of the statistical methods through combining the modal responses linearly by employing pre-calculated linear modal scaling coefficients. The coefficients may be positive or negative, depending on the direction of maximum modal response. The time of maximum response is a crucial parameter since the modal scaling coefficients are calculated at the time when a selected response quantity, namely interstory drift ratio, reaches its maximum value. The details of the procedure are developed in Chapter 2.

1.2 Review of Past Studies

The linear modal combination procedure developed in this study addresses the shortcomings of statistical methods in the combination of modal responses, and proposes a new combination procedure that eliminates these disadvantages. Therefore the review of past studies is presented in two parts. The first part includes a review of previous studies on statistical combination of peak modal responses. The second part reviews other methods available in literature for effective mode superposition analysis.

1.2.1 Review of Previous Studies on Statistical Combination Methods

The idea of using statistical methods in combining the modal maximum responses was first developed by Rosenblueth (1951) in his Ph.D. thesis. He proposed the "square root of the sum of the squares" (SRSS) method in order to combine the modal maximum responses. As its name implies, the total structural response is calculated by taking the square root of the sum of square of modal responses in the SRSS method. It is based on the assumption that the modal contributions to a response quantity are completely independent, hence orthogonal to each other. This method yields acceptable results when the modes are well-separated, or uncoupled. However SRSS method creates significant errors when the structure has closely spaced periods, or coupled modes. In this case, the cross-terms between the modes become important, which SRSS method does not consider at all.

Wilson et al. (1980) proposed an improved statistical combination method which reduces the errors arising from the SRSS method. This method is called the complete quadratic combination (CQC) method. What makes the CQC method more accurate compared to SRSS is that CQC method has cross-modal coupling terms in its formulation. By

definition, there is a cross-modal coefficient in all terms in the CQC combination, and it is the function of modal damping ratios and vibration frequencies of the structure. When those two modes are the same, cross-modal coefficient is 1. Hence, CQC method reduces to the SRSS method theoretically, for perfectly separated modes. However, this is not the case in reality and all modes are correlated to some extent. The significance of cross-modal terms increases as the modal frequencies are spaced closer. It is also necessary to mention that those cross-modal terms are sensitive to positive and negative signs of modal responses. In this study, CQC method is used as the only statistical combination method to compare with the benchmark response history results, as well as the results obtained from linear modal combination procedure, which is the subject of this study.

Rosenblueth and Elorduy (1969) improved the SRSS method that was introduced in Rosenblueth's Ph.D. thesis. This method resembles the CQC method in a way that it also has cross-modal terms in order to account for the interaction between close modes. Nevertheless, the cross-modal terms in Rosenblueth and Elorduy's method have always positive signs, unlike the CQC method. This results in overly conservative responses in some cases. This overestimation may be the reason why their improved method has been neglected in the literature.

The complete Square-Root-of-Sum-of-Squares (c-SRSS) modal combination rule is developed by Heredia-Zavoni (2010). The method is another development over the well-known SRSS method which completely ignores the interaction between different modes. In this study, the total structural response is expressed in terms of uncoupled SDOF modal responses which accounts for the contribution of both modal variances and modal cross-covariances. In other words, the development over SRSS comes with the introduction of modal cross-covariances computed as a function of modal damping and frequencies, an approach similar to the CQC method. Heredia-Zavoni suggested that CQC method yields good results when the ground motion is wide-banded. It does not work accurately though in some cases when the ground motion is narrow-banded. The c-SRSS method gives good estimates for both wide-banded and narrow-banded ground motions according to the author.

1.2.2 Review of Other Methods for Effective Mode Superposition Analysis

Kelly and Sackman (1980) studied the conservatism in summation rules for the systems having closely spaced modes. They stated that closely spaced modes originate from the asymmetry (or torsional unbalance) and light appendages in a structure. In their study, it is indicated that far spaced modes should be treated by modal analysis, closely spaced modes should be treated as a two-degree-of–freedom system. This approach signifies the beat phenomenon. It means that the maximum response of the coupled system occurs far later than the maximum responses of the individual modes. Both mentioned cases which cause coupling among the modes are studied in this thesis as different case studies.

Leger and Wilson (1988) developed a summation procedure for the nonlinear analysis of structures. The proposed method divides the considered number of modes mainly into two groups. For the first group of modes, dynamic analysis shall be conducted. However for the remaining modes with frequencies at least three times higher than the frequency of applied loading, the behavior is considered static. Inertial and damping effects can be ignored, and the responses of higher modes can be taken into account by modifying the mode-displacement summation method with static correction terms. The mode-displacement summation stands for the response history analysis. Static correction terms are calculated with a method called mode-acceleration, since there is a modal acceleration term in those correction expressions. Two different computational variants of the mode-acceleration method are suggested. The first variant is based on the expansion of flexibility matrix in terms of truncated eigenbasis, and the second one is based on expansion of a force vector. For convenience in computation effort, the first one is recommended.

Park et al. (2007) proposed a modal combination rule for combining earthquake load profiles in multi-mode nonlinear static analysis. It is called the factored modal combination (FMC) method. The FMC method is intended to accurately estimate the maximum response values, and total earthquake load profiles for linear and nonlinear analyses, respectively. For the linear analysis case, each modal maximum response parameter is multiplied with a modal combination factor. Each modal combination factor is determined as a function of time, since it changes during the time history. Since the maximum values are desired during the design process, the absolute maximum value of each factor at the instant when the desired parameter (drift, story shear, etc.) attains its maximum value is determined. After the FMC factor is calculated, the maximum response parameter is determined by the superposition of modal responses (addition/subtraction of modal responses). For the nonlinear analysis case, the calculated load combination factors are multiplied with the modal load profiles and superposed in order to obtain the final earthquake load profiles. Finally pushover analyses are performed on the nonlinear structure and the envelope of results are used as FMC results.

Park et al. (2007) in their same paper mentioned the disadvantages of using SRSS and CQC in predicting the elastic load profiles in the response history analysis by noting that the modal response values and the design values occur at different times. In order to predict the seismic load profiles, different approaches are developed in the literature. Requena and Ayala (2000) proposed the combination of modal story loads whereas Lee et al. (2002) proposed the combination of modal story shear forces. SRSS method is used for combinations. Chopra and Goel (2002) proposed the modal pushover analysis (MPA). In MPA, modal lateral load profiles are applied to the system individually, and then the nonlinear modal responses are combined by using the SRSS method, by assuming that they are orthogonal to each other.

Matsumori et al. (1999) developed a procedure in which the modal story shears are combined to estimate different story shear distribution patterns. The purpose of their study was to accurately estimate the story displacements, drifts and girder-end ductility

demand distribution throughout the height as a result of pushover analyses. It is stated that the choice of pattern of the static pushover force distribution is decisive on the results of the analysis, and the higher mode effects are apparent in story shear signals. The authors proposed two different story shear distribution patterns, the first one is the sum of two modal story shears and the second one is the difference of them. Those two distribution patterns are applied to the structure and the envelope of the two results are considered as final results. There are another two distribution types to be applied: the story shear distribution corresponding to the first mode shape, and a design story shear distribution with some distribution factors and coefficients obtained from the Building Standard Law Enforcement Order (BJC, 1981). For the story displacements, drifts and girder-end ductility demands, the sum of two modal story shear distributions forms the envelope at the lower levels, and the difference of them forms at the upper (and middle, for girder-end ductility demand) levels.

Jan et al. (2004) proposed an upper-bound modal combination rule in their study. By conducting response history analysis, they suggested that the major contribution to the displacement response comes from the first two modes. To this respect, an upper-bound pushover analysis procedure is proposed. In this procedure, a higher mode contribution ratio is calculated as the absolute value of the ratio of modal response of second mode to that of first mode. The modal response mentioned here is the multiplication of modal participation factor and the spectral displacement for the specified mode. Then the distribution vector that is combined according to the new combination rule is calculated as the summation of the first mode and second mode contributions, multiplied with the higher mode contribution ratio.

1.3 Objective and Scope

The Linear Modal Combination (LMC) Procedure is presented in this study as a new procedure to combine the modal responses of multi-degree-of-freedom (MDOF) systems. The results obtained with LMC are compared with the results of Complete Quadratic Combination (CQC) method and Linear Response History (RHA) analysis in all of the case studies presented. RHA results are considered as benchmark. The analyses procedures are implemented under three different earthquake ground motions. The LMC procedure is tested on four different systems in this the study. For the two dimensional (2D) case, a three-story plane frame with an appendage at the top was prepared for the initial testing of the suggested formulation. The 2D case study was further extended with a twelve story plane frame where higher modes are significant. For three dimensional (3D) cases, a one-story torsionally coupled space frame was prepared. The coupling between translational and torsional modes was imposed by introducing mass eccentricity in one direction. The 3D case studies were further extended with an eight story space frame with torsional coupling imposed with a mass eccentricity in one direction. Global parameters such as story displacements, interstory drift ratios and story shear forces, and

local parameters such as beam end rotations, beam end moments and column end moments are compared in these case studies.

The main objective of this study is to develop a new method that eliminates the entire statistical phenomenon in the modal combination procedures that mainly relies on the SRSS and CQC methods in their nature. The accuracy of the newly proposed combination procedure is tested on both two dimensional and three dimensional frame systems with both uncoupled and coupled lateral-rotational modes.

This study consists of seven chapters. The titles and contents are as follows:

Chapter 1: Introduction. Problem statement. Review of past studies. Objective and Scope.

Chapter 2: Linear Modal Combination Procedure. The detailed explanation of the method and the formulation for both two dimensional and three dimensional structures.

Chapter 3: Ground Motion Records. The properties of the ground motion records that are employed.

Chapter 4: Case Studies: Simple Structures. Three story plane frame structure with an appendage. One story space frame structure with torsional coupling.

Chapter 5: Case Studies: Prototype Structures. Twelve story plane frame structure. Eight story space frame structure.

Chapter 6: Practical Implementation of Linear Modal Combination Procedure. Reduced Linear Modal Combination Procedure.

Chapter 7: Summary and Conclusions.

CHAPTER 2

LINEAR MODAL COMBINATION PROCEDURE

The linear modal combination procedure (LMC) for both plane frames and space frames are described in this chapter. The formulation of modal scaling coefficients for plane frames is presented in the first section. The frame-wise formulation of the same modal scaling coefficients for space frames are presented in the second section.

The LMC procedure presented herein is based on estimating the level of participation of a specific mode to the total maximum value of a selected response parameter. The objective is to determine the contribution of a specific mode to the maximum value of a selected response parameter within the context of a linear modal combination rule.

Modal scaling coefficients are introduced within the scope of the LMC procedure. For a selected response parameter, modal scaling coefficients essentially indicate the contribution of one specific mode to the total maximum response at the instant when that selected response parameter attains its maximum value during dynamic response under a ground excitation.

The principal response parameter is selected as the interstory drift ratio (IDR). The basis of selecting IDR as the principal response parameter is that the other higher order response parameters (story shear, beam and column deformations, internal forces, etc.) in a specific story attain their maximum values almost synchronously with IDR at that story (Sucuoğlu and Günay, 2011).

LMC procedure, the formulation of modal scaling coefficients and the general implementation algorithm are elaborated hereafter. They are presented for plane frames first, followed by the space frame formulation.

2.1 LMC Procedure for Plane Frames

Interstory drift ratio of the *j*'th story can be expanded in the time domain in terms of its modal components under a ground excitation.

$$\Delta_j(t) = \Gamma_1 \Delta\Phi_{1j} D_1(t) + \Gamma_2 \Delta\Phi_{2j} D_2(t) + \ \ldots \ + \Gamma_N \Delta\Phi_{Nj} D_N(t) \tag{2.1}$$

where

$$\begin{aligned} \Gamma_n &= L_n / M_n \\ L_n &= \boldsymbol{\Phi}_n^T \boldsymbol{m} \boldsymbol{l} \\ M_n &= \boldsymbol{\Phi}_n^T \boldsymbol{m} \boldsymbol{\Phi}_n \\ \Delta\Phi_{n,j} &= \Phi_{n,j} - \Phi_{n,j-1} \end{aligned} \tag{2.2}$$

In Equations 2.1 and 2.2, $\boldsymbol{\Phi}_n$ stands for the *n*'th mode vector, $\Phi_{n,j}$ is the *j*'th element of the *n*'th mode vector, $\boldsymbol{m}$ is the mass matrix and $\boldsymbol{l}$ is the influence vector.

Equation 2.3 presents the same modal expression at the instant when the *j*'th story inter-story drift attains its maximum value during dynamic response. Let $t_{j,max}$ be the instant when *j*'th interstory drift becomes maximum. Then,

$$\Delta_{j,max} = \Delta_j(t_{j,max}) = \sum_{n=1}^{N} \Gamma_n \Delta\Phi_{nj} D_n(t_{j,max}) \tag{2.3}$$

$D_n(t_{j,max})$ in Equation 2.3 satisfies the modal displacement amplitude at $t_{j,max}$ which satisfies Equation 2.4.

$$\ddot{D}_n(t_{j,max}) + 2\xi_n \omega_n \dot{D}_n(t_{j,max}) + \omega_n^2 D_n(t_{j,max}) = -\ddot{u}_g(t_{j,max}) \tag{2.4}$$

If the *n*'th mode participation is isolated from Equation 2.3 and the right hand side is both multiplied and divided by the modal spectral displacement $\overline{D}_n$, we obtain

$$\Delta_{jn}(t_{j,max}) = \Gamma_n \Delta\Phi_{nj} D_n(t_{j,max}) = \Gamma_n \Delta\Phi_{nj} \frac{D_n(t_{j,max})}{\overline{D}_n} \overline{D}_n \tag{2.5}$$

In Equations 2.5 and 2.6, $\overline{D}_n$ is the spectral displacement of the *n*'th mode. The maximum (spectral) modal interstory drift value of the exemplary *n*'th mode is also expressed as,

$$\overline{\Delta}_{jn} = \Gamma_n \Delta\Phi_{nj} \overline{D}_n \tag{2.6}$$

Equations 2.5 and 2.6 can be combined to form Equation 2.7.

$$\Delta_{jn}(t_{j,max}) = \overline{\Delta}_{jn} \frac{D_n(t_{j,max})}{\overline{D}_n} \tag{2.7}$$

Then Equations 2.3 and 2.7 lead to Equation 2.8.

$$\Delta_{j,max} = \overline{\Delta}_{j1} \frac{D_1(t_{j,max})}{\overline{D}_1} + \overline{\Delta}_{j2} \frac{D_2(t_{j,max})}{\overline{D}_2} + \ \dots + \overline{\Delta}_{jN} \frac{D_N(t_{j,max})}{\overline{D}_N} \tag{2.8}$$

or

$$\Delta_{j,max} = \sum_{n=1}^{N} \overline{\Delta}_{jn} \frac{D_n(t_{j,max})}{\overline{D}_n} \tag{2.9}$$

where

$$\alpha_{jn} = \frac{D_n(t_{j,max})}{\overline{D}_n} \tag{2.10}$$

is the modal scaling coefficient that represents the *n*'th mode contribution to the *j*'th interstory drift response.

Finally,

$$\Delta_{j,max} = \sum_{n=1}^{N} \overline{\Delta}_{jn} \alpha_{jn} \tag{2.11}$$

for the *j*'th story. Here,

$$\underline{\alpha}_{jn} = \begin{bmatrix} \alpha_{11} & \cdots & \alpha_{1n} & \cdots & \alpha_{1N} \\ \vdots & \ddots & \vdots & \ddots & \vdots \\ \alpha_{j1} & \cdots & \alpha_{jn} & \cdots & \alpha_{jN} \\ \vdots & \ddots & \vdots & \ddots & \vdots \\ \alpha_{J1} & \cdots & \alpha_{Jn} & \cdots & \alpha_{JN} \end{bmatrix} \tag{2.12}$$

is the modal scaling matrix. *J* stands for the total story number in Equation 2.12 (*j* = 1, 2, … *J*).

The procedure explained above can also be formulated for any response parameter *r* at *j*'th story as given below.

$$r_{max} = \sum_{n=1}^{N} \overline{r}_n \alpha_n \tag{2.13}$$

In Equation 2.13, r_{max} and $\overline{r}_n$ correspond to the response of *r* at t_{max}, and the spectral modal response of the same parameter, respectively. However t_{max} is the instant when this particular response parameter *r* becomes maximum during dynamic response.

Also,

$$\alpha_n = \frac{r_n(t_{max})}{r_n} \tag{2.14}$$

The linear modal combination procedure can be implemented through the following steps.

1. *Eigenvalue Analysis:* The natural periods T_n, modal vectors $\boldsymbol{\Phi}_n$, and other related modal parameters (modal participation factors Γ_n, modal masses M_n, etc.) are calculated.

2. *Modal single-degree-of-freedom (SDOF) Analyses:* Modal SDOF displacement response histories $D_n(t)$ corresponding to each mode are obtained under a particular ground motion record. SDOF analyses are conducted for all significant modes having the specified periods T_n and damping ratios ξ_n.

3. *Response Spectrum Analysis (RSA):* The analyses performed in Step 2 are also used for obtaining the RSA results. The absolute maximum values of each SDOF displacement response history $D_n(t)$'s are obtained and registered as the spectral displacement $\overline{D}_n$ of each mode.

4. *Search for $t_{j,max}$: $t_{j,max}$* for each story are obtained from Equation 2.1.

5. *Modal Scaling Coefficients:* From each SDOF solution $D_n(t)$ in Step 2, the displacement amplitudes that occur at the maximum IDR response of each story, i.e. $D_n(t_{j,max})$ are determined from Equation 2.4. Modal scaling coefficients are calculated by using Equation 2.10. (Story number, j = 1, 2, …, J)

6. *Linear Modal Combination (LMC):* Maximum modal response values from RSA are multiplied by modal scaling coefficients and linearly combined to determine the LMC results, as indicated in Equation 2.13. For any response parameter, there are J number of response values as a result of the LMC procedure. The final response of a selected parameter is estimated by taking the envelope of all results.

2.2 LMC Procedure for Space Frames

The linear modal combination procedure and modal scaling coefficients are based on the premise that when the interstory drift ratio at a certain story attains its maximum value, the other high order parameters (member deformations, internal forces, etc.) also reach their maximum response. This phenomenon is apparent in a 2D plane frame structure

where there is only one frame in the direction of ground motion. The same situation is valid for a 3D space frame structure where any kind of asymmetry does not exist. Inherently, global response parameters which are recorded at the mass center of each story are maximized at the same time as the ones recorded from individual frames in the direction of ground motion. Similarly, the maximum response values are also the same for every node in a specific story, considering that the rigid floor diaphragm is present. Therefore the modal scaling coefficients in the LMC procedure can be established by considering only the IDR's recorded at the mass center of each story. Then, the modal scaling coefficients determined for a typical frame can be used to calculate all local response parameters at any individual frame, consistently.

The approach discussed above is generally not valid for 3D space frames with stiffness or mass asymmetry. Two different examples of such frame systems are presented in Figure 2.1 and Figure 2.2, which are also the case studies of this thesis work. The simple system in Figure 2.1 is created in order to observe the effect of eccentricity ratio on torsional coupling, i.e. observing the variations of stiff edge frame (SE) and flexible edge frame (FE) responses with the eccentricity ratio. For the system in Figure 2.2, the center of mass is shifted from the center of rigidity by fixing the eccentricity to 15% of total floor width. More detailed description on these two systems is given in the following chapters on case studies.

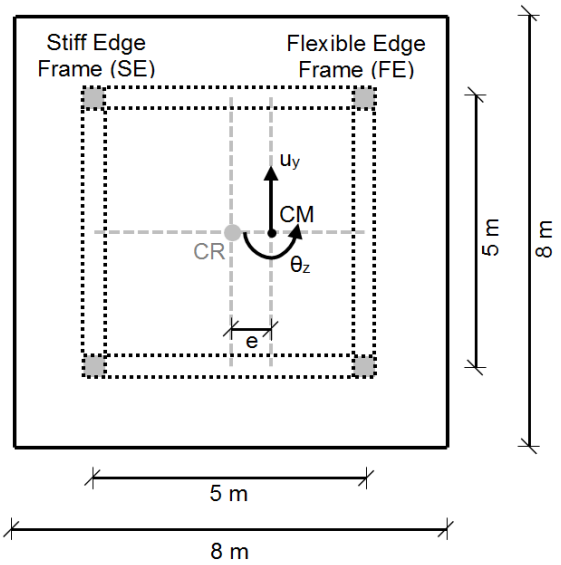

Figure 2.1: Story plan of one story space frame with torsional coupling

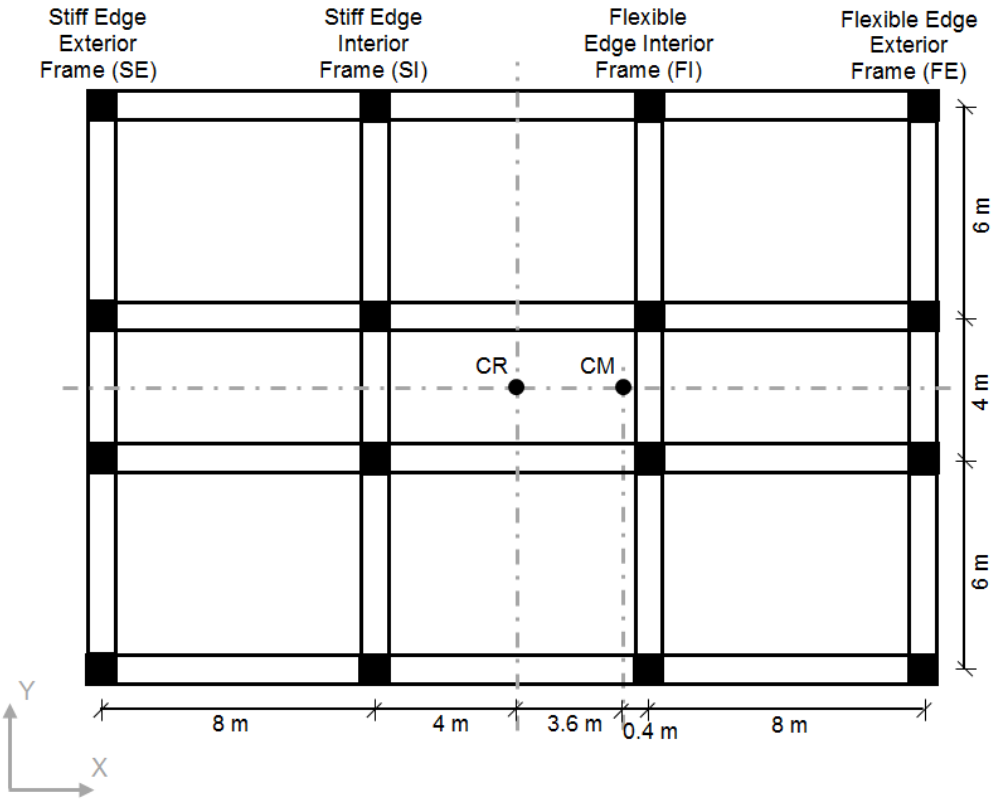

Figure 2.2: Story plan of eight story space frame with torsional coupling

It is considered that during an earthquake ground motion, seismic force resultants act at the mass center of each story level in a building structure. Due to the eccentricity between the centers of rigidity and mass, seismic forces both push the structure and twist it around the center of rigidity. This action induces torsional motion along with translation, creating a displacement gradient between different frame nodes in a specific story level. Hence, the maximum response occurrence time of IDR recorded at the mass center of a story is different from the IDR's recorded at any individual frame, at the same story level. This feature can be observed from Table 2.1, which is obtained under Northridge Earthquake. This time difference is reflected on the modal scaling coefficients that are determined independently for each story. The maximum IDR values for each individual frame also differ significantly from each other in the direction of analysis. An example of maximum IDR profiles of each frame is shown in Figure 2.3. While IDR profiles exhibit such variations among different individual frames, it is not possible to capture the true behavior of each frame by only considering the modal scaling coefficients determined from the IDR of the mass centers of each story.

Table 2.1: Occurrence times of maximum interstory drift ratios in an eight story space frame under ORR090 ground motion of the 1994 Northridge Earthquake

t_{max} values					
Story	**SE**	**SI**	**FI**	**FE**	**CM**
1	8.70	8.72	11.50	10.42	11.50
2	8.70	8.74	12.18	10.46	12.16
3	8.72	8.24	12.20	9.78	12.20
4	8.76	12.18	12.22	9.80	12.22
5	8.56	12.18	9.80	9.80	9.80
6	8.54	12.20	9.78	9.80	9.78
7	8.54	12.20	9.78	9.78	9.78
8	8.86	12.20	9.78	9.78	9.78

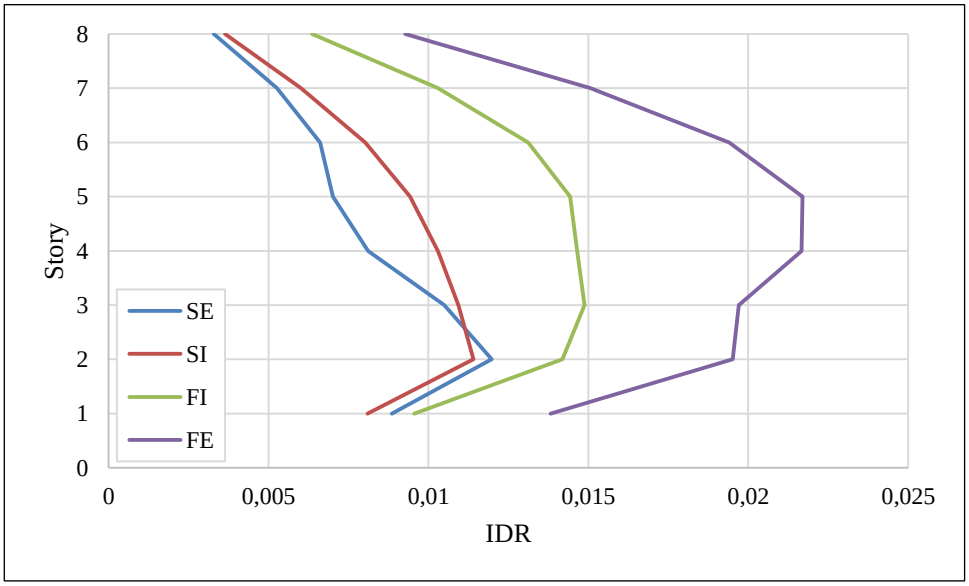

Figure 2.3: Maximum interstory drift ratio profiles of all four frames in the direction of ground motion under ORR090 ground motion of the 1994 Northridge Earthquake

In order to consider the frame-wise variation of IDR's, the LMC procedure is applied to each frame in the direction of ground motion separately, but not to the entire 3D space frame all at once. As a consequence of this approach, one might as well say that the formulation of LMC procedure for space frames is similar to that of the plane frames. The only difference between the two is the frame-wise approach for space frames. When

determining the modal scaling coefficients corresponding to each story, each frame in the direction of ground motion is considered separately. In the previous section, modal scaling coefficient matrix, α_{jn}, was defined for a frame as a 2nd order tensor, the first index representing "the story" and the second index representing "the mode". In this section, a 3rd order tensor is defined for the modal scaling coefficients, where the third index represents "the frame". This 3D coefficient matrix can be considered as a combination of 2D coefficient matrices for each individual frame of the space frame system.

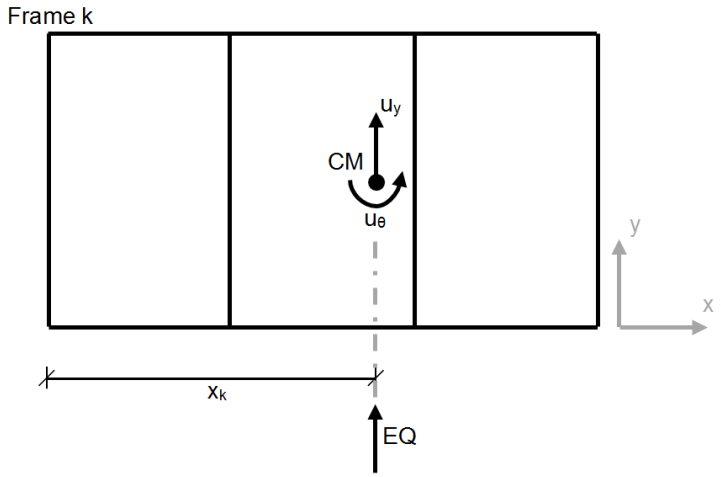

Figure 2.4: Locations of frames with respect to the mass center for a representative *j*'th story

As mentioned above for unsymmetrical plan buildings, the displacement of any frame in a specific story is different from the displacement of the mass center of that story due to torsional coupling effect. The displacement of any frame has contributions from both translational and rotational components of the mode vectors, defined at the center of mass of each story. The same phenomenon is naturally valid for the interstory drift ratios.

In the light of the information above, Equation 2.3 is rewritten for the illustrative Frame *k* in Figure 2.4 as:

$$\Delta_{j,max}^{k} = \Delta_{j}^{k}\left(t_{j,max}^{k}\right) = \sum_{n=1}^{N} \Gamma_n \left(\Delta\Phi_{ny,j} + x_k \Delta\Phi_{n\theta,j}\right) D_n\left(t_{j,max}^{k}\right) \qquad (2.15)$$

where

$$\Delta\Phi_{ny,j} = \Phi_{ny,j} - \Phi_{ny,j-1}$$
$$\Delta\Phi_{n\theta,j} = \Phi_{n\theta,j} - \Phi_{n\theta,j-1} \quad (2.16)$$

In Equations 2.15 and 2.16, $D_n(t^k_{j,max})$ stands for the displacement response of the equivalent SDOF system representing the n'th mode at t_{max} for the j'th story of Frame k. x_k is the distance between Frame k and the center of mass of the j'th story (Figure 2.4). Note that the sign of x_k changes according to the location of frame with respect to the center of mass. $\Phi_{ny,j}$ and $\Phi_{n\theta,j}$ denote the translational and rotational components of the j'th element of the n'th mode vector, respectively. The n'th mode vector $\boldsymbol{\Phi}_n$, is defined at the mass centers of each story, as indicated previously.

Equation 2.17 is obtained when the n'th mode participation is isolated from Equation 2.15 and the right hand side is both multiplied and divided by $\overline{D}_n$, similar to the operation performed in Section 2.1 in obtaining Equation 2.5.

$$\begin{aligned}\Delta^k_{jn}\left(t^k_{j,max}\right) &= \Gamma_n\left(\Delta\Phi_{ny,j} + x_k\Delta\Phi_{n\theta,j}\right)D_n\left(t^k_{j,max}\right)\\ &= \Gamma_n\left(\Delta\Phi_{ny,j} + x_k\Delta\Phi_{n\theta,j}\right)\frac{D_n\left(t^k_{j,max}\right)}{\overline{D}_n}\overline{D}_n\end{aligned} \quad (2.17)$$

The maximum (spectral) modal interstory drift value of the exemplary n'th mode for the j'th story of Frame k is expressed as,

$$\overline{\Delta}^k_{jn} = \Gamma_n\left(\Delta\Phi_{ny,j} + x_k\Delta\Phi_{n\theta,j}\right)\overline{D}_n \quad (2.18)$$

The n'th mode's spectral displacement value $\overline{D}_n$ is the same as defined in Section 2.1, Equation 2.5. Since all modal quantities (eigenvalues and eigenvectors) are defined only at the mass centers of each story, spectral displacement value is independent of any individual frame.

Equations 2.17 and 2.18 can be combined to obtain Equation 2.19.

$$\Delta^k_{jn}\left(t^k_{j,max}\right) = \overline{\Delta}^k_{jn}\frac{D_n\left(t^k_{j,max}\right)}{\overline{D}_n} \quad (2.19)$$

Then Equations 2.15 and 2.19 lead to Equation 2.20, similar to Equation 2.8.

$$\Delta^k_{j,max} = \overline{\Delta}^k_{j1}\frac{D_1\left(t^k_{j,max}\right)}{\overline{D}_1} + \overline{\Delta}^k_{j2}\frac{D_2\left(t^k_{j,max}\right)}{\overline{D}_2} + \ \ldots\ + \overline{\Delta}^k_{jN}\frac{D_N\left(t^k_{j,max}\right)}{\overline{D}_N} \quad (2.20)$$

or

$$\Delta^k_{j,max} = \sum_{n=1}^{N}\overline{\Delta}^k_{jn}\frac{D_n\left(t^k_{j,max}\right)}{\overline{D}_n} \quad (2.21)$$

where

$$\alpha_{jn}^{k} = \frac{D_n\left(t_{j,max}^{k}\right)}{\overline{D}_n} \tag{2.22}$$

Here, α^{k}_{jn} is the modal scaling coefficient that represents the n'th mode's contribution to the j'th interstory drift response of Frame k.

Finally,

$$\Delta_{j,max}^{k} = \sum_{n=1}^{N} \overline{\Delta}_{jn}^{k} \alpha_{jn}^{k} \tag{2.23}$$

for the j'th story of Frame k. Here,

$$\underline{\alpha}_{jn}^{k} = \begin{bmatrix} \alpha_{11}^{k} & \cdots & \alpha_{1n}^{k} & \cdots & \alpha_{1N}^{k} \\ \vdots & \ddots & \vdots & \ddots & \vdots \\ \alpha_{j1}^{k} & \cdots & \alpha_{jn}^{k} & \cdots & \alpha_{jN}^{k} \\ \vdots & \ddots & \vdots & \ddots & \vdots \\ \alpha_{J1}^{k} & \cdots & \alpha_{Jn}^{k} & \cdots & \alpha_{JN}^{k} \end{bmatrix} \tag{2.24}$$

is the modal scaling matrix constructed particularly for Frame k.

The procedure explained above can be formulated for any response parameter r^{k} recorded at j'th story in Frame k as given below.

$$r_{max}^{k} = \sum_{n=1}^{N} \overline{r}_{n}^{k} \alpha_{n}^{k} \tag{2.25}$$

In Equation 2.25, r^{k}_{max} and $\overline{r}_{n}^{k}$ correspond to the response of r at t^{k}_{max}, and the spectral modal response of the same parameter, respectively. However t_{max} is the instant when this particular response parameter r becomes maximum during dynamic response. Also,

$$\alpha_{n}^{k} = \frac{r_n\left(t_{max}^{k}\right)}{\overline{r}_n} \tag{2.26}$$

Development of the procedure presented for illustrative Frame k is valid for all frames in the direction of analysis, regardless of the distance from the center of mass. Accordingly, there is one modal scaling matrix belonging to each frame for a torsionally coupled 3D space frame. For ease of application, a three-dimensional modal scaling matrix can be constructed by assembling all frame wise modal scaling matrices. The indices of the matrix would represent the story number j, the mode number n, and the frame number k, respectively.

The linear modal combination procedure for space frames is applied through the following steps.

1. *Eigenvalue Analysis:* Modal periods T_n, mode vectors $\boldsymbol{\Phi}_n$, and the other related modal parameters (modal participation factors Γ_n, modal masses M_n, etc.) are calculated for each mode.

2. *Modal single-degree-of-freedom (SDOF) Analyses:* Modal SDOF displacement response histories $D_n(t)$ corresponding to each mode are obtained. SDOF analyses are conducted for the significant modes having the specified periods T_n and damping ratios ξ_n under a particular ground motion record.

3. *Response Spectrum Analysis (RSA):* The analyses performed in Step 2 are also used for obtaining the RSA results. The absolute maximum values of each SDOF displacement response history $D_n(t)$'s are obtained and used as the spectral displacement $\overline{D}_n$ of each mode.

4. *Search for t_{max}:* For each Frame k in the direction of analysis, $t^k_{j,max}$ for each story j are obtained from Equation 2.14.

5. *Modal Scaling Coefficients:* From each SDOF solution $D_n(t)$ in Step 2, the displacement amplitudes that occur at the maximum IDR response of each story of each frame, i.e. $D_n(t^k_{j,max})$ are determined. Taking the spectral displacements from Step 3, modal scaling coefficients are calculated by using Equation 2.21.

6. *Linear Modal Combination (LMC):* Maximum modal response values from RSA are multiplied by the associated modal scaling coefficients from Step 5 and linearly combined to determine the LMC results, as indicated in Equation 2.24. Similar to the plane frame cases, this combination procedure is repeated for each individual frame. The envelope of all results for any response parameter is also taken in order to obtain final results.

CHAPTER 3

GROUND MOTION RECORDS

This chapter explains the properties of the ground motions that are employed in the case studies. The analytical responses of the structures in all four case studies are calculated under three different ground motion components. The acceleration time histories of the ground motion components introduced herein are used for the response history analyses of both the multi-degree-of-freedom systems and for the equivalent single-degree-of-freedom modal systems. The response spectra of ground motions are used for the response spectrum analyses (CQC), and accordingly for the linear modal combination (LMC) procedure.

The response of a system to a ground motion is sensitive to the characteristics of that ground motion. Basic characteristics of strong ground motions which influence dynamic structural response are the frequency content, peak values of the ground motion (PGA, PGV, etc.) effective duration or duration of the strong part, and whether it has a dominant acceleration pulse in the record or not. The variation of spectral values over the period is effective in displaying the important characteristics of a ground motion. Spectral acceleration (or displacement) value corresponding to a higher mode period has an influence on the modal contribution of that mode to the total response. If a deliberate coupling is aimed for a system to investigate the coupled response, then the spectral shape of record becomes important.

The ground motion records were obtained from the PEER Strong Motion Database, and no processing was carried out on the original records. Their properties are tabulated in Table 3.1. The table also includes the earthquake titles and component labels of records which are used to assess the results comparatively according to ground motion properties in the following chapters.

Table 3.1: Basic characteristics of the ground motion records

Earthquake	**Date**	**M_w**	**Station**	**Component**	**Record Name**
Northridge	17.01.1994	6,7	Castaic - Old Ridge RT	ORR090	NORTHR
El Centro	15.10.1979	6,5	El Centro Array #4	H-E04140	IMPVALL
Loma Prieta	18.10.1989	7,0	Corralitos	CLS090	LOMAP

Table 3.1 (cont'd)

Earthquake	**Soil Type**	**FD (km)**	**PGA (g)**	**PGV (cm/s)**	**t_{eff} (s)**	**Type**
Northridge	B	20,72	0,568	52,1	9,08	Ordinary
El Centro	D	4,2	0,485	37,4	6,685	Pulse
Loma Prieta	B	3,9	0,479	45,2	7,88	Pulse

Soil Types:
A: Rock
B: Shallow/stiff soil
C: Deep narrow soil
D: Deep broad soil
E: Soft deep soil

M_w: Moment magnitude
FD: Closest distance between the station and the fault rupture
t_{eff}: Effective duration (Trifunac and Brady, 1975)

Acceleration time histories of the records are plotted in Figure 3.1. The acceleration response spectra and displacement response spectra for 5% damping under three earthquake records are presented in Figure 3.2 and Figure 3.3, respectively. The difference in the spectral characteristics of ground motions can be observed from the spectral graphics. It can be observed that Loma Prieta amplifies total acceleration in the 0.5-1.0 second range whereas Northridge and El Centro amplifies displacements at longer periods.

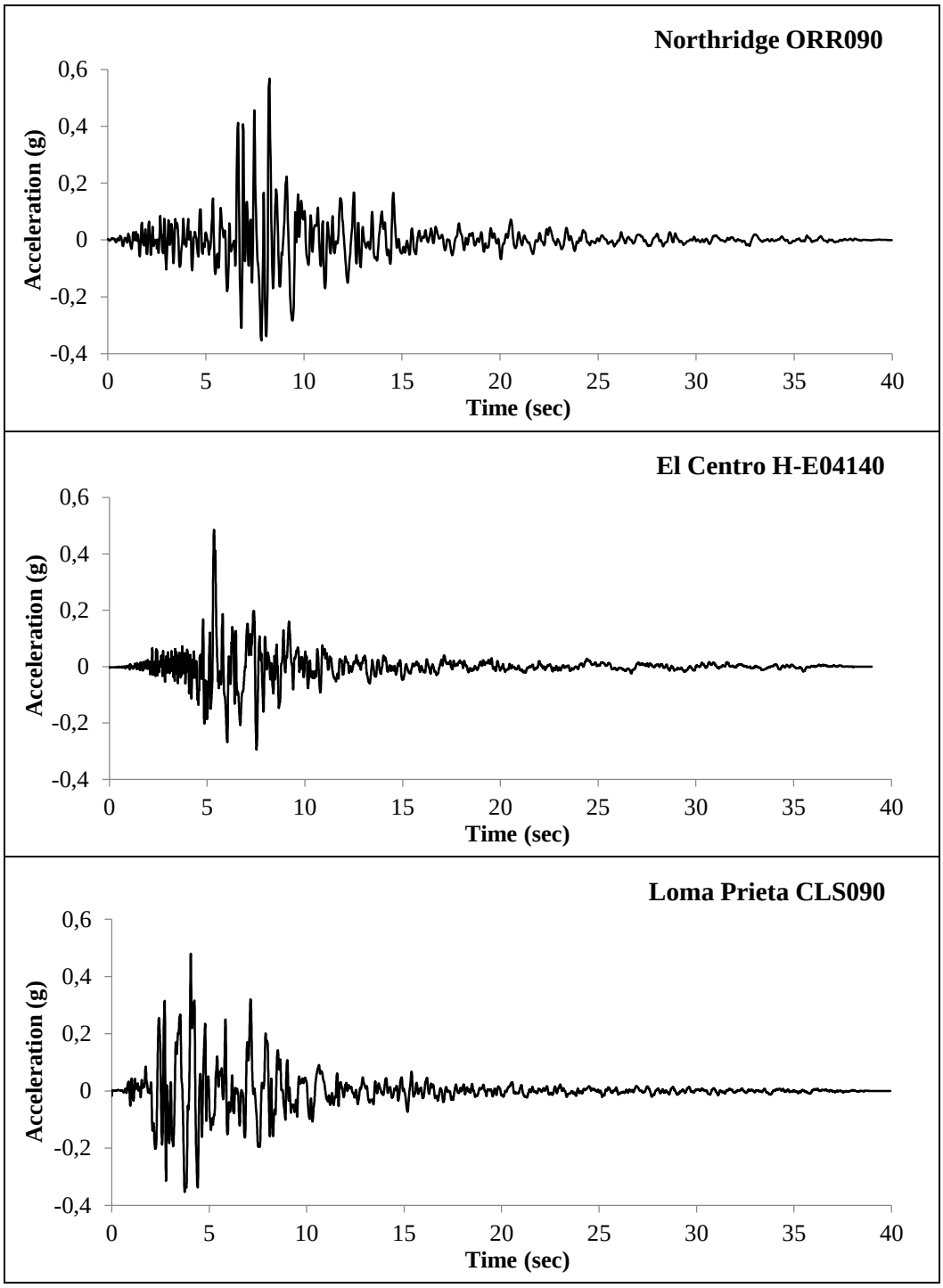

Figure 3.1: Acceleration time histories of the ground motion records

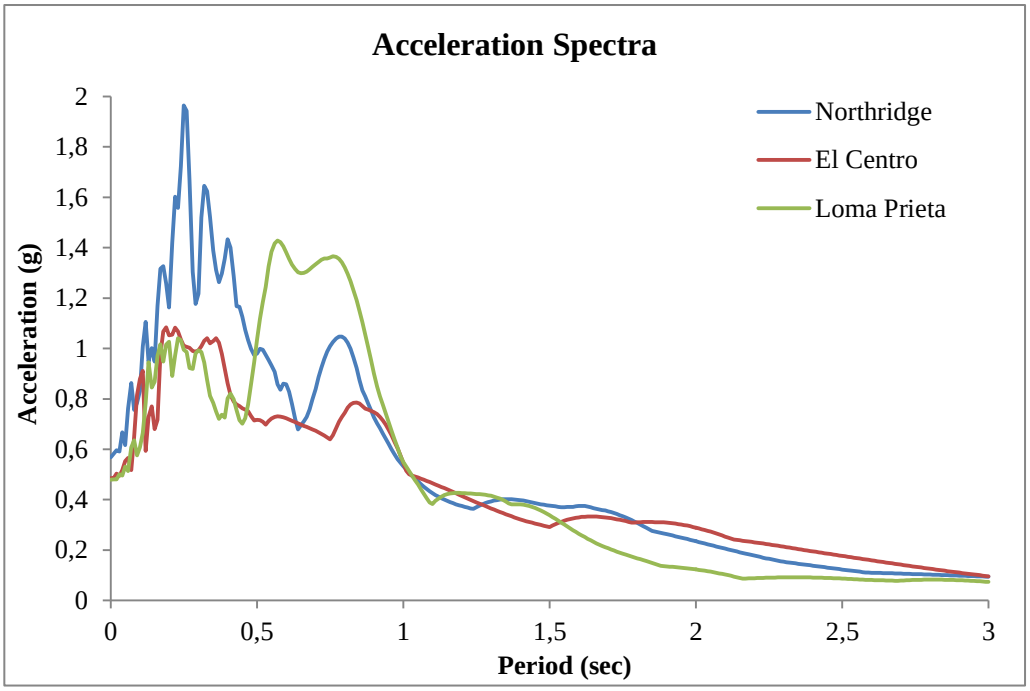

Figure 3.2: Acceleration response spectra of the ground motion records

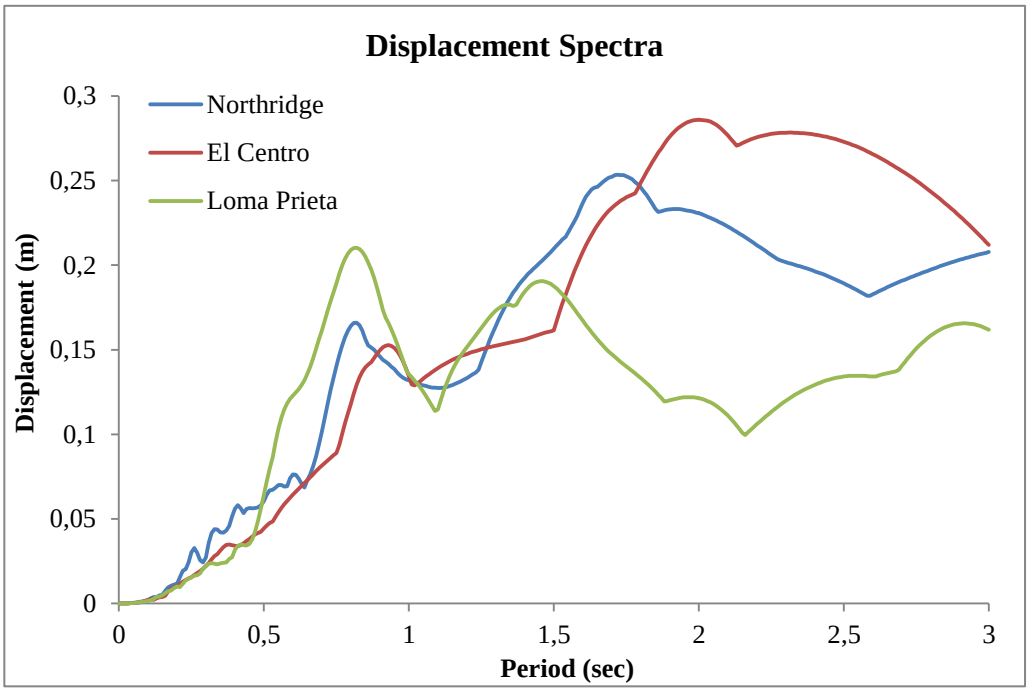

Figure 3.3: Displacement response spectra of the ground motion records

CHAPTER 4

CASE STUDIES: SIMPLE STRUCTURES

The linear modal combination procedure (LMC) which is developed in the previous chapters is tested firstly on two different simple structural systems. The first one is a three story plane frame structure where third story is considered as a light appendage, having much smaller stiffness and mass compared to the regular stories below. The second one is a single story space frame structure with torsional coupling due to the introduced mass eccentricity.

4.1 Three Story Plane Frame Structure with an Appendage

The first case study is utilized in order to observe the effect of strong modal coupling on the dynamic response of the structure. It is modified from a uniform three story frame where the stiffness and mass properties do not change along the height. However, this type of structures have well-separated modes where the ratio of first to second mode period being around 3-3.5. The response from the first mode would be notably dominant compared to those from the higher modes; hence the effect of the higher modes would not be observed much during dynamic response.

The prominent prerequisite of this case study is to create a coupled system. The simplest way to create such coupling is to disturb the uniform stiffness and mass distributions of the structure along its height. As can be observed from Figure 4.1, the stiffness and mass of the third story is reduced from k to k' and from m to m', respectively. Hence the third story represents a light appendage over the two regular stories below. Different k'/k and m'/m ratios were tested during the case study in order to produce a deliberately chosen level of coupling among the vibration modes. The coupling condition in this 3–story structure is determined as the ratio between the first mode and second mode periods. After a trial process, the T_2/T_1 ratio is selected to be around 0.85. The following stiffness and mass ratios give 86% ratio for T_2/T_1, as presented in Table 4.1.

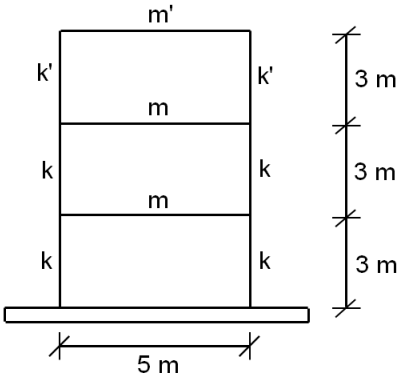

Figure 4.1: Side view of three story plane frame structure

Table 4.1: The ratios of third story stiffness and mass with respect to the first and second story stiffness and mass, respectively

k'/k	***m'/m***
0.005	0.02

As seen in Table 4.1, the stiffness and mass of the third story is decreased significantly and a light appendage at the third story is obtained with this approach. During dynamic response the appendage vibrates with a very different frequency than the rest of the structure, triggering the participation of higher modes to the total response. Consequently, the generated structure with a light appendage has closely coupled modes. Close coupled modal vector amplitudes and modal participation factors also verify the selection of T_2/T_1 ratio. More detailed information on the modal properties is presented in Table 4.2 and Figure 4.2.

It should be noted that *k'/k* and *m'/m* ratios regulate only the modal properties of the structure, not the level of participation of a particular mode to the total response for any response parameter. Strong ground motion records employed in the analyses play an important role on the modal response participations. It is well known that modal responses depend on spectral displacement S_d or spectral acceleration S_a, as well as modal participation factor Γ_n and modal vector amplitude Φ_{nj}. For the LMC procedure, the spectral amplitude term (by definition, it is the spectral displacement) is replaced with $D_n(t_{j,max})$, as introduced in Chapter 2. Since it is directly related to the ground motion record, the magnitude of this spectral amplitude term for every mode is also decisive on how close the modal coupling is.

Only one structural system is certainly not sufficient to observe the coupled response. Hence, four different systems are prepared by simply changing the mass of each story while keeping the *m'/m* ratio constant. Change in mass is directly reflected on the vibration periods of the structure. Different T_1 values for different systems directly change the modal displacement amplitude term (S_d or $D_n(t_{j,max})$) in the modal response participation since the equivalent SDOF solutions change with the period of a particular mode.

Table 4.2: Modal properties of four different structural systems

SYSTEM 1			
Mode *n*	**T_n (s)**	**Γ_n (ton)**	**M_n^* (ton)**
1	0.501	3.208	10.290
2	0.431	-3.120	9.737
3	0.132	-1.643	2.698

SYSTEM 2			
Mode *n*	**T_n (s)**	**Γ_n (ton)**	**M_n^* (ton)**
1	1.002	6.416	41.159
2	0.861	-6.241	38.948
3	0.264	-3.285	10.792

SYSTEM 3			
Mode *n*	**T_n (s)**	**Γ_n (ton)**	**M_n^* (ton)**
1	1.417	9.073	82.319
2	1.218	-8.826	77.896
3	0.374	-4.646	21.585

SYSTEM 4			
Mode *n*	**T_n (s)**	**Γ_n (ton)**	**M_n^* (ton)**
1	2.004	12.831	164.638
2	1.723	-12.482	155.793
3	0.529	-6.570	43.170

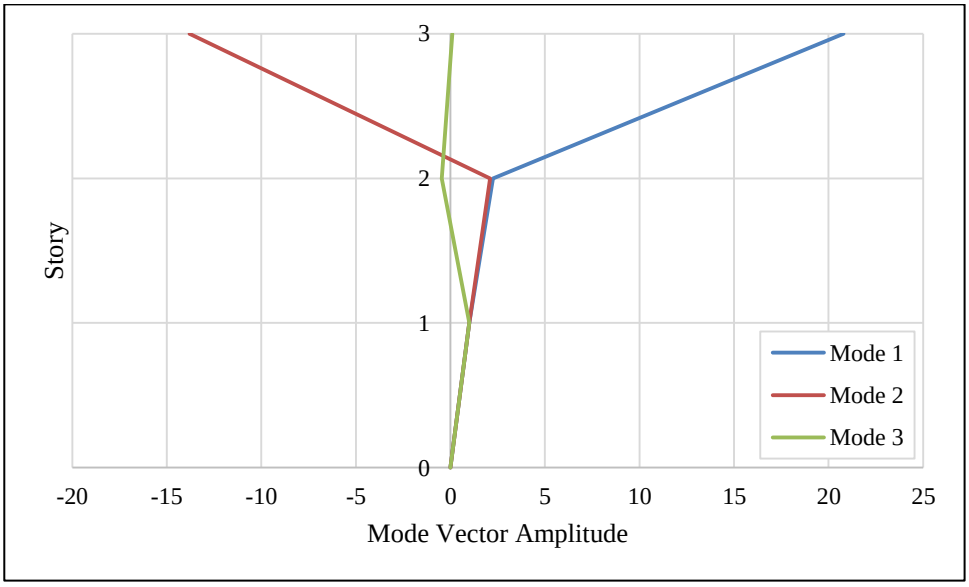

Figure 4.2: Modal vectors of the three story plane frame

In order to better illustrate the modal scaling in the LMC procedure, the maximum modal interstory drifts that are obtained under Loma Prieta earthquake ground motion are presented in Figure 4.3 for each mode. As stated in Chapter 2, the LMC procedure consists of several steps. The third step of the LMC procedure is response spectrum analysis. During that step, the absolute maximum values of previously calculated $D_n(t)$'s are determined and multiplied with the associated modal parameters accordingly in view of Equation 2.6. The result is the maximum modal IDR of a single story j. If this calculation is performed by using the full modal vector $\boldsymbol{\Phi}_n$, the maximum modal IDR profile of each mode along the height is obtained. For convenience, aforementioned equations are presented below again as Equation 4.1.

$$\overline{\Delta}_{jn} = \Gamma_n \Delta\Phi_{nj} \overline{D}_n \tag{4.1}$$

Equation 4.1 can be written for the entire system.

$$\overline{\boldsymbol{\Delta}}_{\boldsymbol{n}} = \Gamma_n \boldsymbol{\Delta\Phi}_{\boldsymbol{n}} \overline{D}_n \tag{4.2}$$

The modal IDR profile $\overline{\boldsymbol{\Delta}}_{\boldsymbol{n}}$ which is calculated by using Equation 4.2 is the representation of the n'th mode contribution to the total IDR profile. They are illustrated in Figure 4.3 for all 3 modes.

After the modal scaling coefficients are determined through searching for $t_{j,max}$ values for each story, which also constitutes the fourth step of the LMC procedure, the total IDR response is calculated by multiplying the modal scaling coefficients with the maximum modal IDR profiles of the associated modes that are illustrated in Figure 4.3 and Equation 4.2. The j'th story component of the IDR profile is determined by using Equation 4.3, written below.

$$\Delta_{j,max} = \sum_{n=1}^{N} \overline{\Delta}_{jn} \alpha_{jn} \tag{4.3}$$

It is useful to remind that α_{jn} is the modal scaling coefficient that represents the n'th mode contribution to the IDR response of the j'th story.

Within the scope of LMC procedure, there are a total j number of IDR profiles, each of which is representing the instant when the IDR response of each story j reaches the maximum value. The j'th story IDR is determined exactly in this procedure when the system is linear elastic.

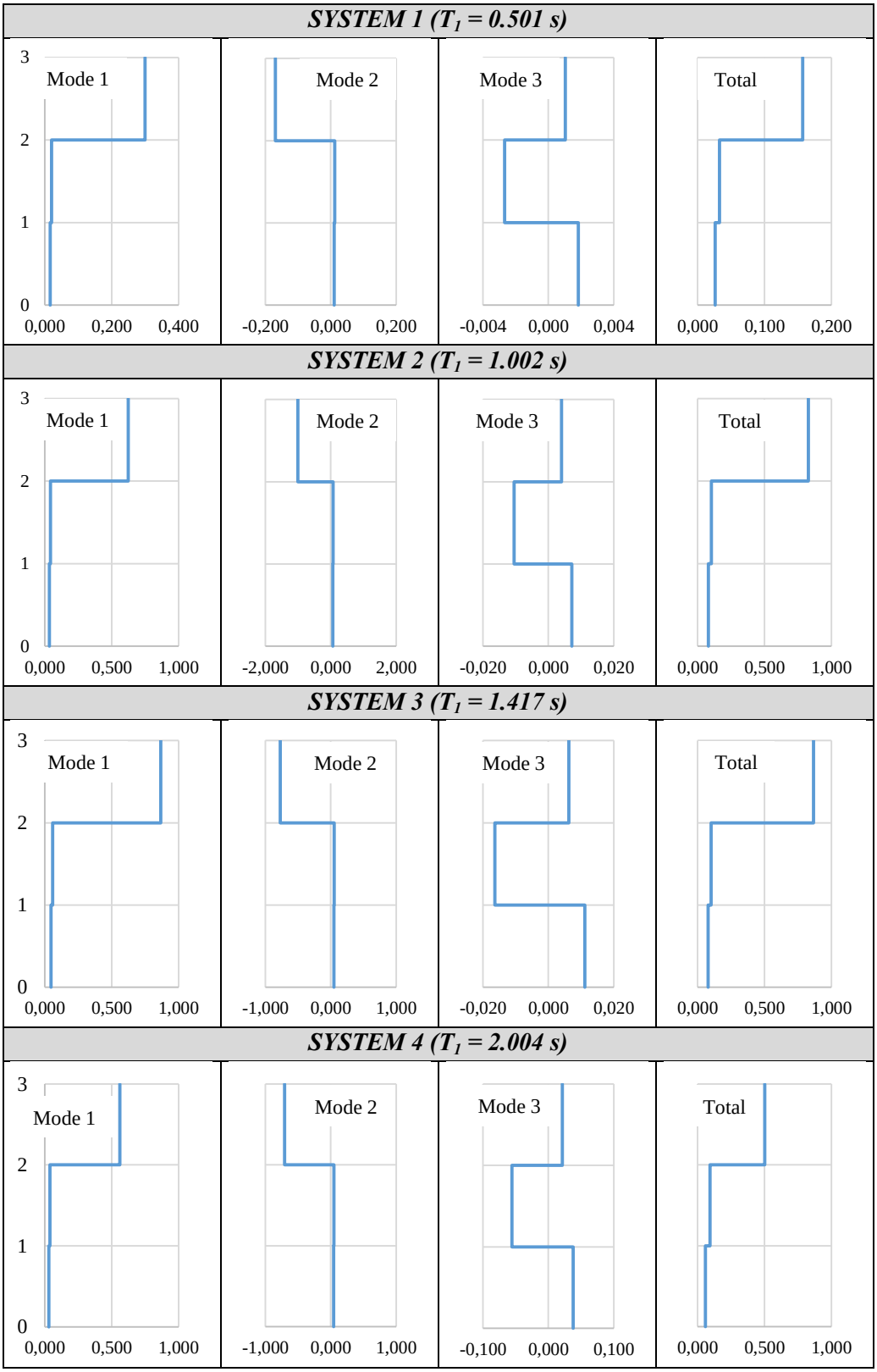

Figure 4.3: Maximum modal interstory drift ratio profiles under Loma Prieta 1989 CLS090

Analytical model of the three story structure is prepared by using the OpenSees software framework. Since the LMC procedure is tested for linear elastic behavior only, the structure is modeled with members having linear geometry and linear elastic material behavior. For a linear elastic system, cross sectional area A and moment of inertia I are the only parameters that define a member, while modulus of elasticity E is the only parameter which defines material properties. The geometric and material properties of the system which correspond to the vibration properties presented in Table 4.2 and Figure 4.2 are listed below:

- Beam and column lengths are 3 meters and 5 meters, respectively.
- Cross section areas of all members are 30x30 cm^2.
- Modulus of elasticity is defined as 22360 MPa, corresponding to that of concrete having a compressive strength of 21.7 MPa. This value is calculated according to $E_c = 4800\sqrt{f_c}$ (ACI 318-99, 1999).
- Lumped masses corresponding to each translational DOF are assigned at each story level. The masses m of the systems having the fundamental periods T_1 equal to 0.501, 1.002, 1.417 and 2.004 seconds are 11.25, 45, 90 and 180 tons, respectively.
- Rayleigh damping is used for estimating the damping of structural system. First and third modes are fixed to 5% damping.

Story displacements, interstory drift ratios, story shear forces and node rotations are obtained analytically under three different earthquake ground motions that are defined in Chapter 3. However the results are not indicative exclusively since the structure is a made-up model. All design parameters are determined in such a way that they result in preferred modal properties. Therefore only the error ratios (in percentage errors) of the CQC and LMC procedures with respect to the benchmark response history analysis (RHA) results are presented. For each response parameter, the absolute difference between the responses calculated from CQC or LMC, and RHA is calculated. Then it is divided with the absolute value of the RHA result. This calculation is done for both CQC and LMC procedures. t_{max} values, modal scaling coefficients, and the percentage errors of CQC method and LMC procedures are presented from Table 4.3 to Table 4.7 for three ground motion components that are introduced in Chapter 3, respectively.

Table 4.3: t_{max} values of four systems with different coupled mode periods under three different ground excitations

GM	**Northridge**			
Story	***System 1*** ***(T_1 = 0.50 s)***	***System 2*** ***(T_1 = 1.00 s)***	***System 3*** ***(T_1 = 1.42 s)***	***System 4*** ***(T_1 = 2.00 s)***
1	9.480	8.580	8.740	10.020
2	9.480	8.480	8.860	8.260
3	8.220	9.280	11.160	12.280

GM	**El Centro**			
Story	***System 1*** ***(T_1 = 0.50 s)***	***System 2*** ***(T_1 = 1.00 s)***	***System 3*** ***(T_1 = 1.42 s)***	***System 4*** ***(T_1 = 2.00 s)***
1	6.150	7.455	6.415	6.800
2	6.140	7.490	6.295	7.740
3	6.735	8.170	7.375	11.030

GM	**Loma Prieta**			
Story	***System 1*** ***(T_1 = 0.50 s)***	***System 2*** ***(T_1 = 1.00 s)***	***System 3*** ***(T_1 = 1.42 s)***	***System 4*** ***(T_1 = 2.00 s)***
1	4.125	4.050	7.945	7.015
2	4.145	4.445	7.925	3.835
3	3.835	5.205	8.945	9.155

Table 4.4: Modal scaling coefficients of four different systems

(a) under Northridge 1994 ORR090

SYSTEM 1			
	Mode		
Story	**1**	**2**	**3**
1	0,99137	0,91036	0,30273
2	0,99137	0,91036	0,30273
3	-0,25663	0,75799	-0,69301

SYSTEM 3			
	Mode		
Story	**1**	**2**	**3**
1	-0,75080	-1,00000	-0,87639
2	-0,75853	-0,74600	0,78616
3	0,68530	-0,34792	0,08367

SYSTEM 2			
	Mode		
Story	**1**	**2**	**3**
1	-0,94503	-0,86746	-0,82333
2	-0,64145	-0,98552	0,67242
3	0,30218	-0,76111	0,42712

SYSTEM 4			
	Mode		
Story	**1**	**2**	**3**
1	0,74195	0,75686	0,55364
2	0,98116	0,82095	-0,43777
3	0,22640	-0,90462	0,53714

(b) under El Centro 1979 H-E04140

SYSTEM 1			
	Mode		
Story	**1**	**2**	**3**
1	0,78956	0,86534	-0,08418
2	0,73583	0,92918	-0,21470
3	0,94818	-0,28815	0,35873

SYSTEM 3			
	Mode		
Story	**1**	**2**	**3**
1	0,99905	0,83477	0,47962
2	0,84792	0,99595	-0,71332
3	-0,67895	0,07396	-0,40284

SYSTEM 2			
	Mode		
Story	**1**	**2**	**3**
1	-0,76991	-0,88700	-0,23715
2	-0,91193	-0,75870	-0,02654
3	0,57949	-0,75181	0,34884

SYSTEM 4			
	Mode		
Story	**1**	**2**	**3**
1	0,70622	0,75114	0,91433
2	-0,79786	-0,88317	0,50982
3	0,84310	-0,47034	0,12247

(c) under Loma Prieta 1989 CLS090

SYSTEM 1			
	Mode		
Story	**1**	**2**	**3**
1	-0,99038	-0,98214	0,07447
2	-0,99712	-0,99862	0,38416
3	0,86533	0,60946	0,11337

SYSTEM 3			
	Mode		
Story	**1**	**2**	**3**
1	0,80573	0,92080	-0,30170
2	0,76386	0,96159	-0,35953
3	-0,63351	0,40933	0,11133

SYSTEM 2			
	Mode		
Story	**1**	**2**	**3**
1	0,86037	0,87473	-0,30149
2	-0,69226	-0,96092	0,74856
3	0,29073	-0,64319	0,56519

SYSTEM 4			
	Mode		
Story	**1**	**2**	**3**
1	0,97989	0,76733	-0,10403
2	-0,72747	-0,47657	0,75204
3	0,08008	-0,65340	-0,23785

Table 4.5: Percent errors of CQC and LMC procedures for several response parameters under Northridge 1994 ORR090

SYSTEM 1				
CQC Errors (%)				
Story	**Story Displacement**	**Interstory Drift Ratio**	**Story Shear Force**	**Node Rotation**
1	16.66	16.66	17.39	15.43
2	15.22	13.37	9.86	12.38
3	27.19	18.72	16.94	17.72
LMC Errors (%)				
Story	**Story Displacement**	**Interstory Drift Ratio**	**Story Shear Force**	**Node Rotation**
1	0.05	0.05	0.05	0.04
2	0.04	0.04	0.05	0.03
3	1.67	0.03	0.02	0.02

SYSTEM 3				
CQC Errors (%)				
Story	**Story Displacement**	**Interstory Drift Ratio**	**Story Shear Force**	**Node Rotation**
1	21.13	21.13	27.91	10.80
2	10.46	12.03	20.49	15.36
3	12.69	12.20	12.24	12.21
LMC Errors (%)				
Story	**Story Displacement**	**Interstory Drift Ratio**	**Story Shear Force**	**Node Rotation**
1	0.01	0.01	1.28	5.10
2	8.73	0.02	2.99	0.93
3	0.40	0.16	0.17	0.17

SYSTEM 2				
CQC Errors (%)				
Story	**Story Displacement**	**Interstory Drift Ratio**	**Story Shear Force**	**Node Rotation**
1	20.69	20.69	25.70	12.08
2	11.16	15.32	21.32	16.54
3	12.49	8.19	7.12	7.59
LMC Errors (%)				
Story	**Story Displacement**	**Interstory Drift Ratio**	**Story Shear Force**	**Node Rotation**
1	0.03	0.03	0.03	2.72
2	4.37	0.04	2.46	0.03
3	0.66	0.15	0.15	0.15

SYSTEM 4				
CQC Errors (%)				
Story	**Story Displacement**	**Interstory Drift Ratio**	**Story Shear Force**	**Node Rotation**
1	3.86	3.87	7.50	9.81
2	11.50	16.31	23.84	17.96
3	8.68	0.84	0.84	0.10
LMC Errors (%)				
Story	**Story Displacement**	**Interstory Drift Ratio**	**Story Shear Force**	**Node Rotation**
1	0.04	0.04	0.33	0.02
2	0.02	0.02	11.62	1.13
3	0.16	0.27	0.26	0.26

Table 4.6: Percent errors of CQC and LMC procedures for several response parameters under El Centro 1979 H-E04140

SYSTEM 1				
CQC Errors (%)				
Story	**Story Displacement**	**Interstory Drift Ratio**	**Story Shear Force**	**Node Rotation**
1	1.90	1.90	0.19	3.38
2	3.48	4.32	5.73	3.07
3	9.71	6.76	6.04	6.38
LMC Errors (%)				
Story	**Story Displacement**	**Interstory Drift Ratio**	**Story Shear Force**	**Node Rotation**
1	0.16	0.16	0.05	0.15
2	0.15	0.16	0.39	0.20
3	0.14	0.04	0.05	0.04

SYSTEM 3				
CQC Errors (%)				
Story	**Story Displacement**	**Interstory Drift Ratio**	**Story Shear Force**	**Node Rotation**
1	17.32	17.32	19.58	17.05
2	17.81	23.30	27.11	24.60
3	46.26	58.32	60.20	59.32
LMC Errors (%)				
Story	**Story Displacement**	**Interstory Drift Ratio**	**Story Shear Force**	**Node Rotation**
1	0.03	0.03	1.56	3.67
2	2.44	0.03	0.93	0.07
3	0.07	0.07	0.07	0.07

SYSTEM 2				
CQC Errors (%)				
Story	**Story Displacement**	**Interstory Drift Ratio**	**Story Shear Force**	**Node Rotation**
1	5.48	5.48	5.99	3.86
2	3.58	1.51	0.11	2.31
3	9.72	10.62	10.77	10.71
LMC Errors (%)				
Story	**Story Displacement**	**Interstory Drift Ratio**	**Story Shear Force**	**Node Rotation**
1	0.03	0.03	0.11	0.32
2	0.53	0.11	2.59	0.87
3	0.42	0.16	0.15	0.15

SYSTEM 4				
CQC Errors (%)				
Story	**Story Displacement**	**Interstory Drift Ratio**	**Story Shear Force**	**Node Rotation**
1	5.52	5.52	15.24	4.99
2	6.24	11.77	14.29	12.45
3	11.20	10.24	9.93	10.08
LMC Errors (%)				
Story	**Story Displacement**	**Interstory Drift Ratio**	**Story Shear Force**	**Node Rotation**
1	0.03	0.03	0.58	0.01
2	0.03	0.07	0.06	0.05
3	0.32	0.01	0.02	0.02

Table 4.7: Percent errors of CQC and LMC procedures for several response parameters under Loma Prieta 1989 CLS090

SYSTEM 1				
CQC Errors (%)				
Story	**Story Displacement**	**Interstory Drift Ratio**	**Story Shear Force**	**Node Rotation**
1	17.06	17.06	17.65	18.81
2	19.01	20.30	21.87	19.78
3	61.59	90.68	98.21	94.68
LMC Errors (%)				
Story	**Story Displacement**	**Interstory Drift Ratio**	**Story Shear Force**	**Node Rotation**
1	0.01	0.01	2.22	0.26
2	0.23	0.06	0.06	0.09
3	0.23	0.33	0.35	0.34

SYSTEM 3				
CQC Errors (%)				
Story	**Story Displacement**	**Interstory Drift Ratio**	**Story Shear Force**	**Node Rotation**
1	1.99	1.99	5.72	7.25
2	7.80	10.39	11.85	9.77
3	10.83	13.60	14.03	13.84
LMC Errors (%)				
Story	**Story Displacement**	**Interstory Drift Ratio**	**Story Shear Force**	**Node Rotation**
1	0.18	0.18	0.16	0.02
2	0.02	0.18	0.08	0.21
3	2.45	0.05	0.08	0.05

SYSTEM 2				
CQC Errors (%)				
Story	**Story Displacement**	**Interstory Drift Ratio**	**Story Shear Force**	**Node Rotation**
1	2.56	2.56	1.31	6.39
2	7.21	11.89	16.76	14.44
3	24.57	23.37	23.08	23.20
LMC Errors (%)				
Story	**Story Displacement**	**Interstory Drift Ratio**	**Story Shear Force**	**Node Rotation**
1	0.01	0.01	0.56	0.55
2	0.74	0.05	0.05	0.82
3	0.29	0.35	0.34	0.34

SYSTEM 4				
CQC Errors (%)				
Story	**Story Displacement**	**Interstory Drift Ratio**	**Story Shear Force**	**Node Rotation**
1	19.88	19.88	54.37	7.66
2	9.43	3.86	4.68	5.79
3	63.75	53.07	52.06	53.01
LMC Errors (%)				
Story	**Story Displacement**	**Interstory Drift Ratio**	**Story Shear Force**	**Node Rotation**
1	0.10	0.10	13.74	2.00
2	3.36	0.02	2.67	0.11
3	0.68	0.14	0.76	0.00

The LMC procedure is based on the notion that all response parameters at a particular story can be obtained at the instant when the interstory drift ratio (IDR) of that story attains its maximum value during its response history. Using the modal scaling coefficients determined at those instants, any desired parameter can be calculated, including IDR itself. Based on this notion, IDR is implicitly determined. The percentage errors observed for IDR from the LMC procedure are numerical errors resulting from the OpenSees analyses. Otherwise they should be zero. The results are presented in Tables 4.5, 4.6 and 4.7.

The first outcome that clearly stands out from the error comparisons presented above is that the errors that CQC method produces is significantly larger than the errors obtained from the LMC procedure. While CQC method errors may rise up to 98% in certain cases, LMC errors are generally less than 1%. Therefore the discussion about the error levels is made below only considering the CQC method results.

The randomness of the errors in a system-wise approach is another important outcome to be highlighted. Considering all three ground motions together, there is no correlation between the systems with different periods, and the errors produced. For instance, System 3 produces the highest level of errors in average under El Centro ground motion while System 1 produces the largest errors under Loma Prieta ground motion. In the story wise comparisons, the story that gives the highest errors for all observed parameters is generally the third story. Only under Northridge ground motion the story with highest errors changes with different systems.

Among different response parameters, story shear force generally gives slightly more error under all three ground motions for almost all the systems considered in this case study. This phenomenon is particularly obvious under El Centro and Loma Prieta ground motions. Since story shear force is a higher order parameter, it is natural that we observe larger errors compared to the other response parameters.

Table 4.3 includes the t_{max} values that are obtained at the time of maximum IDR of each story for all four systems under three different earthquake ground motions. The values in the table indicate that the interstory drift ratios at the first and second stories attain their maximum values at very close times for the first three systems. On the other hand, this behavior is not observed in System 4. All three stories behave different from each other and reach their maximum IDR's at different times. However for all four systems, the maximum value of the third story IDR occurs at a considerably different time than the first and second stories.

Modal scaling coefficients are presented in Table 4.4 for all systems under all three earthquake ground motions. As can be seen from the table, the modal scaling coefficients are random in terms of modes and stories.

The modal SDOF displacement response histories of each mode as well as the total IDR response histories of each story for all four systems under Loma Prieta earthquake ground motion are shown from Figure 4.4 to Figure 4.11. The occurrence time of the maximum modal displacement responses and maximum IDR's can be investigated from the response history graphs. It can be inferred from these graphs that the first and second stories exhibit a very similar behavior throughout the response history. For System 4 this trend is disturbed, all three stories show different behavior. For Systems 1, 2 and 3, co-acting first and second story IDR's attains their maximum values at the same or successive cycles, therefore their instants and amplitudes are very close to each other. This trend is visible in the figures below.

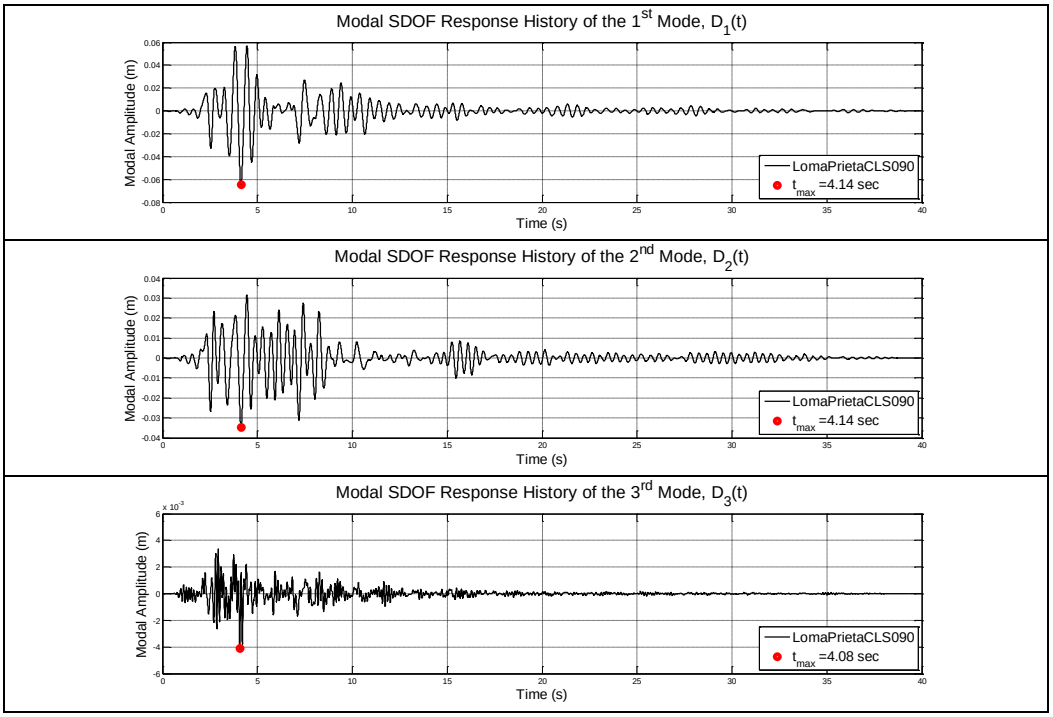

Figure 4.4: Modal SDOF response histories for each mode of System 1 under Loma Prieta 1989 CLS090

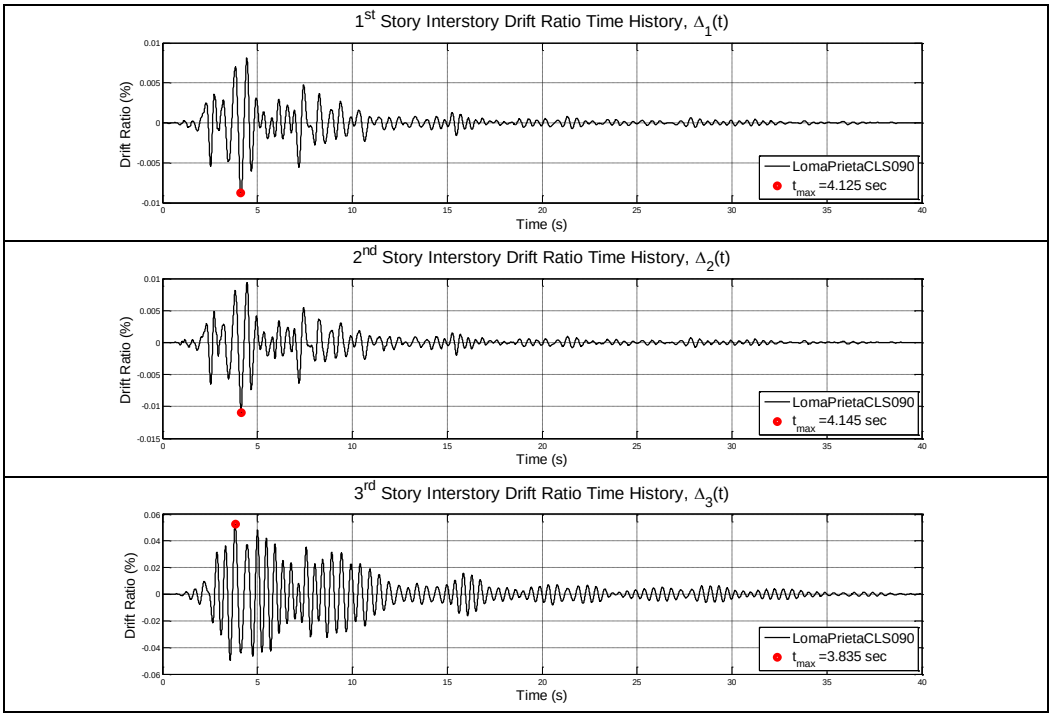

Figure 4.5: Response histories of IDR of each story of System 1 under Loma Prieta 1989 CLS090

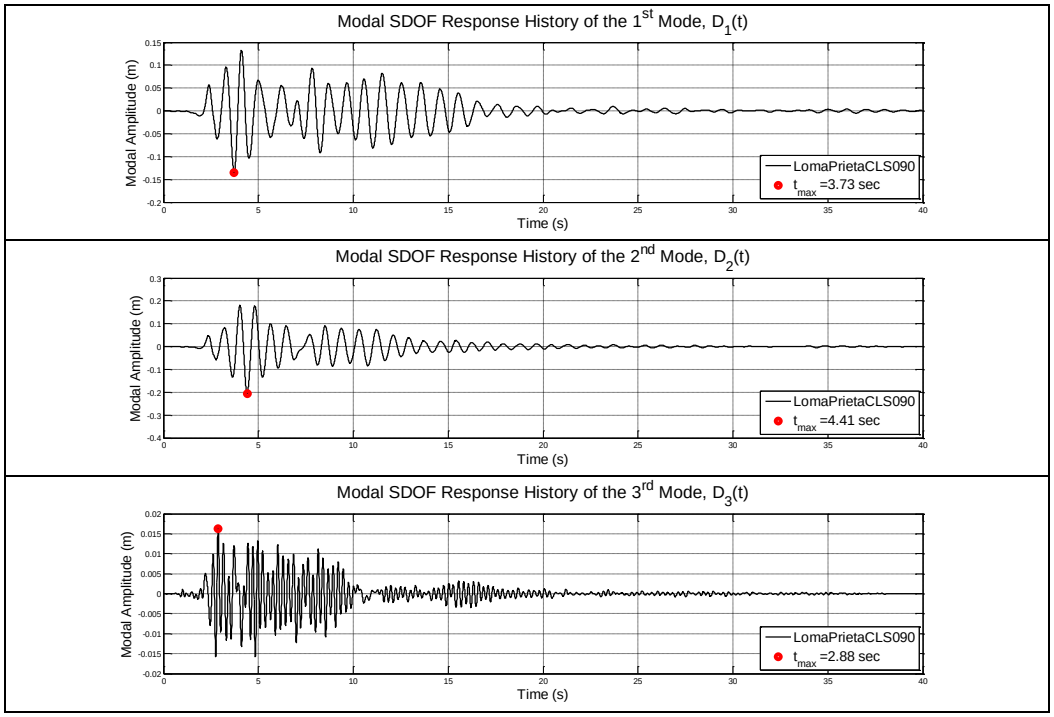

Figure 4.6: Modal SDOF response histories for each mode of System 2 under Loma Prieta 1989 CLS090

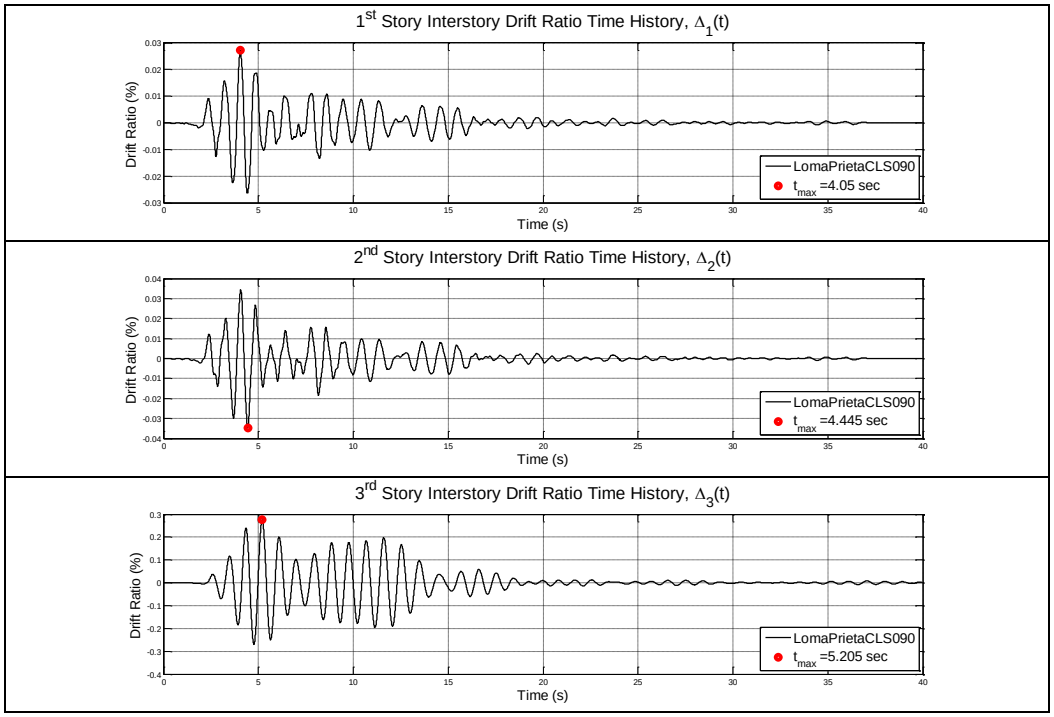

Figure 4.7: Response histories of IDR of each story of System 2 under Loma Prieta 1989 CLS090

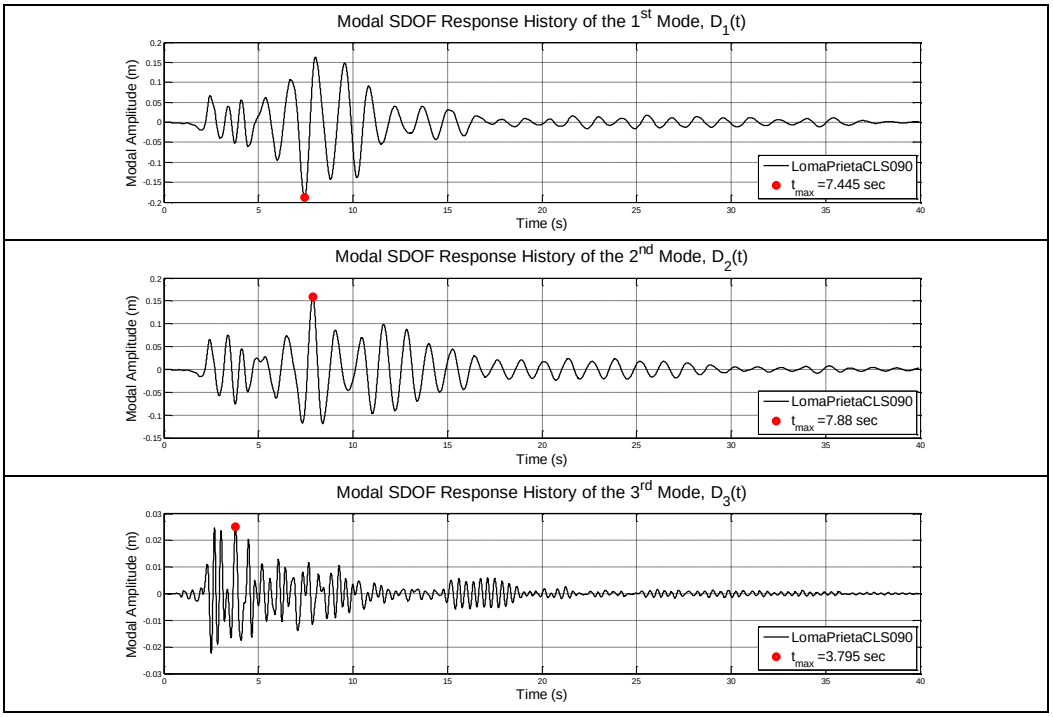

Figure 4.8: Modal SDOF response histories for each mode of System 3 under Loma Prieta 1989 CLS090

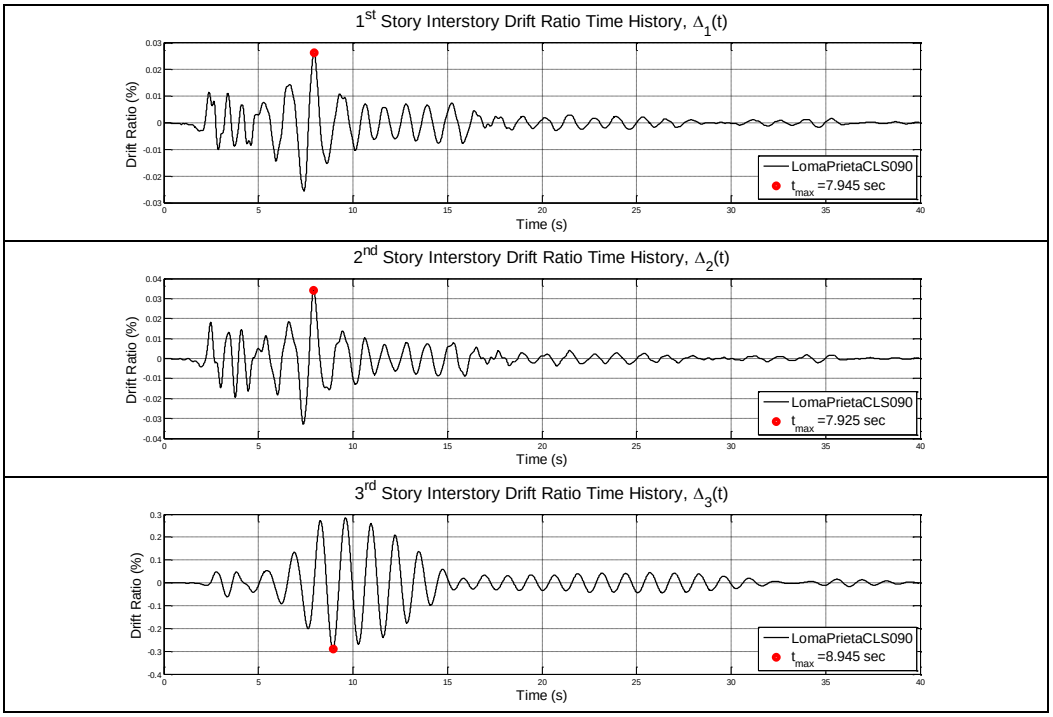

Figure 4.9: Response histories of IDR of each story of System 3 under Loma Prieta 1989 CLS090

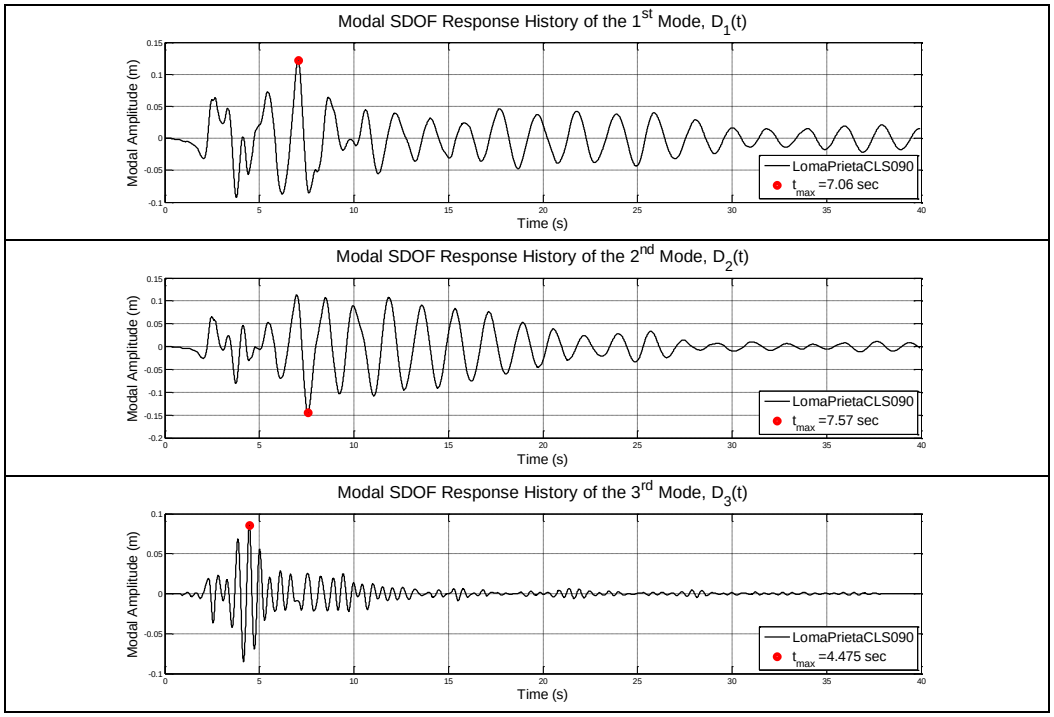

Figure 4.10: Modal SDOF response histories for each mode of System 4 under Loma Prieta 1989 CLS090

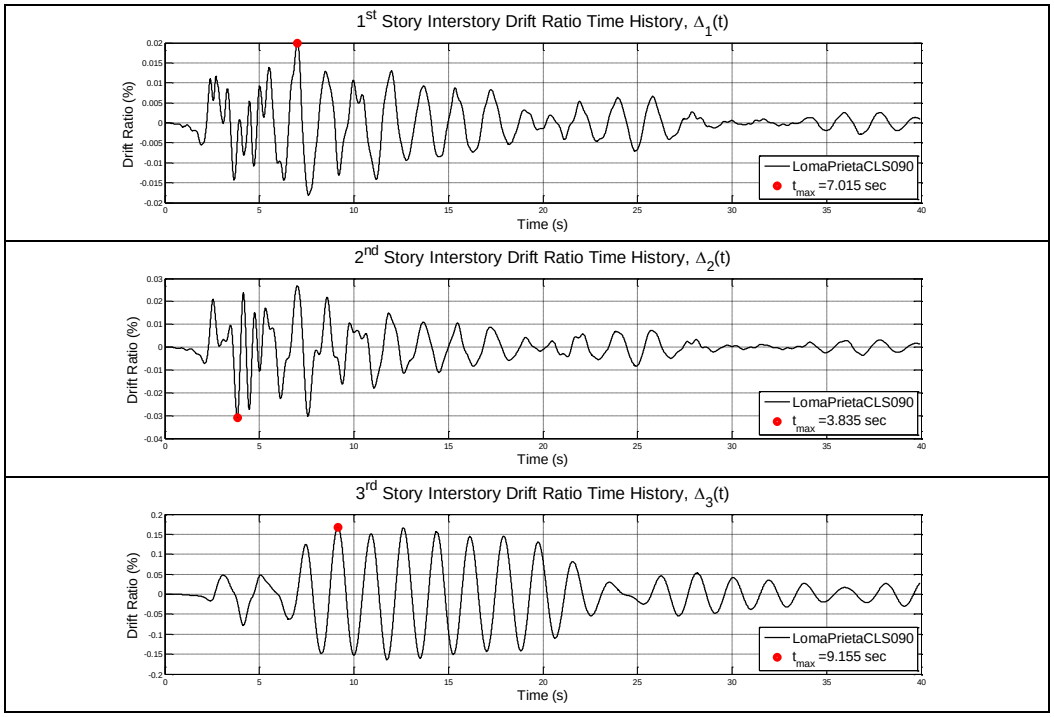

Figure 4.11: Response histories of IDR of each story of System 4 under Loma Prieta 1989 CLS090

4.2 One Story Space Frame Structure with Torsional Coupling

The second case study is a one story space frame. This simple structural system is utilized to observe the effect of torsional coupling on the response of three dimensional buildings.

The structural system which is illustrated in Figure 4.12 and Figure 4.13 is the simplest three dimensional structure that can be conceived. It is composed of four columns, four beams and a rigid slab carrying the mass of the structure, m. All mass is considered to be lumped at the center of mass (CM), which is located on the slab. The center of mass defined on this slab is also the point where the global degrees of freedom are defined. u_y and θ_z are the global degrees of freedom that are used in this case study. u_x is uncoupled from the other two since the structure is symmetric in the X direction. On the slab, there are four other nodes which connect the beams with each other and also connect them to the columns. The structural model of this frame contains two frames in the direction of analysis. The first one is the stiff edge (SE) frame, which is far from the center of mass and the second one is the flexible edge (FE) frame, which is closer to the center of mass. The global responses observed at those two frames are recorded at those four nodes. The frame-wise approach in 3D structures was described in detail in Chapter 2, Section 2.2.

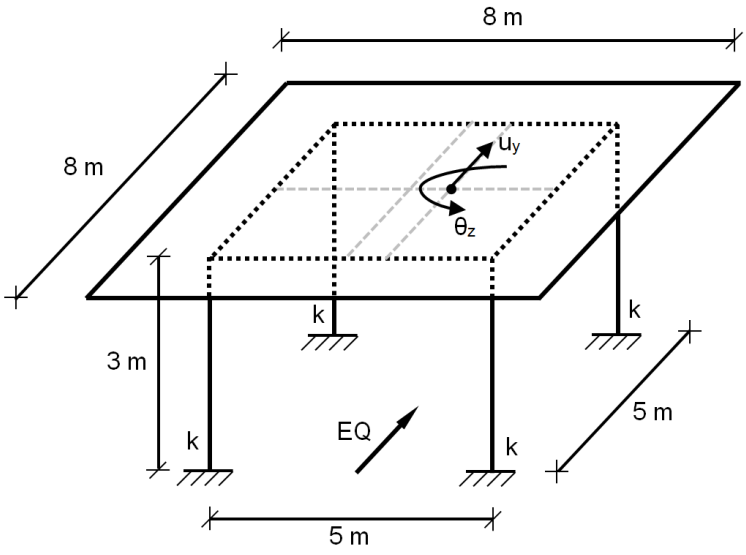

Figure 4.12: Three dimensional view of one story space frame structure

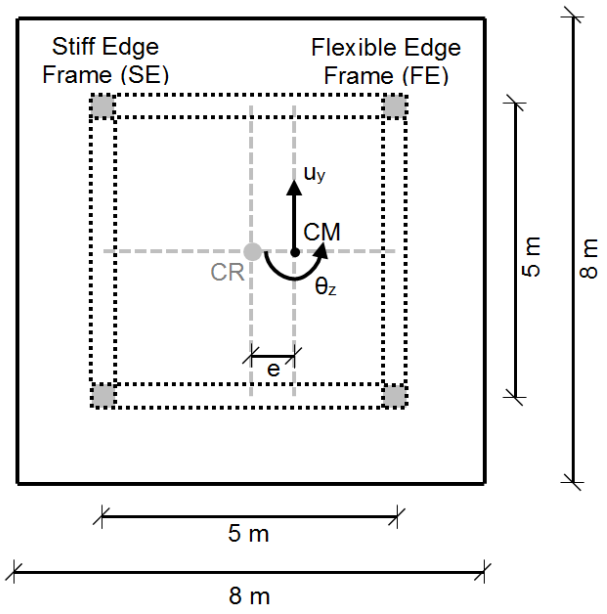

Figure 4.13: Plan view of one story space frame structure

The original structure here is designed to be symmetrical with respect to both horizontal axes, X and Y. That is, the center of mass and the center of rigidity (CR) coincide. Cross sections of columns are symmetric likewise, and stiffness coefficients are also the same. With these conditions, the structure behaves as a 2D SDOF system in the direction of ground motion. In order to observe the effect of unsymmetrical behavior in global and local coordinates, either stiffness or mass asymmetry should be created. Since shifting the center of mass is simpler, the location of mass center is changed by introducing an eccentricity ratio *e* in one direction. The eccentricity ratio *e* is defined with respect to the total length of one side of the slab. As can be seen in Figure 4.13, this eccentricity is introduced in X direction.

In the previous 2D case study, the stiffness and mass reduction at the third story was kept constant and the mass of the system was changed in order to obtain four different systems with different fundamental periods T_1. In this case study on the other hand, the stiffness and mass of the system is kept constant and the eccentricity ratio *e* is changed in order to obtain different systems that have different levels of torsional coupling. The eccentricity ratios selected for this case study are 5%, 15% and 25%. The modal properties of the three selected systems are presented in Table 4.8.

The modal properties and the modal vectors (Table 4.8a and Table 4.8b) obtained by eigenvalue analysis indicate that the first mode is the translation-dominant mode in Y direction. The second mode is pure translational mode in X direction. It is shown in Table 4.8 that the second mode participation factor and u_y and θ_z components of the

second mode vector are zero. Hence, second mode does not contribute to the total response at all under a ground motion excitation in Y direction. The third mode is a torsional dominant mode. T_1/T_3 ratios are 1.18, 1.28 and 1.42 for the eccentricity ratios of 5%, 15% and 25%, respectively.

Table 4.8: (a) Modal properties and (b) modal vectors of three systems having different eccentricity ratios

(a)

SYSTEM 1 (e = 5%)			
Mode	T_n **(s)**	Γ_n **(ton)**	M_n^* **(ton)**
1	0.497	-9.795	95.943
2	0.493	0.000	0.000
3	0.421	-2.014	4.057
SYSTEM 2 (e = 15%)			
Mode	T_n **(s)**	Γ_n **(ton)**	M_n^* **(ton)**
1	0.523	-8.957	80.223
2	0.493	0.000	0.000
3	0.409	-4.447	19.777
SYSTEM 3 (e = 25%)			
Mode	T_n **(s)**	Γ_n **(ton)**	M_n^* **(ton)**
1	0.563	-8.366	69.992
2	0.493	0.000	0.000
3	0.397	5.478	30.008

(b)

SYSTEM 1 (e = 5%)			
DOF	**Mode 1**	**Mode 2**	**Mode 3**
$\mathbf{u_x}$	0.00000	-0.10000	0.00000
$\mathbf{u_y}$	-0.09795	0.00000	-0.02014
$\boldsymbol{\theta_z}$	0.00615	0.00000	-0.02990
SYSTEM 2 (e = 15%)			
DOF	**Mode 1**	**Mode 2**	**Mode 3**
$\mathbf{u_x}$	0.00000	-0.10000	0.00000
$\mathbf{u_y}$	-0.08957	0.00000	-0.04447
$\boldsymbol{\theta_z}$	0.01327	0.00000	-0.02673
SYSTEM 3 (e = 25%)			
DOF	**Mode 1**	**Mode 2**	**Mode 3**
$\mathbf{u_x}$	0.00000	0.10000	0.00000
$\mathbf{u_y}$	-0.08366	0.00000	0.05478
$\boldsymbol{\theta_z}$	0.01566	0.00000	0.02392

The analytical model of the structural system is prepared in the OpenSees software platform. The model for this case study is designed by using only linear elastic members and material relations, similar to the first case study presented in this chapter. The requirements for defining a linear elastic member in OpenSees are defined in the previous section. The geometric and material properties of this representative model are as following:

- Length of beams and columns are 5 meters and 3 meters, respectively.
- The cross sectional areas of all members are 30x30 cm^2.
- The plan dimensions of the slab are 8x8 m^2.
- The modulus of elasticity E is defined as 22360 MPa.

- The translational mass m of the system is defined at the center of mass, as 100 tons. The rotational mass I_0 changes with the eccentricity ratio e. I_0 is 1072.92, 1122.92 and 1222.92 ton.m^2 for the eccentricity ratios of 5%, 15% and 25%, respectively. I_0 is calculated by using Equation 4.4.

$$I_0 = m\left(\frac{a^2 + b^2}{12} + e^2\right) \tag{4.4}$$

Story displacements, story shear forces and column bottom end moments are the response parameters that are recorded and observed in this case study, under the same three ground motion components. Interstory drift is the same as story displacement since this is a single story structure. For this reason only the story displacement is presented even though the principal response parameter of LMC procedure is the interstory drift ratio. t_{max} values, modal scaling coefficients, and percentage errors of CQC and LMC procedures with respect to the benchmark RHA are presented from Table 4.9 to Table 4.13. The error definition is the same as defined in the previous section.

Table 4.9: $t_{\max}$ values for three systems with different eccentricity ratios (in seconds) under three different ground excitations

GM	**Northridge**		
DOF	***System 1 (e = 5%)***	***System 2 (e = 15%)***	***System 3 (e = 25%)***
$\mathbf{u_y}$	9.480	9.500	8.340
$\mathbf{\Theta_z}$	10.040	9.800	7.960
$\mathbf{u_{S.E.}}$	9.480	9.440	8.360
$\mathbf{u_{F.E.}}$	7.900	9.520	7.940

GM	**El Centro**		
DOF	***System 1 (e = 5%)***	***System 2 (e = 15%)***	***System 3 (e = 25%)***
$\mathbf{u_y}$	6.695	5.490	5.505
$\mathbf{\Theta_z}$	6.720	6.500	6.290
$\mathbf{u_{S.E.}}$	5.480	5.495	5.505
$\mathbf{u_{F.E.}}$	6.700	6.750	5.505

GM	**Loma Prieta**		
DOF	***System 1 (e = 5%)***	***System 2 (e = 15%)***	***System 3 (e = 25%)***
$\mathbf{u_y}$	4.135	4.155	4.505
$\mathbf{\Theta_z}$	3.815	4.755	4.525
$\mathbf{u_{S.E.}}$	4.135	4.140	4.140
$\mathbf{u_{F.E.}}$	4.135	4.160	4.510

Table 4.10: Modal scaling coefficients for the three systems

(a) under Northridge 1994 ORR090

	SYSTEM 1 (e = 5%)		*SYSTEM 2 (e = 15%)*		*SYSTEM 3 (e = 25%)*	
DOF	**Mode 1**	**Mode 3**	**Mode 1**	**Mode 3**	**Mode 1**	**Mode 3**
$\mathbf{u}_{\mathbf{S.E.}}$	0.99900	0.81328	0.63148	0.84674	-0.80227	-1.00000
$\mathbf{u}_{\mathbf{F.E.}}$	1.00000	0.37752	1.00000	0.04584	0.99740	-0.21166

(b) under El Centro 1979 H-E04140

	SYSTEM 1 (e = 5%)		*SYSTEM 2 (e = 15%)*		*SYSTEM 3 (e = 25%)*	
DOF	**Mode 1**	**Mode 3**	**Mode 1**	**Mode 3**	**Mode 1**	**Mode 3**
$\mathbf{u}_{\mathbf{S.E.}}$	-0.89884	-0.59902	-0.97094	-0.60590	-1.00000	-0.64436
$\mathbf{u}_{\mathbf{F.E.}}$	0.99881	-0.21633	1.00000	-0.28497	-1.00000	-0.64436

(c) under Loma Prieta 1989 CLS090

	SYSTEM 1 (e = 5%)		*SYSTEM 2 (e = 15%)*		*SYSTEM 3 (e = 25%)*	
DOF	**Mode 1**	**Mode 3**	**Mode 1**	**Mode 3**	**Mode 1**	**Mode 3**
$\mathbf{u}_{\mathbf{S.E.}}$	-1.00000	-1.00000	-0.98011	-0.97389	-0.71738	-0.90161
$\mathbf{u}_{\mathbf{F.E.}}$	-1.00000	-1.00000	-1.00000	-0.88591	1.00000	0.39601

Table 4.11: Response results and percent errors for several response parameters under Northridge 1994 ORR090

SYSTEM 1 (e = 5%)						
Response				*Error (%)*		
Frame	**THA**	**CQC**	**LMC**	**Frame**	**CQC**	**LMC**
Story Displacement (m)				**Story Displacement**		
S.E.	0.05627	0.05123	0.05627	**S.E.**	8.96	0.00
F.E.	0.06277	0.06357	0.06277	**F.E.**	1.27	0.00
Story Shear Force (kN)				**Story Shear Force**		
S.E.	455.62	413.07	455.62	**S.E.**	9.34	0.00
F.E.	513.23	520.70	513.23	**F.E.**	1.46	0.00
Column Bottom End Moments (kN.m)				**Column Bottom End Moment**		
S.E.	416.53	378.34	416.53	**S.E.**	9.17	0.00
F.E.	467.14	473.55	467.14	**F.E.**	1.37	0.00

SYSTEM 2 (e = 15%)						
Response				*Error (%)*		
Frame	**THA**	**CQC**	**LMC**	**Frame**	**CQC**	**LMC**
Story Displacement (m)				**Story Displacement**		
S.E.	0.04649	0.04702	0.04649	**S.E.**	1.13	0.00
F.E.	0.06800	0.06795	0.06800	**F.E.**	0.08	0.00
Story Shear Force (kN)				**Story Shear Force**		
S.E.	378.75	382.09	378.75	**S.E.**	0.88	0.00
F.E.	564.01	562.74	564.01	**F.E.**	0.23	0.00
Column Bottom End Moments (kN.m)				**Column Bottom End Moment**		
S.E.	345.30	348.67	345.30	**S.E.**	0.98	0.00
F.E.	510.08	509.24	510.08	**F.E.**	0.16	0.00

SYSTEM 3 (e = 25%)						
Response				*Error (%)*		
Frame	**THA**	**CQC**	**LMC**	**Frame**	**CQC**	**LMC**
Story Displacement (m)				**Story Displacement**		
S.E.	0.05534	0.04703	0.05534	**S.E.**	15.01	0.00
F.E.	0.05845	0.06121	0.05845	**F.E.**	4.72	0.00
Story Shear Force (kN)				**Story Shear Force**		
S.E.	449.21	387.55	449.21	**S.E.**	13.72	0.00
F.E.	490.99	508.96	490.99	**F.E.**	3.66	0.00
Column Bottom End Moments (kN.m)				**Column Bottom End Moment**		
S.E.	410.21	351.44	410.20	**S.E.**	14.32	0.00
F.E.	441.53	459.73	441.53	**F.E.**	4.12	0.00

Table 4.12: Response results and percent errors for several response parameters under El Centro 1979 H-E04140

SYSTEM 1 (e = 5%)						
Response				*Error (%)*		
Frame	**THA**	**CQC**	**LMC**	**Frame**	**CQC**	**LMC**
Story Displacement (m)				**Story Displacement**		
S.E.	0.03551	0.03729	0.03551	**S.E.**	5.01	0.00
F.E.	0.04861	0.04719	0.04861	**F.E.**	2.91	0.00
Story Shear Force (kN)				**Story Shear Force**		
S.E.	286.66	300.28	286.65	**S.E.**	4.75	0.00
F.E.	399.47	386.64	399.47	**F.E.**	3.21	0.00
Column Bottom End Moments (kN.m)				**Column Bottom End Moment**		
S.E.	262.44	275.22	262.44	**S.E.**	4.87	0.00
F.E.	362.77	351.60	362.77	**F.E.**	3.08	0.00

SYSTEM 2 (e = 15%)						
Response				***Error (%)***		
Frame	**THA**	**CQC**	**LMC**	**Frame**	**CQC**	**LMC**
Story Displacement (m)				**Story Displacement**		
S.E.	0.03130	0.02997	0.03130	**S.E.**	4.25	0.00
F.E.	0.04842	0.04827	0.04842	**F.E.**	0.30	0.00
Story Shear Force (kN)				**Story Shear Force**		
S.E.	249.45	241.63	249.44	**S.E.**	3.13	0.00
F.E.	403.66	399.92	403.66	**F.E.**	0.93	0.00
Column Bottom End Moments (kN.m)				**Column Bottom End Moment**		
S.E.	229.71	221.30	229.71	**S.E.**	3.66	0.00
F.E.	364.22	361.84	364.22	**F.E.**	0.65	0.00

SYSTEM 3 (e = 25%)						
Response				***Error (%)***		
Frame	**THA**	**CQC**	**LMC**	**Frame**	**CQC**	**LMC**
Story Displacement (m)				**Story Displacement**		
S.E.	0.02939	0.03040	0.02939	**S.E.**	3.41	0.00
F.E.	0.05245	0.05000	0.05245	**F.E.**	4.67	0.00
Story Shear Force (kN)				**Story Shear Force**		
S.E.	231.59	248.24	231.59	**S.E.**	7.19	0.00
F.E.	432.99	416.44	432.99	**F.E.**	3.82	0.00
Column Bottom End Moments (kN.m)				**Column Bottom End Moment**		
S.E.	214.38	226.00	214.38	**S.E.**	5.42	0.00
F.E.	392.40	375.91	392.40	**F.E.**	4.20	0.00

Table 4.13: Response results and percent errors for several response parameters under Loma Prieta 1989 CLS090

SYSTEM 1 (e = 5%)						
Response				***Error (%)***		
Frame	**THA**	**CQC**	**LMC**	**Frame**	**CQC**	**LMC**
Story Displacement (m)				**Story Displacement**		
S.E.	0.05616	0.05135	0.05616	**S.E.**	8.57	0.00
F.E.	0.06424	0.06675	0.06424	**F.E.**	3.90	0.00
Story Shear Force (kN)				**Story Shear Force**		
S.E.	453.57	412.61	453.57	**S.E.**	9.03	0.00
F.E.	524.14	547.03	524.13	**F.E.**	4.37	0.00
Column Bottom End Moments (kN.m)				**Column Bottom End Moment**		
S.E.	415.16	378.54	415.16	**S.E.**	8.82	0.00
F.E.	477.53	497.39	477.53	**F.E.**	4.16	0.00

SYSTEM 2 (e = 15%)						
Response				***Error (%)***		
Frame	**THA**	**CQC**	**LMC**	**Frame**	**CQC**	**LMC**
Story Displacement (m)				**Story Displacement**		
S.E.	0.05253	0.04159	0.05253	**S.E.**	20.82	0.00
F.E.	0.08184	0.08210	0.08184	**F.E.**	0.32	0.00
Story Shear Force (kN)				**Story Shear Force**		
S.E.	418.05	328.56	418.05	**S.E.**	21.41	0.00
F.E.	673.89	680.70	673.88	**F.E.**	1.01	0.00
Column Bottom End Moments (kN.m)				**Column Bottom End Moment**		
S.E.	385.21	303.73	385.21	**S.E.**	21.15	0.00
F.E.	611.42	615.70	611.42	**F.E.**	0.70	0.00

SYSTEM 3 (e = 25%)						
Response				***Error (%)***		
Frame	**THA**	**CQC**	**LMC**	**Frame**	**CQC**	**LMC**
Story Displacement (m)				**Story Displacement**		
S.E.	0.03845	0.03473	0.03845	**S.E.**	9.68	0.00
F.E.	0.09810	0.09685	0.09810	**F.E.**	1.28	0.00
Story Shear Force (kN)				**Story Shear Force**		
S.E.	302.20	271.01	301.56	**S.E.**	10.32	0.21
F.E.	816.72	808.29	816.72	**F.E.**	1.03	0.00
Column Bottom End Moments (kN.m)				**Column Bottom End Moment**		
S.E.	279.98	251.81	279.73	**S.E.**	10.06	0.09
F.E.	737.40	728.98	737.40	**F.E.**	1.14	0.00

The development of the LMC procedure for both plane frame and space frame structures was presented in Chapter 2. It was stated that it is not consistent to use the modal scaling coefficients determined at the center of mass when determining the local response parameters at the associated members. The contribution of rotational motion about the global vertical axis is the resultant of translational motion with a moment arm. Therefore it was concluded to determine the modal scaling coefficients for each frame separately.

The first outcome of this second case study is that the LMC procedure yields exact results for all observed parameters as the benchmark RHA results. Since the structure has only one story, both story shear force and the column bottom end moments, and story displacement (and interstory drift ratio) concurrently reach their maximum response. This condition is not affected by torsional motion accompanying translational motion when an individual frame in the direction of motion is considered solely. The direction of analysis is Y direction, as can be seen in Figure 4.12. Total translation in Y direction is the summation of pure translation in Y direction and the Y component of torsion.

Total translational displacement in each individual frame causes internal forces and deformations. For this reason, each individual frame behaves like a SDOF system and all parameters reach maximum response at the same time.

Another finding from the presented results is that the CQC errors obtained from the stiff edge frame are always larger than those obtained from the flexible edge frame. Under El Centro ground motion, CQC errors are relatively low, which fluctuate around 5% for the SE frame. Under the other two ground motions the errors are between 10% and 20% for the SE frame. Besides, average errors for a particular system show random behavior from one ground motion to another. For instance, under Northridge ground motion, System 2 SE frame gives 1% and System 3 SE frame gives around 15% error, respectively. However under Loma Prieta ground motion, the errors at System 2 SE frame are around 20% and those on System 3 SE frame are about 10%.

CHAPTER 5

CASE STUDIES: PROTOTYPE STRUCTURES

The case studies which are employed in this chapter to test the LMC procedure are a twelve story plane frame structure and an eight story space frame structure, respectively.

5.1 Twelve Story Plane Frame Structure

5.1.1 Modeling

The first case study of this chapter, which is also the third case study of the thesis, is a twelve story symmetric-plane frame structure. The side view of this structure is shown in Figure 5.1. The analytical model of the twelve story structure is prepared by using the OpenSees software framework. Similar to the simple structures presented in the previous chapter, members having linear elastic material and geometric properties are used in the modeling of this structure. Cross sectional area A, moment of inertia I and modulus of elasticity E are the parameters that define the member properties. The geometric and material properties are listed below.

- There are three spans on the structural system. The exterior spans are 6 meters and interior span is 4 meters.
- The height of the first story is 4 meters, while that of the other stories are 3.2 meters.
- Cross section areas of the beams:
    - From 1st to 4th stories, they are 30x55 cm^2.
    - From 5th to 8th stories, they are 30x50 cm^2.
    - From 9th to 12th stories, they are 30x45 cm^2.
- Cross section areas of the columns:
    - From 1st to 4th stories, they are 50x50 cm^2.
    - From 5th to 8th stories, they are 45x45 cm^2.
    - From 9th to 12th stories, they are 40x40 cm^2.
- Modulus of elasticity is defined as 25000 MPa.

- Rigid diaphragms are introduced at each story level.
- Rayleigh damping is used for estimating the damping of structural system in response history analyses. First and third modes are fixed to 5% damping.
- Cracked section stiffness is used for each member of the structure. For beams, 40% of the gross moment of inertia is taken when calculating the cracked section stiffness. For columns, this ratio is 60%.

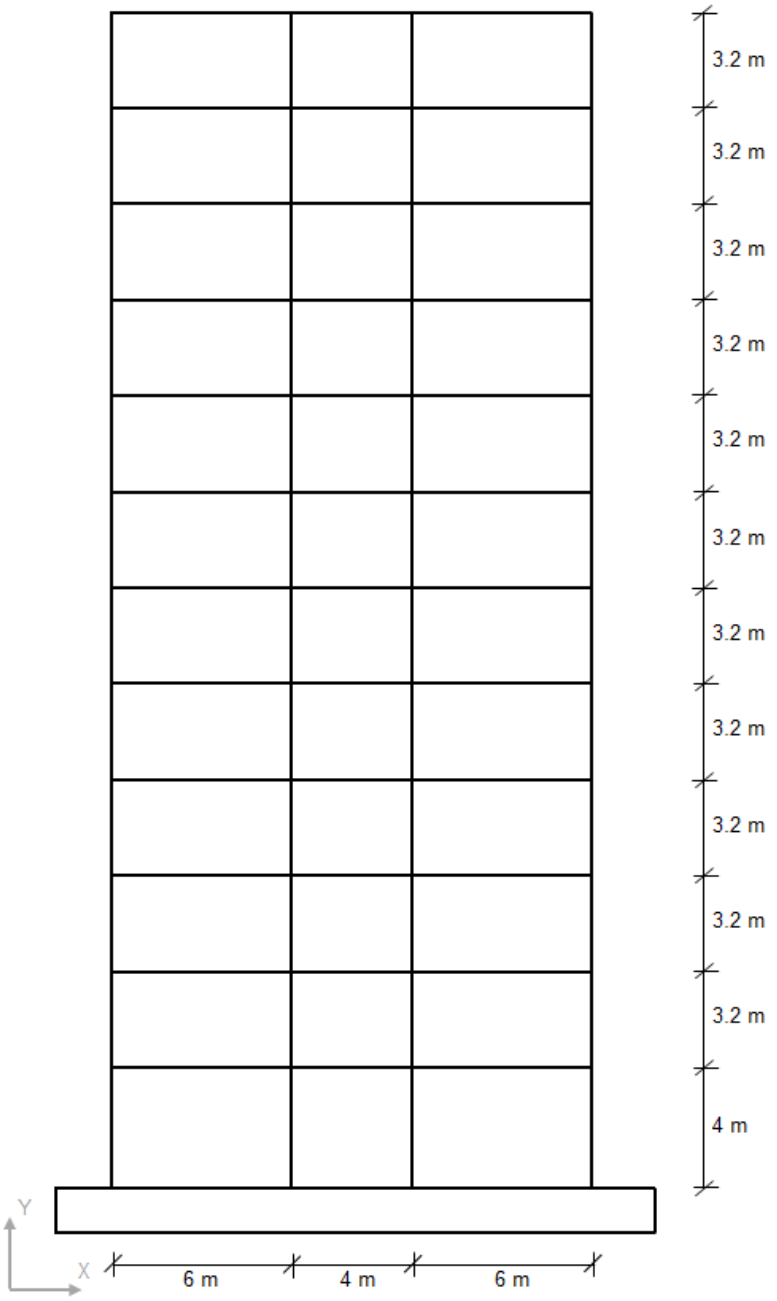

Figure 5.1: Side view of twelve story plane frame structure

5.1.2 Modal Analysis Results

The modal analysis results for the first three modes are presented in this section. The analysis is conducted on the linear elastic model with previously specified cracked section stiffnesses. Detailed information on the modal properties is given in Table 5.1. Mass-normalized modal vectors of the system are also presented in Figure 5.2.

Table 5.1: Modal properties of the twelve story plane frame structure for the first three modes

Mode *n*	**T_n (s)**	**Effective Modal Mass (ton)**	**Effective Modal Mass Ratio**
1	2,387	434,296	0,790
2	0,815	66,609	0,121
3	0,475	21,753	0,040

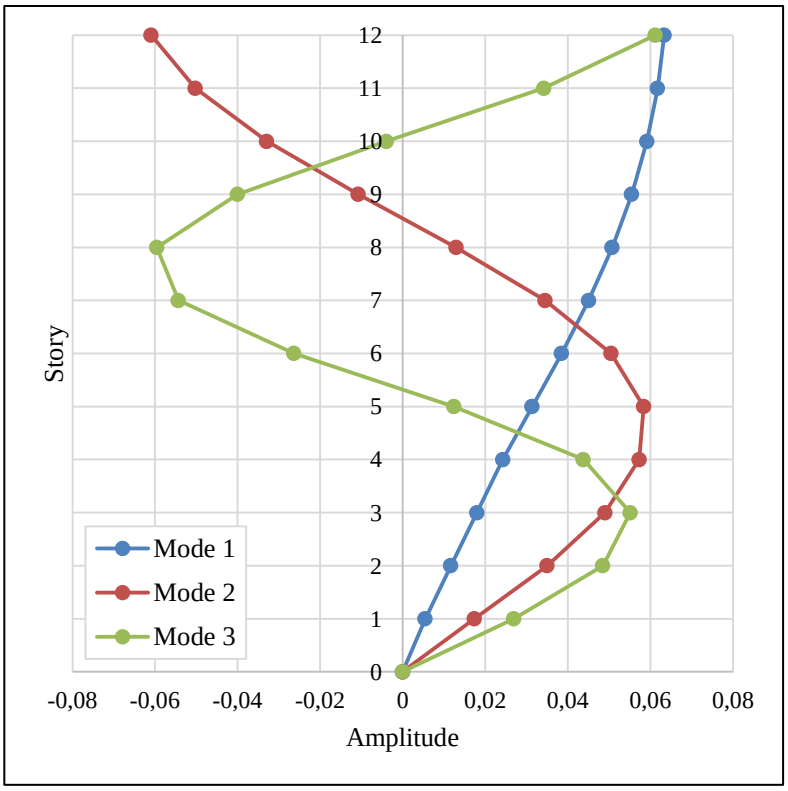

Figure 5.2: Modal vectors of the twelve story plane frame structure

5.1.3 Presentation of Results

The observed parameters in this case study are the story displacement, interstory drift ratio, mean beam end rotation, mean beam end moment and exterior and interior column end moments. The results of these parameters obtained from response history analysis (RHA), response spectrum analysis with CQC method (CQC), and linear modal combination procedure (LMC) are compared with each other. t_{max} values of each story of the twelve story plane frame structure are given in Table 5.2. The distributions of these parameters and beam end moments are presented from Figure 5.3 to Figure 5.8 for three earthquake ground motions that are introduced in Chapter 3. The percentage errors of CQC method results for those parameters and also for beam end moments are also given in Table 5.3 to Table 5.8.

The distributions of response parameters that are presented in the figures below reveal that under Northridge and El Centro ground motion components, the trend in the height-wise distributions are notably similar. Up to 5^{th} story, CQC produces very close results to the RHA, which is considered as the benchmark. However, between 5^{th} and 10^{th} stories CQC gives large errors compared to the other stories. Between 10^{th} and 12^{th} stories, the error decreases slightly. It means that for these two earthquake ground motions, higher mode effects are much more visible at the upper story levels.

The trend of response distributions is different under Loma Prieta ground motion. CQC gives very close results to the RHA between 5^{th} and 8^{th} stories. Other than those stories, the errors are larger. The largest errors are obtained at the first five stories. The reason of this different behavior could be the participation of the third mode along with the second mode.

Since CQC method combines the modal responses implicitly with a statistical approach, the errors grow large when the modes other than the first mode participate in the total response. Nevertheless, the LMC procedure scales the modal responses and directly combines them without removing their directional information. Therefore, LMC procedure either yields exact results or gives negligible errors. The numerical values of all those mentioned CQC errors can be observed from the CQC error tables below.

When t_{max} values given in Table 5.2 are observed, it is observed that the maximum IDR occurrence times of each story are grouped into three different time interval. This is notably apparent for Northridge and Loma Prieta ground motion components. For Northridge ground motion, the three groups are from the 1^{st} to 5^{th} stories, from 6^{th} to 9^{th} stories, and from 10^{th} to 12^{th} stories. For Loma Prieta ground motion they are from 1 to 5^{th} stories, 6^{th} story, and from 7 to 12^{th} stories. The regions of those story groups are compatible with the regions that CQC method produces different error levels.

Table 5.2: t_{max} values of the twelve story plane frame under three different ground motions

Story	Northridge 1994 ORR090	El Centro 1979 H-E04140	Loma Prieta 1989 CLS090
1	9,300	8,180	4,355
2	9,300	8,185	4,370
3	9,340	7,000	4,390
4	9,400	7,020	4,415
5	9,460	7,170	4,455
6	8,420	7,255	3,880
7	8,460	7,275	4,780
8	8,480	7,280	4,735
9	8,480	7,280	4,730
10	9,680	7,270	4,740
11	9,700	7,250	4,755
12	9,700	7,235	4,760

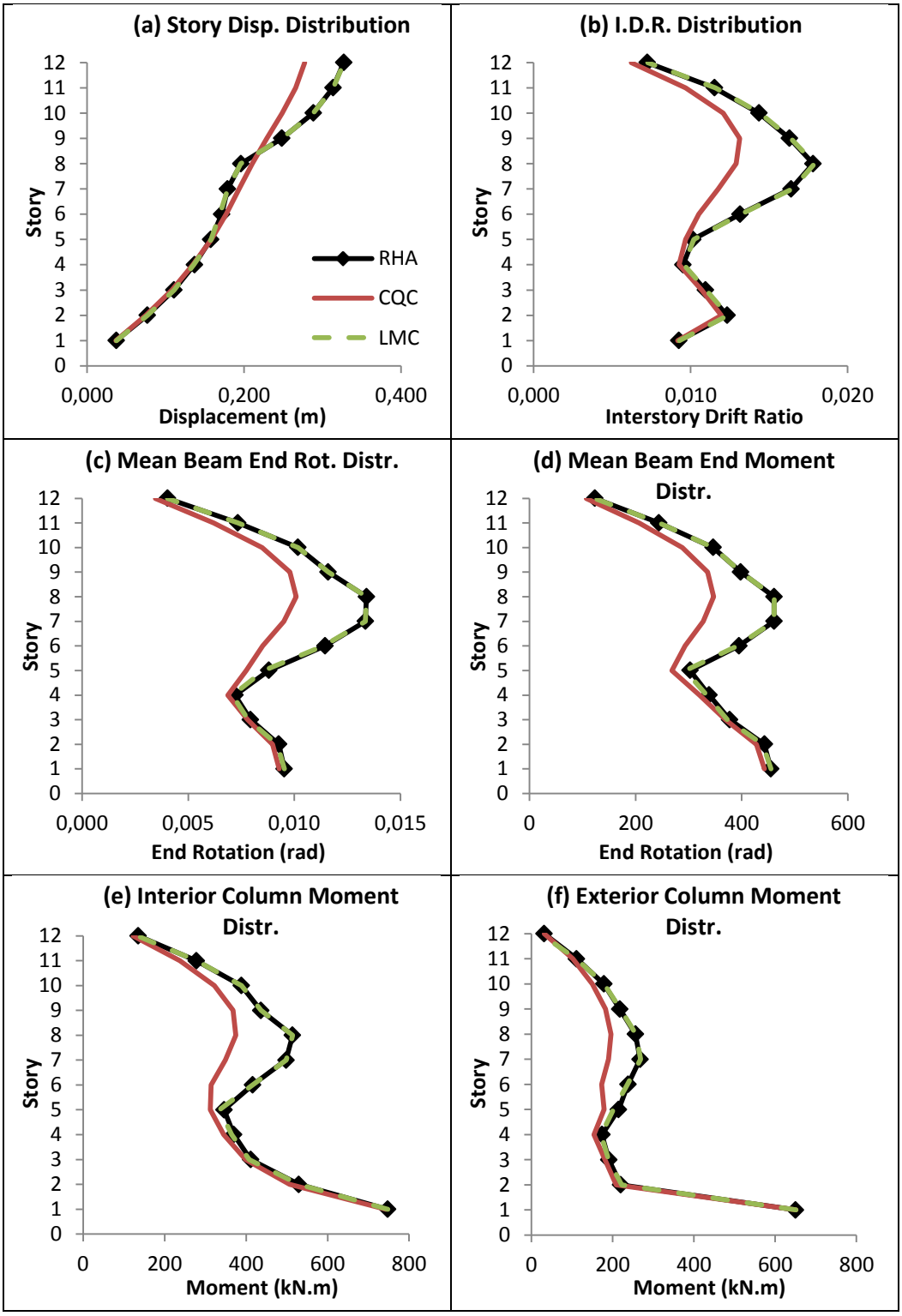

Figure 5.3: Distributions of several response parameters under Northridge 1994 ORR090 (a) Story displacement (b) Interstory drift ratio (c) Mean beam end rotation (d) Mean beam end moment (e) Interior column bottom end moment (f) Exterior column bottom end moment

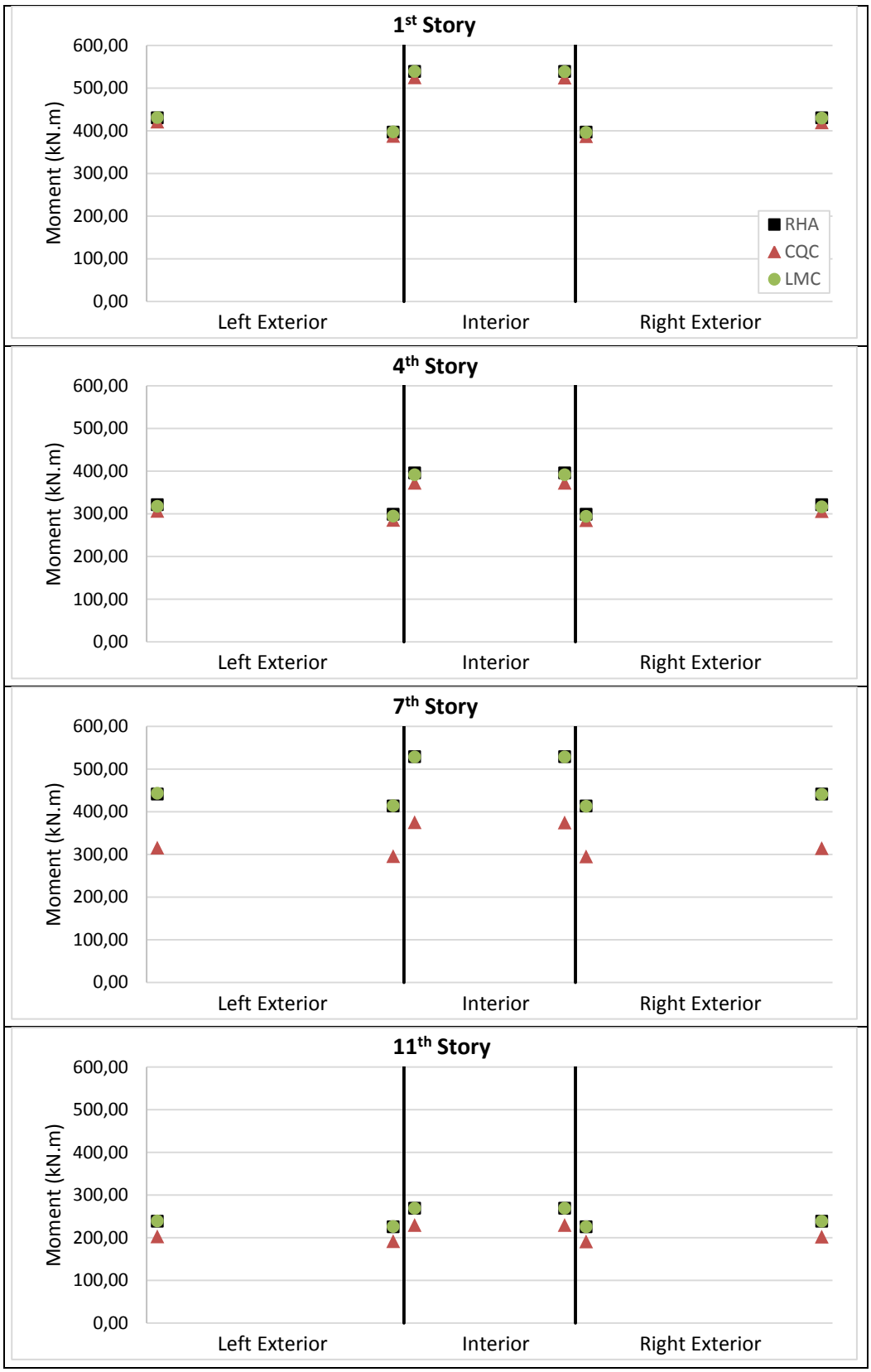

Figure 5.4: Beam end moments at particular stories under Northridge 1994 ORR090

Table 5.3: CQC errors (%) for several response parameters under Northridge 1994 ORR090

CQC Errors (%)					
Story	**Interstory Drift Ratio**	**Story Shear Force**	**Mean Beam End Rotation**	**Interior Column Moment**	**Exterior Column Moment**
1	0,90	0,39	2,55	0,53	0,16
2	2,98	4,50	3,20	4,27	5,13
3	2,13	3,27	1,74	3,01	4,96
4	2,72	4,42	4,62	6,79	11,40
5	4,68	8,35	12,04	9,78	16,56
6	19,99	20,93	25,64	24,57	27,25
7	28,25	29,72	28,80	29,92	29,02
8	27,56	29,38	24,76	27,03	23,53
9	19,53	20,51	15,59	15,65	16,28
10	15,88	16,65	16,62	16,96	15,87
11	15,97	15,74	15,64	14,53	8,56
12	14,15	11,71	14,25	9,24	0,68

Table 5.4: CQC errors (%) for beam end moments under Northridge 1994 ORR090

CQC Errors (%) for Beam End Moments						
Beam	**Left Exterior**		**Interior**		**Right Exterior**	
End	**i**	**j**	**i**	**j**	**i**	**j**
Story 1	2,31	2,45	2,79	2,83	2,69	2,67
Story 2	3,12	3,17	3,63	3,66	3,35	3,39
Story 3	1,74	1,77	2,65	2,68	1,95	2,01
Story 4	4,78	4,72	6,16	6,18	4,91	5,05
Story 5	11,65	11,76	10,56	10,58	11,91	11,88
Story 6	25,52	25,58	25,78	25,81	25,73	25,76
Story 7	28,75	28,78	29,28	29,31	28,95	29,01
Story 8	24,60	24,68	24,80	24,83	24,88	24,90
Story 9	15,42	15,52	15,89	15,93	15,74	15,77
Story 10	16,42	16,54	16,92	16,97	16,80	16,82
Story 11	15,27	15,48	15,07	15,14	15,79	15,76
Story 12	13,62	14,05	12,06	12,14	14,36	14,14

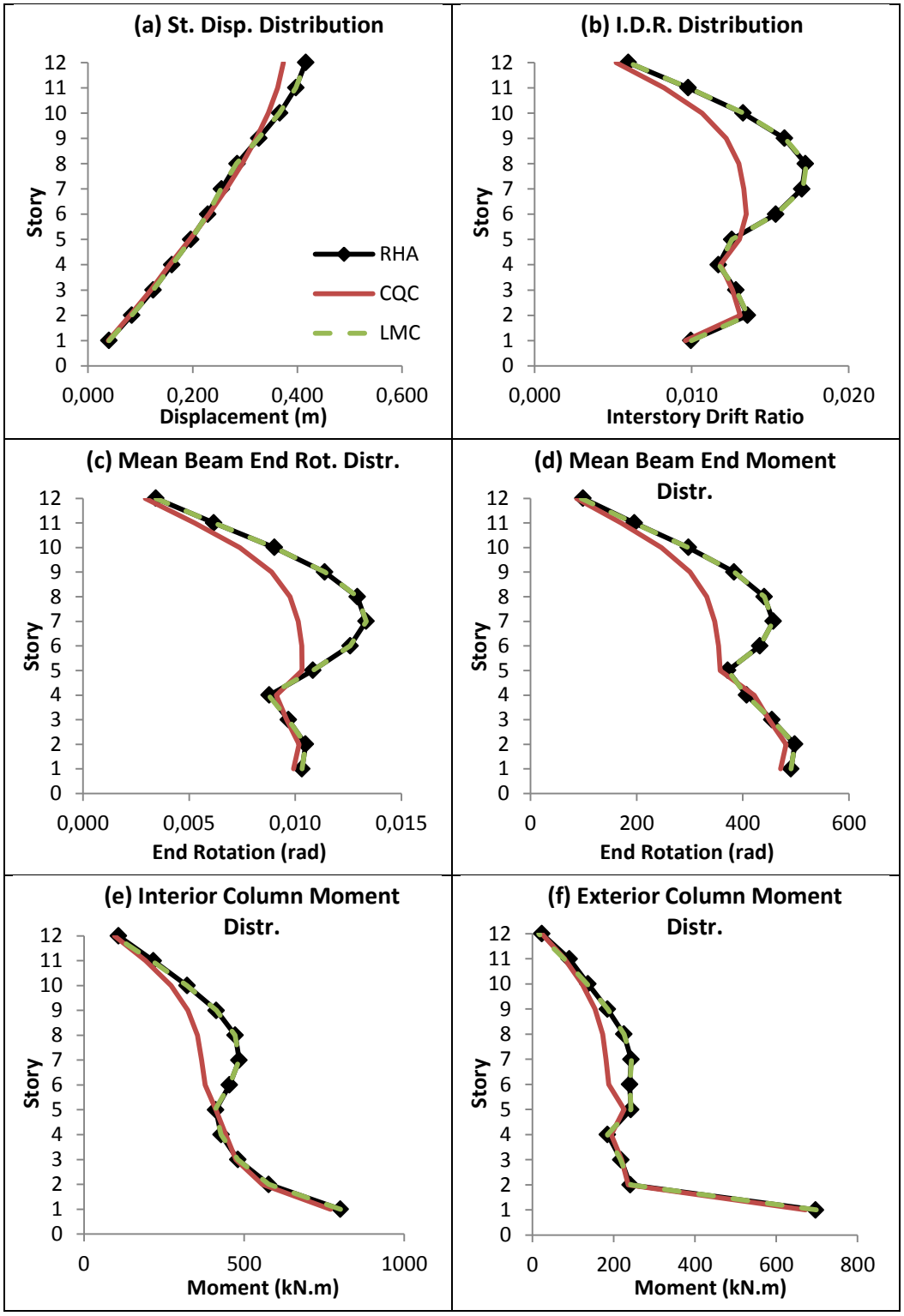

Figure 5.5: Distributions of several response parameters under El Centro 1979 H-E04140 (a) Story displacement (b) Interstory drift ratio (c) Mean beam end rotation (d) Mean beam end moment (e) Interior column bottom end moment (f) Exterior column bottom end moment

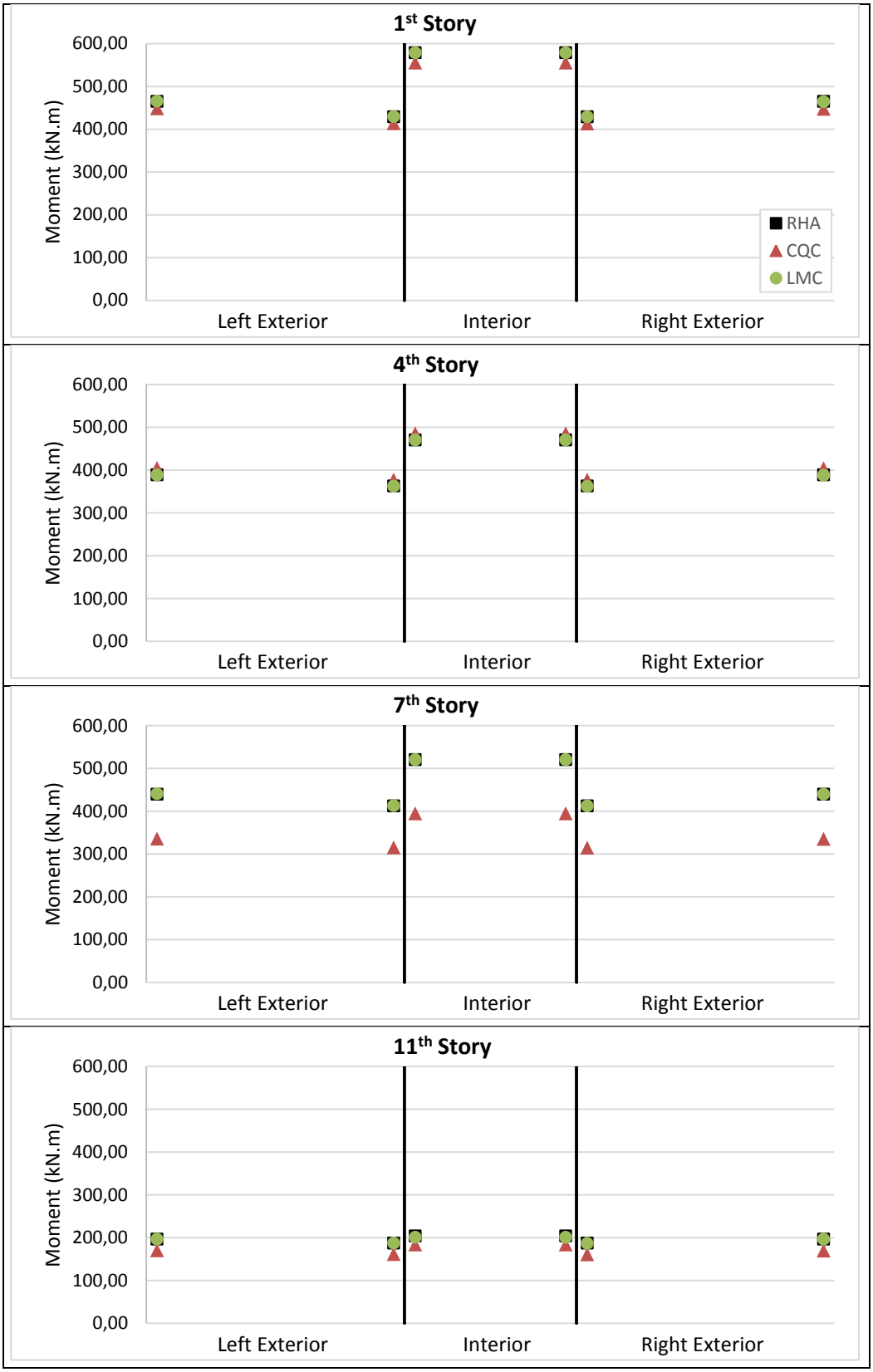

Figure 5.6: Beam end moments at particular stories under El Centro 1979 H-E04140

Table 5.5: CQC errors (%) for several response parameters under El Centro 1979 H-E04140

CQC Errors (%)					
Story	**Interstory Drift Ratio**	**Story Shear Force**	**Mean Beam End Rotation**	**Interior Column Moment**	**Exterior Column Moment**
1	3,64	3,64	3,81	3,82	3,50
2	3,48	3,71	2,90	3,49	2,01
3	1,74	2,11	0,85	1,29	0,74
4	1,03	0,81	3,80	3,32	4,74
5	3,79	5,36	4,67	0,01	6,96
6	12,27	12,09	18,14	16,76	21,45
7	21,77	22,57	23,97	24,25	25,35
8	24,64	25,26	24,52	24,99	23,20
9	23,30	22,97	21,93	21,41	16,75
10	19,67	17,95	18,15	15,60	10,85
11	15,69	12,34	14,93	11,41	13,05
12	12,99	12,22	14,53	11,61	0,99

Table 5.6: CQC errors (%) for beam end moments under El Centro 1979 H-E04140

CQC Errors (%) for Beam End Moments						
Beam	**Left Exterior**		**Interior**		**Right Exterior**	
End	**i**	**j**	**i**	**j**	**i**	**j**
Story 1	3,75	3,80	4,22	4,24	3,93	3,95
Story 2	2,94	2,95	3,75	3,77	3,05	3,09
Story 3	0,89	0,89	1,56	1,57	0,98	1,02
Story 4	3,80	3,79	3,08	3,06	3,70	3,68
Story 5	4,29	4,43	3,09	3,11	4,50	4,41
Story 6	18,03	18,06	18,03	18,04	18,14	18,15
Story 7	23,94	23,96	24,36	24,38	24,06	24,09
Story 8	24,43	24,49	24,72	24,75	24,61	24,62
Story 9	21,68	21,80	21,30	21,33	21,95	21,90
Story 10	17,57	17,83	15,81	15,85	18,03	17,87
Story 11	13,93	14,31	10,19	10,25	14,54	14,30
Story 12	12,31	13,54	9,81	9,89	13,75	12,67

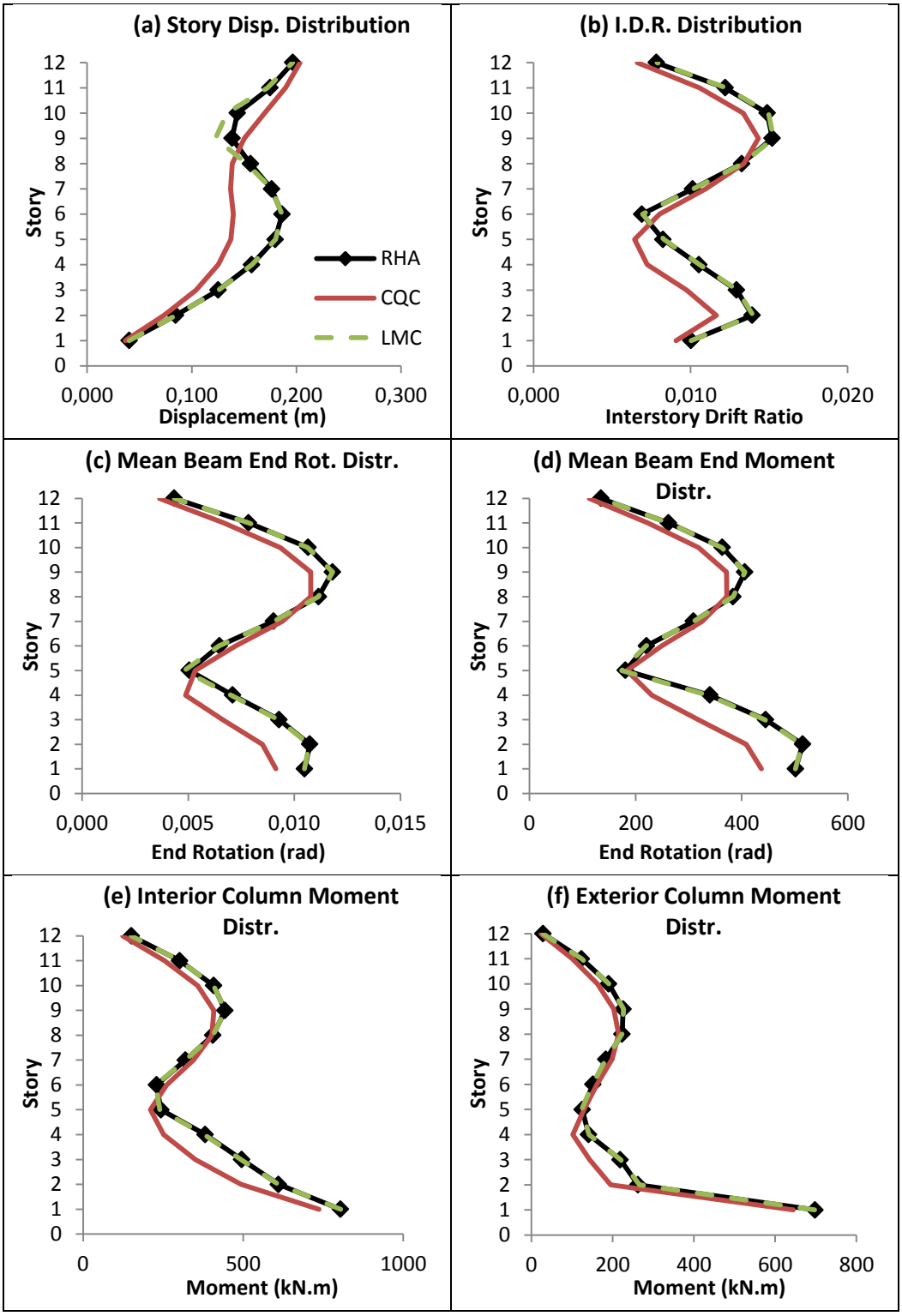

Figure 5.7: Distributions of several response parameters under Loma Prieta 1989 CLS090 (a) Story displacement (b) Interstory drift ratio (c) Mean beam end rotation (d) Mean beam end moment (e) Interior column bottom end moment (f) Exterior column bottom end moment

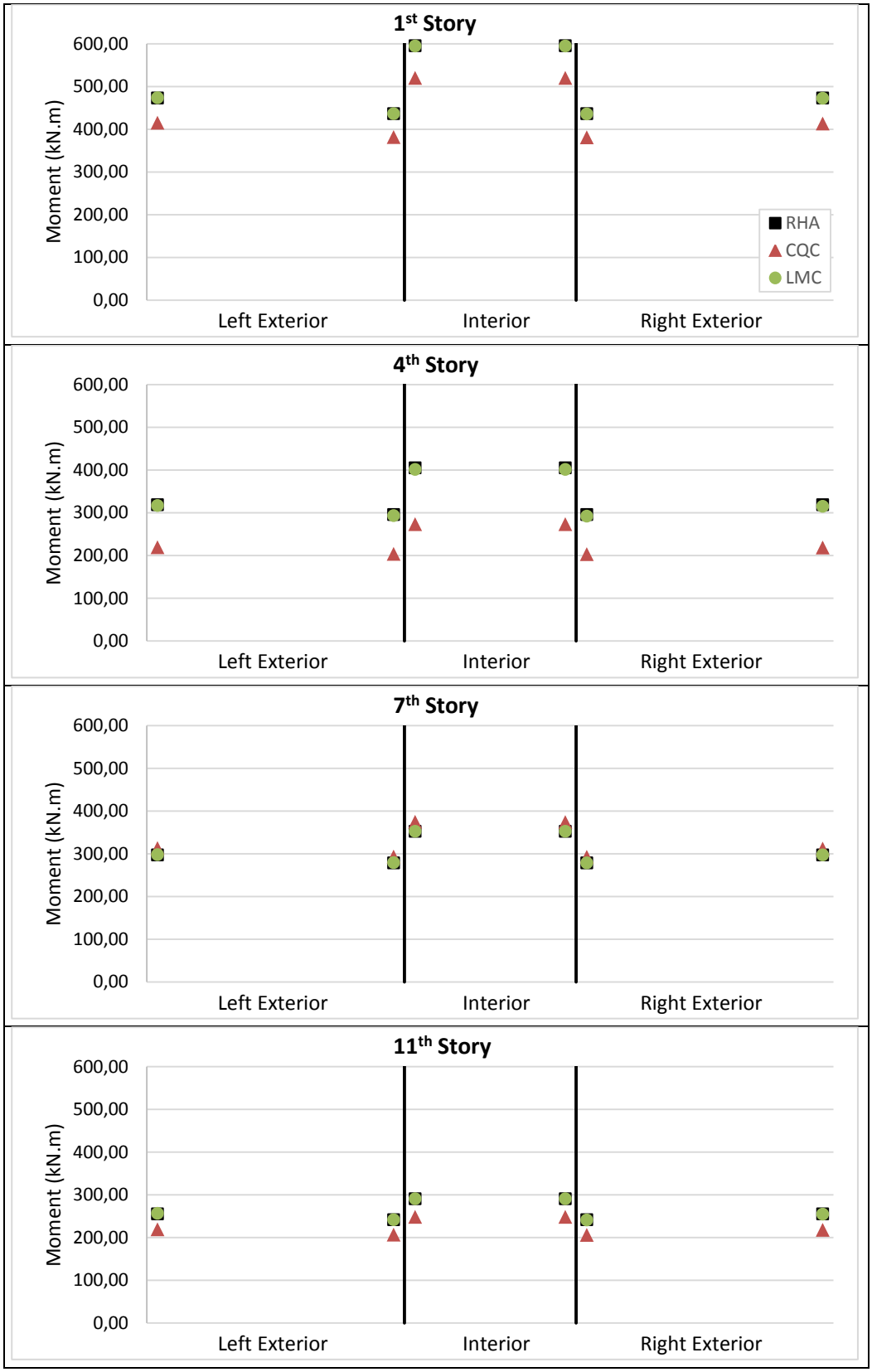

Figure 5.8: Beam end moments at particular stories under Loma Prieta 1989 CLS090

Table 5.7: CQC errors (%) for several response parameters under Loma Prieta 1989 CLS090

CQC Errors (%)					
Story	**Interstory Drift Ratio**	**Story Shear Force**	**Mean Beam End Rotation**	**Interior Column Moment**	**Exterior Column Moment**
1	9,54	6,53	12,98	8,37	7,66
2	16,45	16,53	20,80	19,29	25,75
3	24,58	25,64	28,66	29,14	34,48
4	31,25	33,08	31,37	34,09	27,87
5	22,14	27,08	5,28	13,68	3,85
6	16,37	13,05	12,00	13,65	6,21
7	8,14	9,32	4,55	7,95	8,27
8	1,00	2,22	3,31	0,91	3,65
9	5,87	6,45	8,67	7,98	10,19
10	10,24	11,19	12,36	12,32	14,56
11	13,44	14,98	14,98	15,83	18,36
12	15,48	17,16	16,08	17,54	17,64

Table 5.8: CQC errors (%) for beam end moments under Loma Prieta 1989 CLS090

CQC Errors (%) for Beam End Moments						
Beam	**Left Exterior**		**Interior**		**Right Exterior**	
End	**i**	**j**	**i**	**j**	**i**	**j**
Story 1	12,58	12,83	12,83	12,86	13,08	12,94
Story 2	20,59	20,66	20,35	20,38	20,86	20,88
Story 3	28,47	28,57	28,45	28,47	28,72	28,70
Story 4	31,57	31,50	32,81	32,84	31,65	31,79
Story 5	3,92	4,35	2,03	2,07	4,15	3,62
Story 6	12,67	12,42	13,99	13,94	12,13	12,22
Story 7	5,14	4,86	5,95	5,90	4,58	4,71
Story 8	2,91	3,10	2,64	2,69	3,36	3,32
Story 9	8,36	8,51	8,35	8,39	8,76	8,75
Story 10	12,09	12,22	12,21	12,26	12,48	12,49
Story 11	14,75	14,87	14,97	15,02	15,11	15,12
Story 12	16,01	16,07	16,07	16,12	16,23	16,30

5.2 Eight Story Space Frame Structure

5.2.1 Modeling

The last case study of this thesis is carried out on an eight story space frame structure with torsional coupling. The plan view and side view of the structure are shown in Figure 5.9 and Figure 5.10, respectively. The analytical model of the structure is prepared by the OpenSees software framework. The geometric and material properties are listed below.

- The structure is composed of three spans in both lateral directions. In X direction, all three spans are 8 meters. In Y direction, on the other hand, the exterior spans are 6 meters and interior span is 4 meters.
- Except the first story, the story height is uniform. The height of the first story is 3.5 meters while that of the other stories are 3 meters.
- Cross sectional area of all beams are 30x55 cm^2.
- Cross sectional area of columns are 50x50 cm^2 throughout the height of structure.
- Modulus of elasticity is defined as 25000 MPa.
- Rigid diaphragms are introduced at each story level.
- Rayleigh damping is used for estimating the damping of structural system in response history analyses. First and third modes are fixed to 5% damping.
- Cracked section stiffness is used for each member of the structure. The ratio of cracking for beams and columns are 50% and 60%, respectively.

When a three dimensional frame structure which has uniform beams and columns in their geometry and material is symmetrical with respect to both principal lateral directions, the response of the structure to the ground excitation would only be in the direction of the analysis, as remarked before in Chapter 2. In other words, when the center of mass and the center of rigidity coincide, identical responses would be obtained from all individual frames in the direction of analysis. Only one planar frame would be sufficient for further investigation of the structure under a ground excitation in one direction. Therefore, there is no need to construct a three dimensional model if the structure is completely symmetric and the response in the orthogonal direction does not affect the response in the direction of motion.

In this case study, it is aimed to represent the response of an unsymmetrical plan structure to seismic forces. In practice when the structure is not symmetric, there is an eccentricity between the center of mass and the center of rigidity for a particular story, resulting in lateral-torsional coupling. In order to investigate the effect of torsional coupling on the response history and LMC procedure, the center of mass is shifted in X direction from the center of rigidity by introducing an eccentricity of 15% of the total floor width, as can be observed in Figure 5.9.

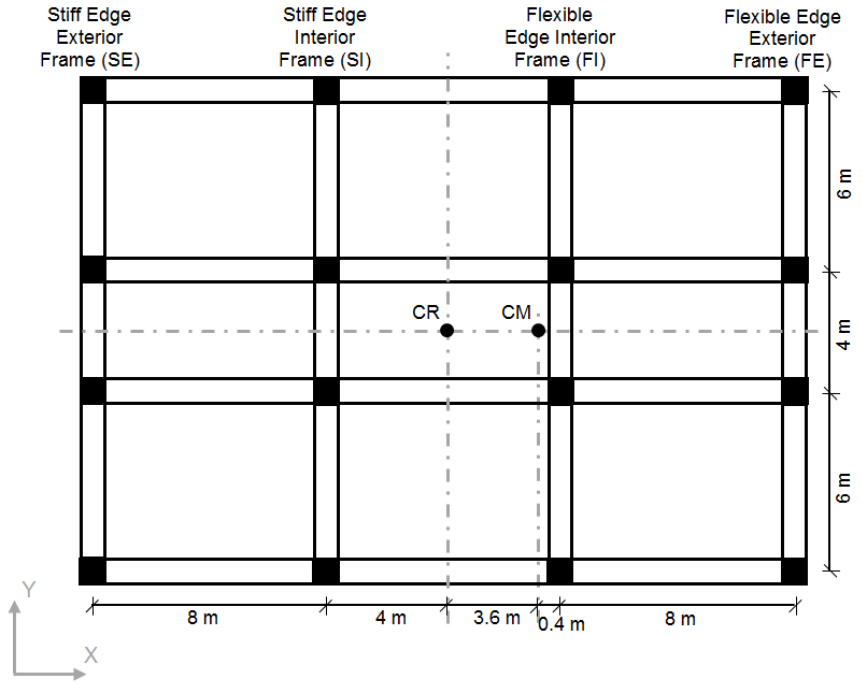

Figure 5.9: Plan view of eight story space frame of structure with torsional coupling

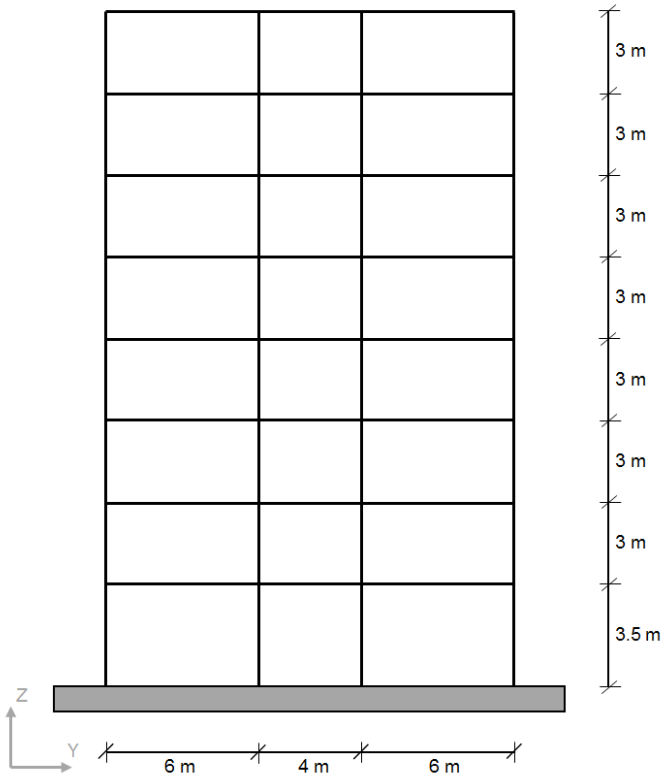

Figure 5.10: Side view of eight story space frame structure in the direction of analysis

5.2.2 Modal Analysis Results

In this section, modal analysis results for the first nine modes in X and Y directions, and about Z direction are given. The presented results are obtained under the eigenvalue analysis that is performed on the linear elastic model with cracked section stiffnesses. Detailed information on the modal properties are given in Table 5.9. The first column of the table represents the mode number along with the primary direction of the mode. For instance, 1-X represents the first mode in X direction whereas 1-Y and 1-θ stand for the first modes in Y direction and about Z axis, respectively. The second column includes corresponding periods of each mode. Other columns indicate the effective modal masses and their ratios in both X and Y directions. As can be seen in the table in Y direction, the effective modal masses of X-direction dominant modes are zero. Likewise in X direction, the effective modal masses of the coupling modes in Y direction and about Z direction are zero. This behavior is due to the one-way eccentricity in X direction. The modes in X direction do not participate in the response during a ground excitation which is applied only in Y direction.

Table 5.9: Modal properties of the eight story space frame structure for the first three modes in the principal global directions

Modes	T_n **(s)**	**X Direction**		**Y Direction**	
		Effective Modal Mass (ton)	**Effective Modal Mass Ratio**	**Effective Modal Mass (ton)**	**Effective Modal Mass Ratio**
1-X	1.674	1567.20	0.822	0	0
1-Y	1.644	0	0	1217.72	0.639
1-θ	1.108	0	0	366.38	0.192
2-X	0.530	190.18	0.10	0	0
2-Y	0.528	0	0	144.70	0.076
2-θ	0.356	0	0	43.88	0.023
3-Y	0.296	0	0	52.14	0.027
3-X	0.292	73.66	0.039	0	0
3-θ	0.199	0	0	18.34	0.009

5.2.3 Presentation of Results

The comparative analysis results of response history analysis (RHA), response spectrum analysis with CQC method (CQC) and linear modal combination procedure (LMC) are presented in this section. Interstory drift ratio, story shear force, mean beam chord rotations, column end moments and beam end moments are recorded during the analyses performed under three ground motions that are introduced in Chapter 3. t_{max} values of each individual frame under all three ground motion components are shown in Table 5.10. Height-wise distributions of observed parameters are presented from Figure 5.11 to Figure 5.25. The percentage errors of CQC method for those parameters and also for beam end moments are presented in Table 5.11 to Table 5.16.

LMC procedure either yields exact results or exhibit minor errors. During the analysis of this case study, each frame is considered individually and the maximum response of each mode is scaled with the modal scaling coefficients representing each individual frame. Since the errors are very small, as can be seen from the distribution graphs, it is not necessary to present LMC procedure errors.

The response distributions of observed parameters and the percentage error tables indicate that the response of the eight story space frame shows variations with changing earthquake ground motion. For a single earthquake ground motion, the trend of parameter distributions is similar according to the errors that CQC method produces.

For Northridge ground motion component, the smallest errors are obtained from SE frame, while FE frame produces the largest errors. CQC method underestimates the RHA results at the upper stories of all frames. At lower stories, this behavior is a bit different. CQC method starts to overestimate the exact result in the flexible edge region of the structure. The numerical values of the CQC errors also show that at mid-level stories (4^{th} to 7^{th} story), the errors are generally around 25%, which can be considered high.

The CQC method generally gives better results for every parameter under El Centro ground motion. However, under this ground motion, the smallest errors are observed at FE frame, as opposed to the case under Northridge ground motion. The error variation throughout the height is also different. The errors are the highest at two stories, which are between 20 and 30%.

The structure show different behavior under Loma Prieta ground motion. CQC method, in this case, produces a high level of error at the 1^{st} and 2^{nd} stories. Except SE frame, the errors of all parameters at the first story are between 32 and 40%. The errors at the upper level stories at the highest level at the SI frame in this case.

Table 5.10 presents the t_{max} values of each frame separately under all three earthquake ground motions. An investigation of t_{max} values concludes that for all ground motions, the maximum occurrence times of IDR of each story at all individual frames are generally grouped into three different time interval, similar to the previous case study, twelve

story plane frame structure. Some exceptions of this grouping is the SE frame, which shows two different time groups under El Centro and Loma Prieta ground motions.

Table 5.10: t_{max} values of each frame of eight story space frame under three different ground motions

GM	Northridge				
Story	**SE**	**SI**	**FI**	**FE**	**CM**
1	8,700	8,72	11,5	10,42	11,5
2	8,700	8,74	12,18	10,46	12,16
3	8,720	8,24	12,2	9,78	12,2
4	8,760	12,18	12,22	9,8	12,22
5	8,560	12,18	9,8	9,8	9,8
6	8,54	12,2	9,78	9,8	9,78
7	8,54	12,2	9,78	9,78	9,78
8	8,86	12,2	9,78	9,78	9,78

GM	El Centro				
Story	**SE**	**SI**	**FI**	**FE**	**CM**
1	6,320	7,53	7,515	7,51	7,52
2	6,310	7,55	7,54	7,535	7,54
3	6,290	7,57	7,565	7,56	7,565
4	6,245	7,59	7,59	7,59	7,59
5	6,235	5,705	7,635	7,645	7,635
6	6,235	5,715	5,755	5,775	5,755
7	6,24	5,72	5,75	5,765	5,75
8	6,245	5,725	5,75	5,76	5,745

GM	Loma Prieta				
Story	**SE**	**SI**	**FI**	**FE**	**CM**
1	8,280	9,905	9,18	9,16	9,18
2	8,285	9,9	7,49	7,57	7,485
3	8,290	3,77	7,51	7,57	7,505
4	3,780	3,79	7,53	7,575	7,525
5	3,775	3,8	7,55	7,57	7,545
6	3,76	4,16	4,165	7,57	4,165
7	3,745	4,16	4,15	4,15	4,155
8	3,74	4,16	4,145	4,14	4,145

SE: Stiff Edge Interior Frame FI: Flexible Edge Interior Frame
SI: Stiff Edge Interior Frame FE: Flexible Edge Exterior Frame
CM: Center of Mass

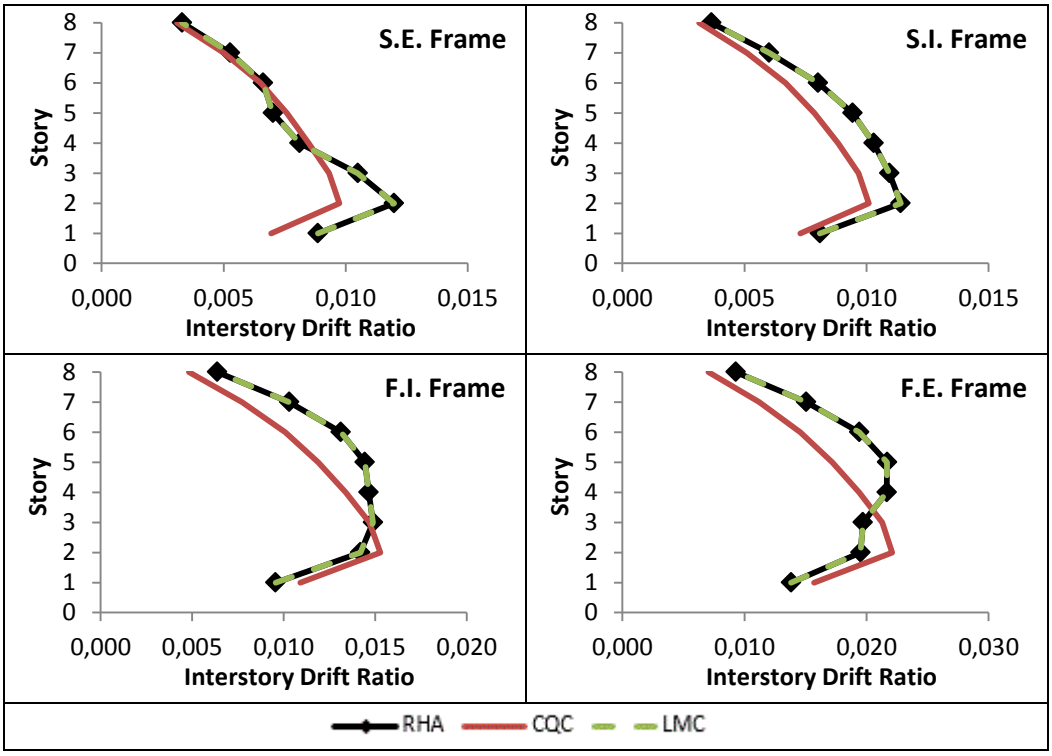

Figure 5.11: Interstory drift ratio distributions under Northridge 1994 ORR090

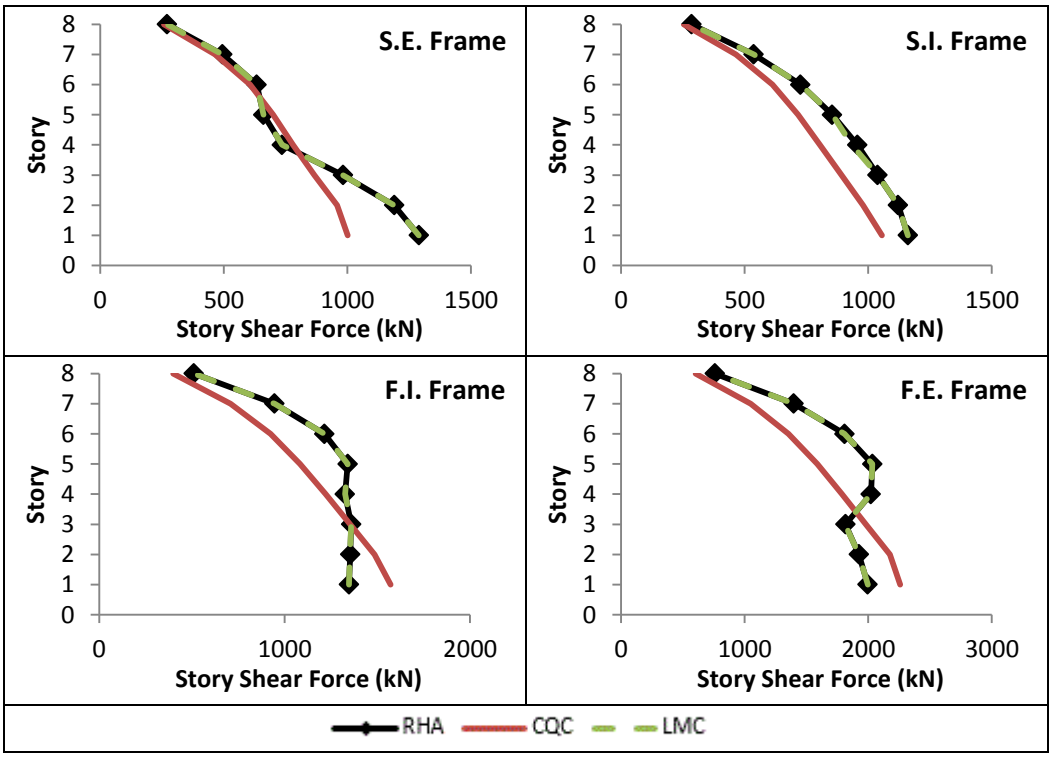

Figure 5.12: Story shear force distributions under Northridge 1994 ORR090

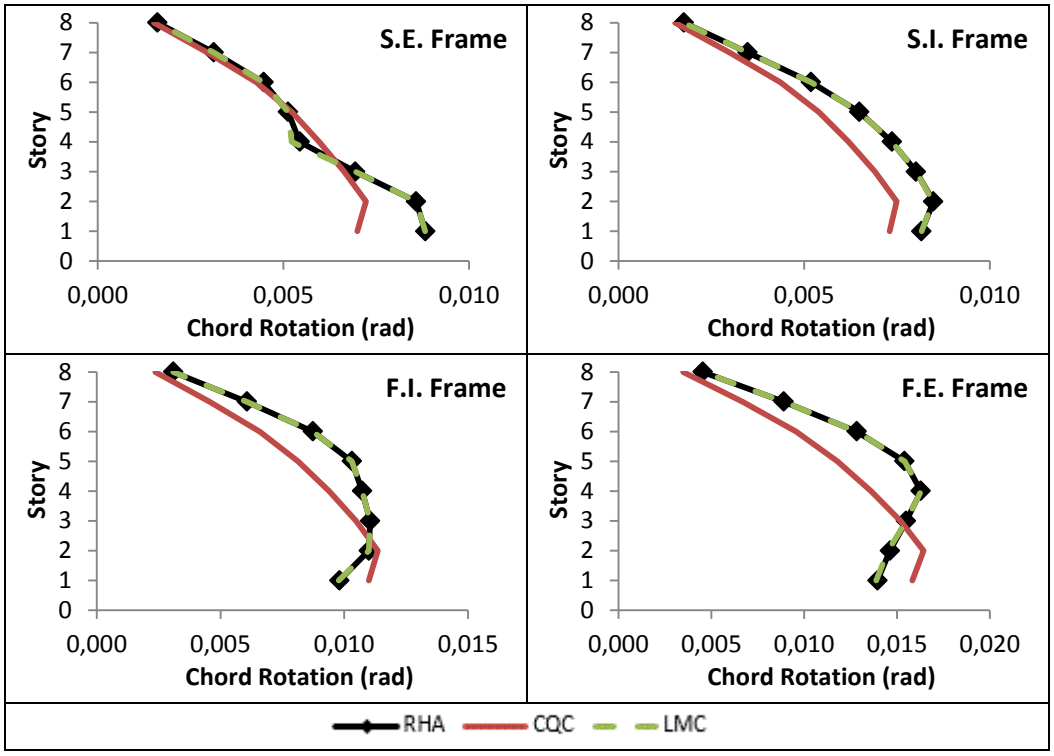

Figure 5.13: Mean beam chord rotation distributions under Northridge 1994 ORR090

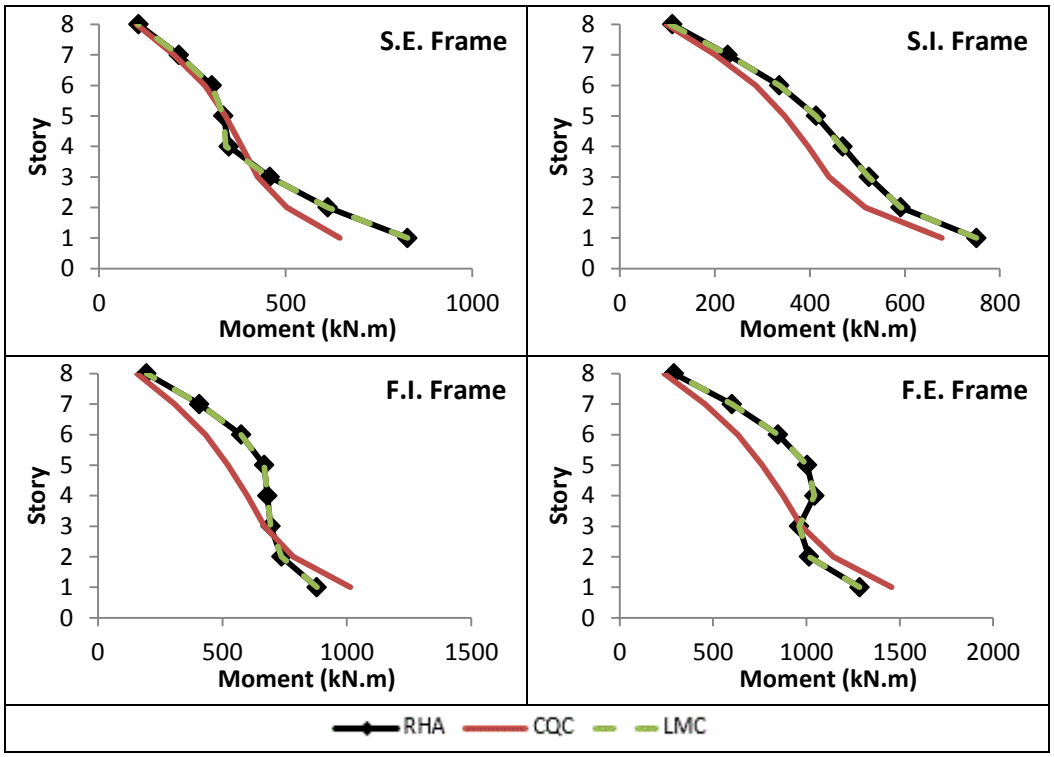

Figure 5.14: Interior column bottom end moment distr. under Northridge 1994 ORR090

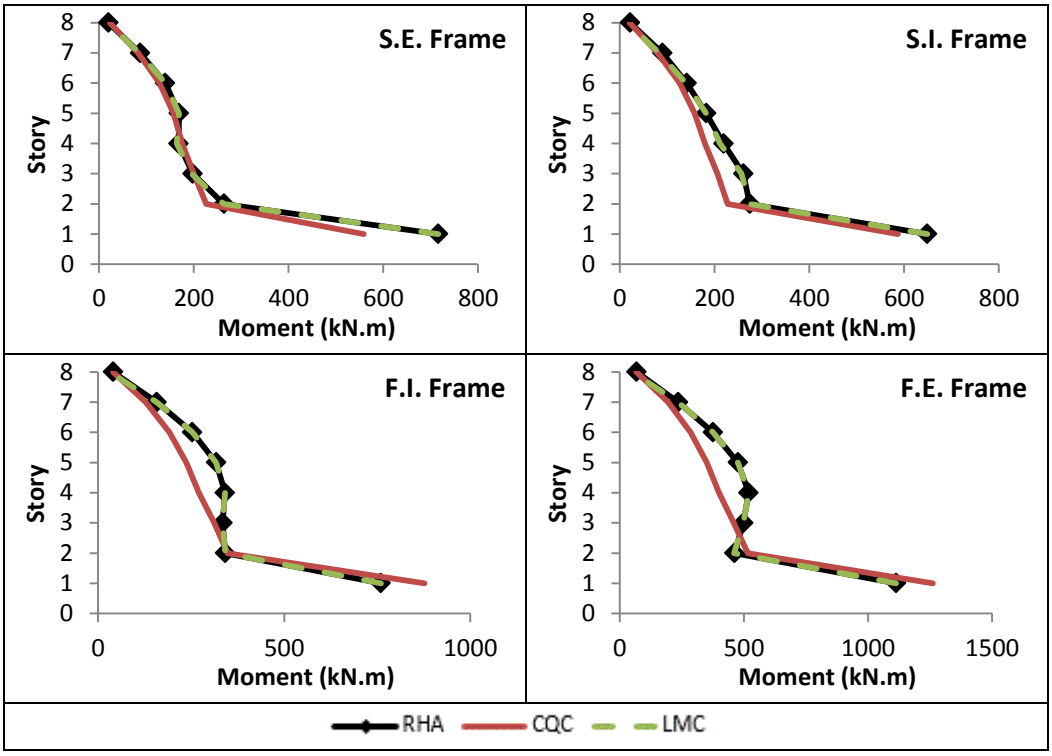

Figure 5.15: Exterior column bottom end moment distributions under Northridge 1994 ORR090

Table 5.11: CQC errors (%) for several response parameters under Northridge 1994 ORR090

Stiff Edge Exterior Frame					
Story	**Interstory Drift Ratio**	**Story Shear Force**	**Mean Beam End Rotation**	**Interior Column Moment**	**Exterior Column Moment**
1	21,58	22,32	20,74	21,95	21,98
2	18,69	19,44	15,78	17,86	14,09
3	11,16	11,68	4,32	6,96	0,92
4	4,58	5,97	9,58	9,95	4,32
5	8,16	5,88	2,17	1,58	6,82
6	1,54	4,24	4,34	6,07	8,68
7	5,04	5,99	5,46	6,03	5,00
8	6,27	4,88	5,80	5,59	16,16
Stiff Edge Interior Frame					
Story	**Interstory Drift Ratio**	**Story Shear Force**	**Mean Beam End Rotation**	**Interior Column Moment**	**Exterior Column Moment**
1	9,98	9,09	10,56	9,68	9,50
2	11,45	12,62	11,69	12,65	17,03
3	11,53	14,05	13,79	15,99	21,01
4	14,18	15,82	15,77	15,55	17,96
5	16,58	16,08	16,81	16,12	13,45
6	16,63	15,61	15,94	14,75	10,80
7	15,31	13,45	14,08	11,89	10,94
8	13,95	11,12	13,39	11,08	4,61
Flexible Edge Interior Frame					
Story	**Interstory Drift Ratio**	**Story Shear Force**	**Mean Beam End Rotation**	**Interior Column Moment**	**Exterior Column Moment**
1	14,19	16,62	12,03	15,19	15,44
2	7,61	9,65	3,22	6,34	1,71
3	1,31	0,41	5,12	3,66	6,71
4	8,55	7,93	12,45	11,94	20,52
5	17,65	19,22	21,08	21,74	25,24
6	23,22	23,97	24,70	24,88	24,45
7	25,07	25,06	24,90	24,49	18,93
8	24,34	21,88	23,60	19,62	0,08
Flexible Edge Exterior Frame					
Story	**Interstory Drift Ratio**	**Story Shear Force**	**Mean Beam End Rotation**	**Interior Column Moment**	**Exterior Column Moment**
1	13,55	13,16	13,43	13,34	13,29
2	13,25	12,96	12,36	12,84	11,59
3	7,99	9,17	2,03	1,50	7,79
4	10,48	11,62	16,51	16,13	23,13
5	20,74	21,97	23,48	23,93	26,32
6	24,82	25,01	25,48	25,40	24,03
7	25,52	24,99	24,89	24,00	16,99
8	24,08	20,58	23,04	17,65	0,63

Table 5.12: CQC errors (%) for beam end moments under Northridge 1994 ORR090

Stiff Edge Exterior Frame						
Beam	**Left Exterior**		**Interior**		**Right Exterior**	
End	**i**	**j**	**i**	**j**	**i**	**j**
Story 1	20,72	20,62	20,88	20,88	20,62	20,72
Story 2	15,63	15,57	16,18	16,18	15,57	15,63
Story 3	4,12	4,01	4,92	4,92	4,01	4,12
Story 4	9,58	9,63	9,52	9,52	9,63	9,58
Story 5	2,26	2,35	1,85	1,85	2,35	2,26
Story 6	4,11	3,99	5,05	5,05	3,99	4,11
Story 7	5,21	5,14	6,19	6,19	5,14	5,21
Story 8	5,47	5,19	7,34	7,34	5,19	5,47
Stiff Edge Interior Frame						
Beam	**Left Exterior**		**Interior**		**Right Exterior**	
End	**i**	**j**	**i**	**j**	**i**	**j**
Story 1	10,49	10,47	10,74	10,74	10,47	10,49
Story 2	11,63	11,53	11,92	11,92	11,53	11,63
Story 3	13,80	13,77	13,82	13,82	13,77	13,80
Story 4	15,79	15,80	15,70	15,70	15,80	15,79
Story 5	16,82	16,84	16,75	16,75	16,84	16,82
Story 6	16,05	16,11	15,59	15,59	16,11	16,05
Story 7	14,51	14,61	12,84	12,84	14,61	14,51
Story 8	13,63	14,08	11,96	11,96	14,08	13,63
Flexible Edge Interior Frame						
Beam	**Left Exterior**		**Interior**		**Right Exterior**	
End	**i**	**j**	**i**	**j**	**i**	**j**
Story 1	12,01	11,80	12,30	12,30	11,80	12,01
Story 2	3,01	2,98	3,75	3,75	2,98	3,01
Story 3	5,23	5,29	4,78	4,78	5,29	5,23
Story 4	12,53	12,49	12,32	12,32	12,49	12,53
Story 5	21,01	20,95	21,33	21,33	20,95	21,01
Story 6	24,60	24,55	25,01	25,01	24,55	24,60
Story 7	24,89	24,89	24,94	24,94	24,89	24,89
Story 8	23,89	24,00	22,56	22,56	24,00	23,89
Flexible Edge Exterior Frame						
Beam	**Left Exterior**		**Interior**		**Right Exterior**	
End	**i**	**j**	**i**	**j**	**i**	**j**
Story 1	13,41	13,41	13,47	13,47	13,41	13,41
Story 2	12,26	12,23	12,62	12,62	12,23	12,26
Story 3	2,25	2,33	1,41	1,41	2,33	2,25
Story 4	16,58	16,54	16,39	16,39	16,54	16,58
Story 5	23,41	23,38	23,67	23,67	23,38	23,41
Story 6	25,42	25,39	25,67	25,67	25,39	25,42
Story 7	24,98	25,01	24,63	24,63	25,01	24,98
Story 8	23,53	23,77	21,19	21,19	23,77	23,53

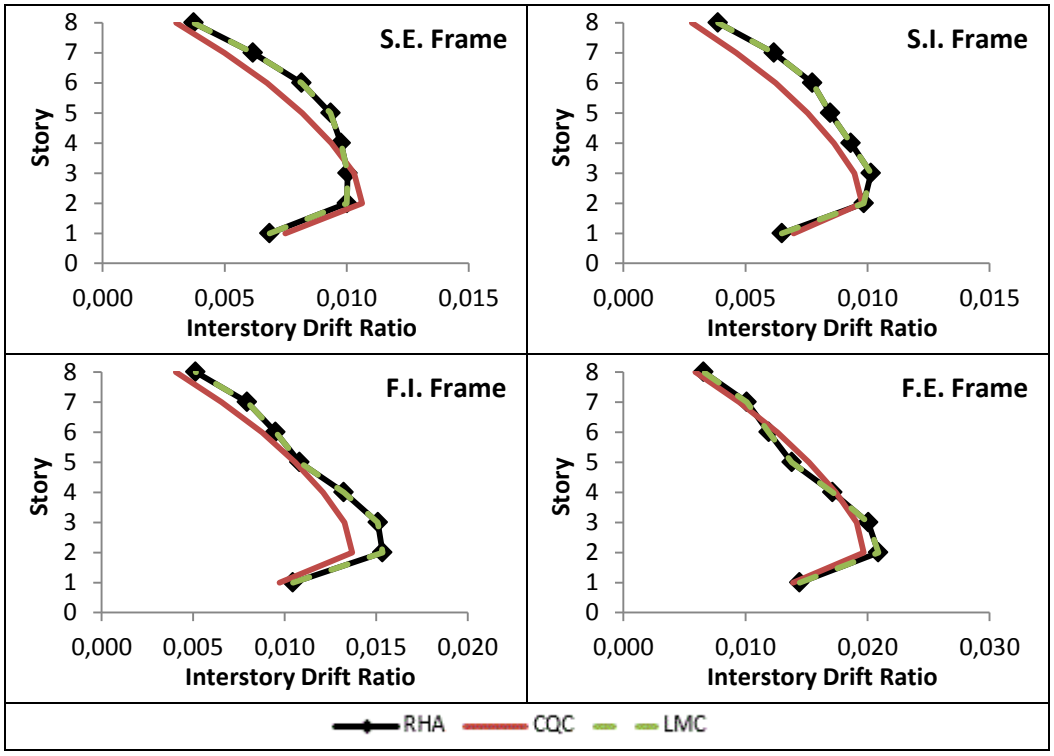

Figure 5.16: Interstory drift ratio distributions under El Centro 1979 H-E04140

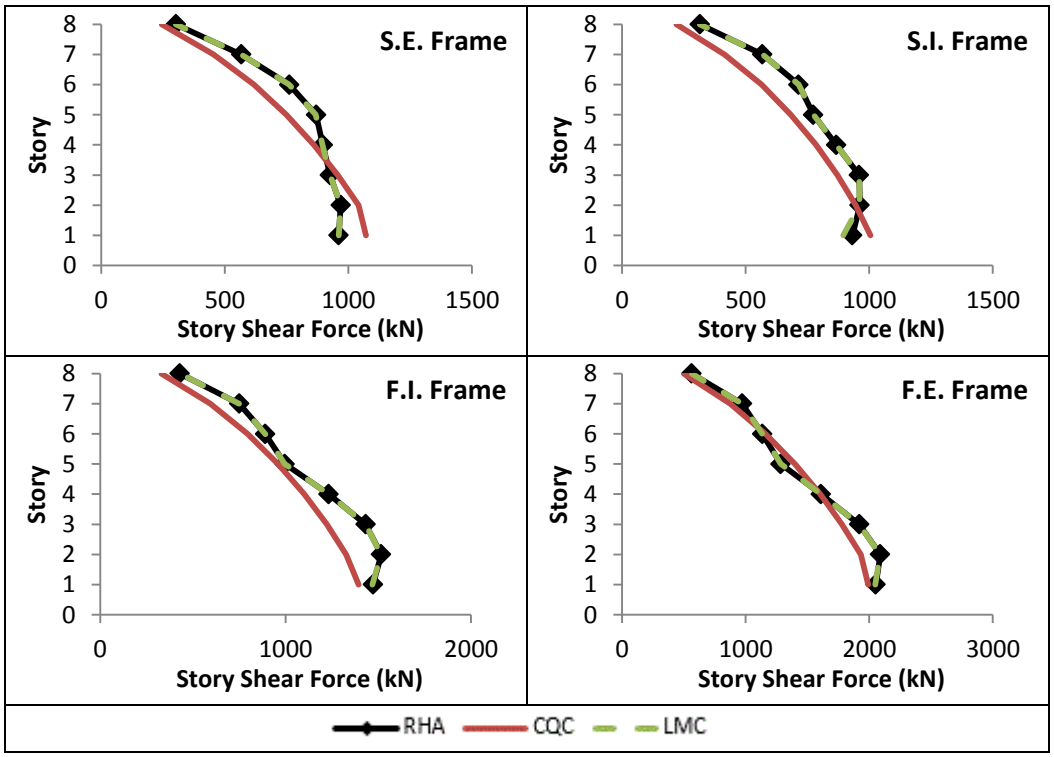

Figure 5.17: Story shear force distributions under El Centro 1979 H-E04140

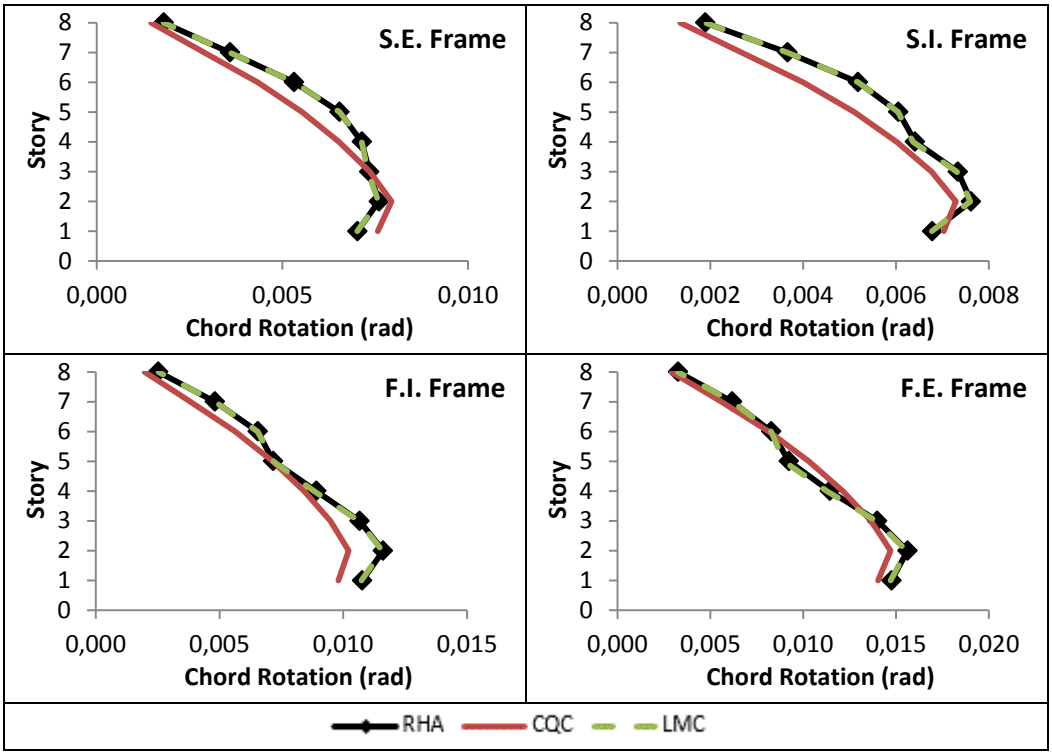

Figure 5.18: Mean beam chord rotation distributions under El Centro 1979 H-E04140

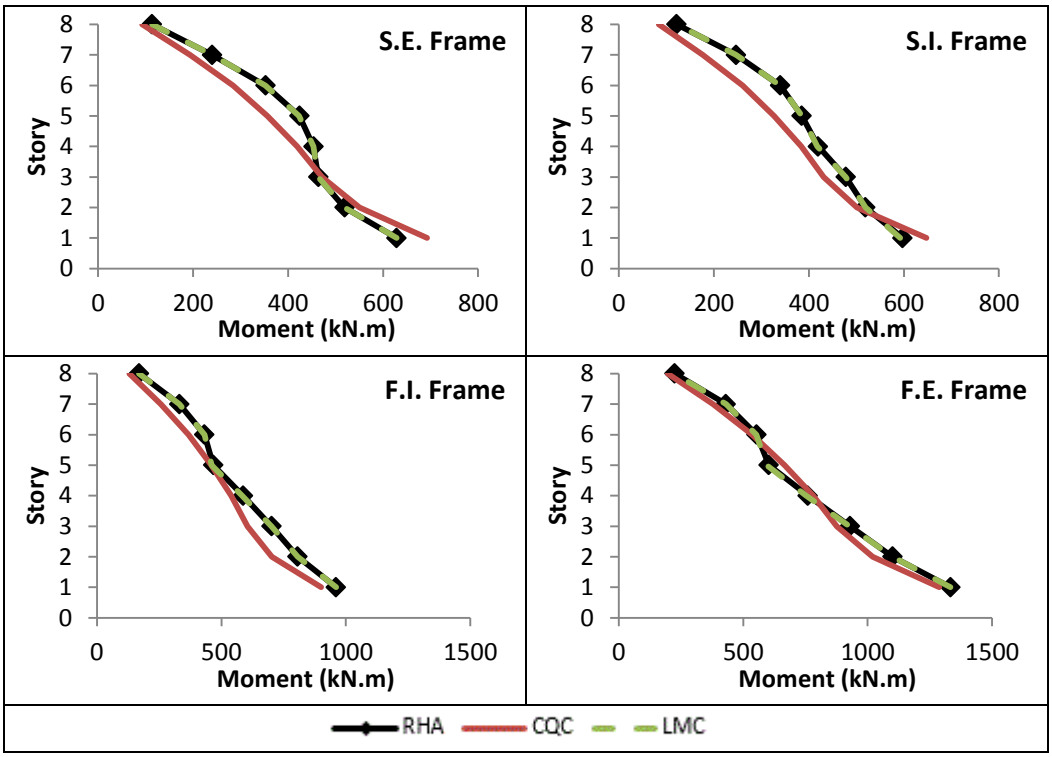

Figure 5.19: Interior column bottom end moment distr. under El Centro 1979 H-E04140

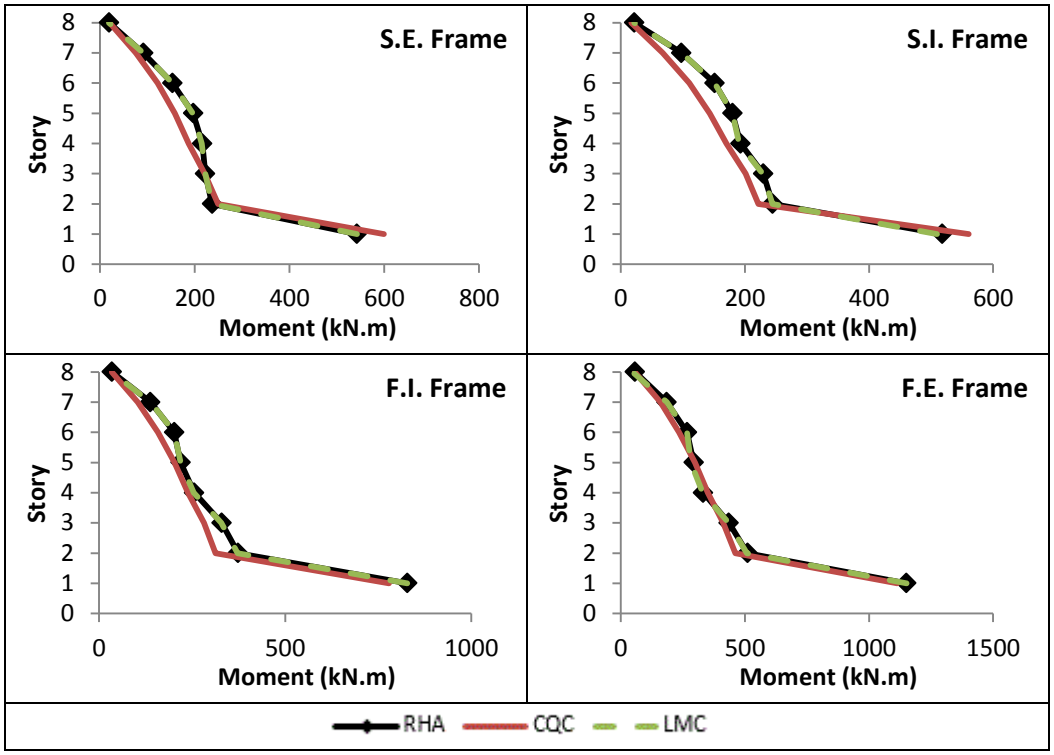

Figure 5.20: Exterior column bottom end moment distributions under El Centro 1979 H-E04140

Table 5.13: CQC errors (%) for several response parameters under El Centro 1979 H-E04140

Stiff Edge Exterior Frame					
Story	**Interstory Drift Ratio**	**Story Shear Force**	**Mean Beam End Rotation**	**Interior Column Moment**	**Exterior Column Moment**
1	9,38	11,49	7,80	10,23	10,53
2	6,21	7,49	4,47	6,02	5,19
3	2,63	3,43	0,20	1,64	0,64
4	3,98	3,99	8,55	7,57	13,29
5	12,42	13,87	15,38	15,93	19,73
6	17,28	18,74	18,51	19,41	20,46
7	18,96	19,71	19,19	19,48	17,33
8	19,03	19,09	18,85	17,98	2,56
Stiff Edge Interior Frame					
Story	**Interstory Drift Ratio**	**Story Shear Force**	**Mean Beam End Rotation**	**Interior Column Moment**	**Exterior Column Moment**
1	7,47	7,74	3,57	8,41	8,24
2	0,75	1,73	4,29	3,56	9,37
3	6,67	9,12	7,72	9,79	12,35
4	7,35	9,43	6,22	8,43	11,77
5	10,97	11,78	15,70	15,23	20,32
6	19,51	20,98	22,84	23,32	27,03
7	25,04	27,05	27,03	28,43	30,79
8	27,74	29,94	28,53	30,75	22,12
Flexible Edge Interior Frame					
Story	**Interstory Drift Ratio**	**Story Shear Force**	**Mean Beam End Rotation**	**Interior Column Moment**	**Exterior Column Moment**
1	7,05	5,32	8,95	6,29	6,00
2	10,84	12,52	12,04	12,81	16,35
3	12,13	14,65	11,11	13,86	14,50
4	8,61	10,64	5,53	8,31	6,52
5	2,26	3,67	0,34	1,89	7,70
6	7,85	10,67	13,86	14,92	22,01
7	17,50	20,74	20,44	22,62	24,87
8	21,07	23,08	21,98	23,40	2,63
Flexible Edge Exterior Frame					
Story	**Interstory Drift Ratio**	**Story Shear Force**	**Mean Beam End Rotation**	**Interior Column Moment**	**Exterior Column Moment**
1	3,81	2,97	4,92	3,44	3,25
2	5,75	7,56	5,89	7,28	9,59
3	4,81	7,34	2,47	5,77	5,35
4	1,52	0,40	6,11	2,82	5,69
5	10,25	8,86	11,67	10,50	1,33
6	5,80	2,29	1,65	3,20	12,24
7	6,26	9,87	9,38	12,09	14,14
8	10,27	11,24	10,83	12,15	0,60

Table 5.14: CQC errors (%) for beam end moments under El Centro 1979 H-E04140

Stiff Edge Exterior Frame						
Beam	**Left Exterior**		**Interior**		**Right Exterior**	
End	**i**	**j**	**i**	**j**	**i**	**j**
Story 1	7,78	7,73	7,90	7,90	7,73	7,78
Story 2	4,38	4,38	4,68	4,68	4,38	4,38
Story 3	0,08	0,04	0,53	0,53	0,04	0,08
Story 4	8,60	8,60	8,44	8,44	8,60	8,60
Story 5	15,33	15,29	15,56	15,56	15,29	15,33
Story 6	18,41	18,37	18,80	18,80	18,37	18,41
Story 7	19,14	19,13	19,35	19,35	19,13	19,14
Story 8	18,99	19,01	18,43	18,43	19,01	18,99
Stiff Edge Interior Frame						
Beam	**Left Exterior**		**Interior**		**Right Exterior**	
End	**i**	**j**	**i**	**j**	**i**	**j**
Story 1	3,70	3,55	3,43	3,43	3,55	3,70
Story 2	4,35	4,24	4,28	4,28	4,24	4,35
Story 3	7,68	7,60	7,92	7,92	7,60	7,68
Story 4	6,16	6,10	6,44	6,44	6,10	6,16
Story 5	15,64	15,60	15,89	15,89	15,60	15,64
Story 6	22,69	22,58	23,34	23,34	22,58	22,69
Story 7	26,73	26,62	27,95	27,95	26,62	26,73
Story 8	28,21	27,85	30,21	30,21	27,85	28,21
Flexible Edge Interior Frame						
Beam	**Left Exterior**		**Interior**		**Right Exterior**	
End	**i**	**j**	**i**	**j**	**i**	**j**
Story 1	8,87	8,90	9,09	9,09	8,90	8,87
Story 2	12,04	11,93	12,17	12,17	11,93	12,04
Story 3	11,02	10,94	11,40	11,40	10,94	11,02
Story 4	5,45	5,38	5,82	5,82	5,38	5,45
Story 5	0,29	0,23	0,53	0,53	0,23	0,29
Story 6	13,62	13,45	14,66	14,66	13,45	13,62
Story 7	19,98	19,82	21,80	21,80	19,82	19,98
Story 8	21,53	21,08	24,16	24,16	21,08	21,53
Flexible Edge Exterior Frame						
Beam	**Left Exterior**		**Interior**		**Right Exterior**	
End	**i**	**j**	**i**	**j**	**i**	**j**
Story 1	4,86	4,85	5,06	5,06	4,85	4,86
Story 2	5,86	5,75	6,09	6,09	5,75	5,86
Story 3	2,36	2,26	2,84	2,84	2,26	2,36
Story 4	6,21	6,30	5,76	5,76	6,30	6,21
Story 5	11,75	11,87	11,32	11,32	11,87	11,75
Story 6	1,33	1,08	2,75	2,75	1,08	1,33
Story 7	8,77	8,57	11,18	11,18	8,57	8,77
Story 8	10,23	9,67	13,61	13,61	9,67	10,23

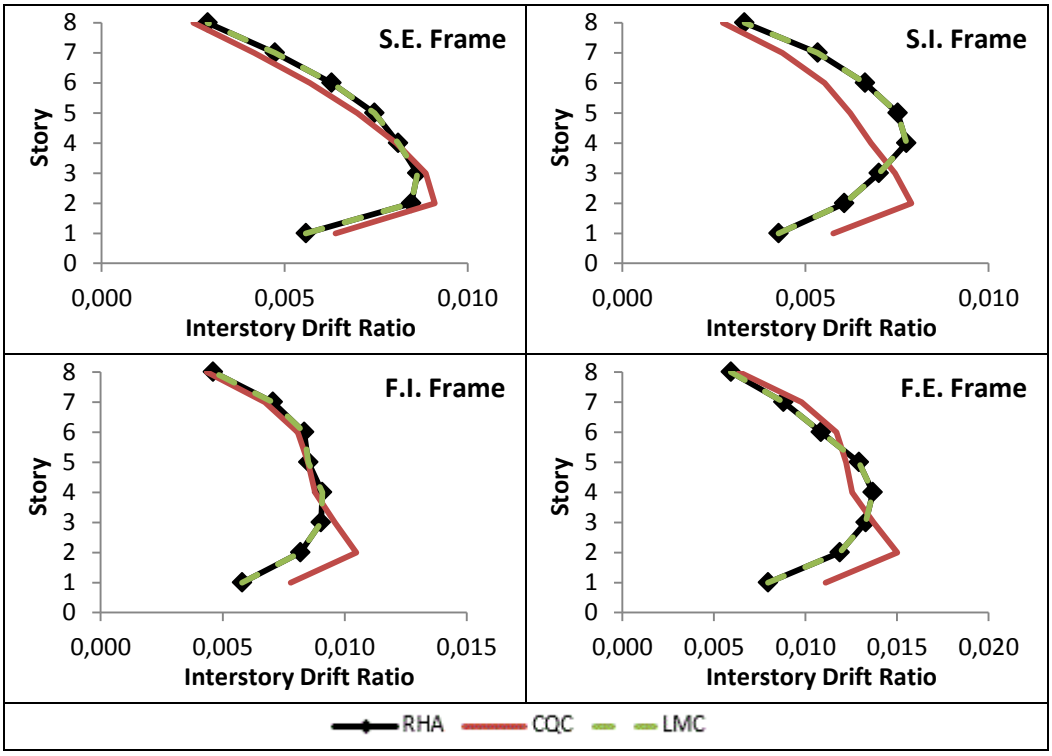

Figure 5.21: Interstory drift ratio distributions under Loma Prieta 1989 CLS090

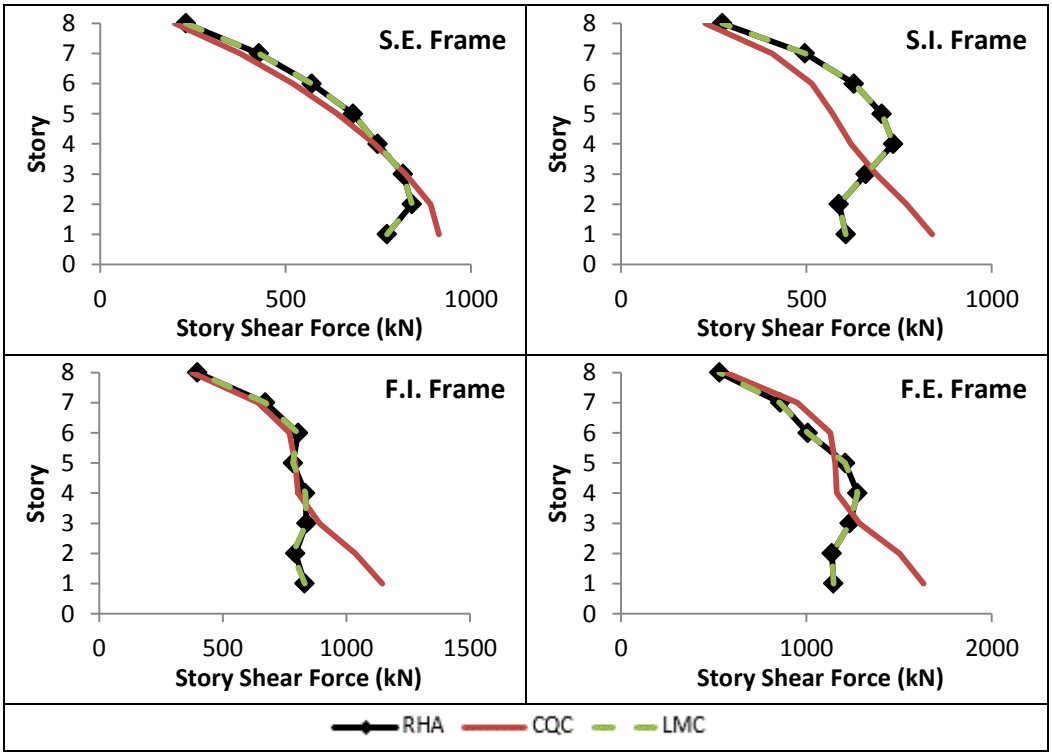

Figure 5.22: Story shear force distributions under Loma Prieta 1989 CLS090

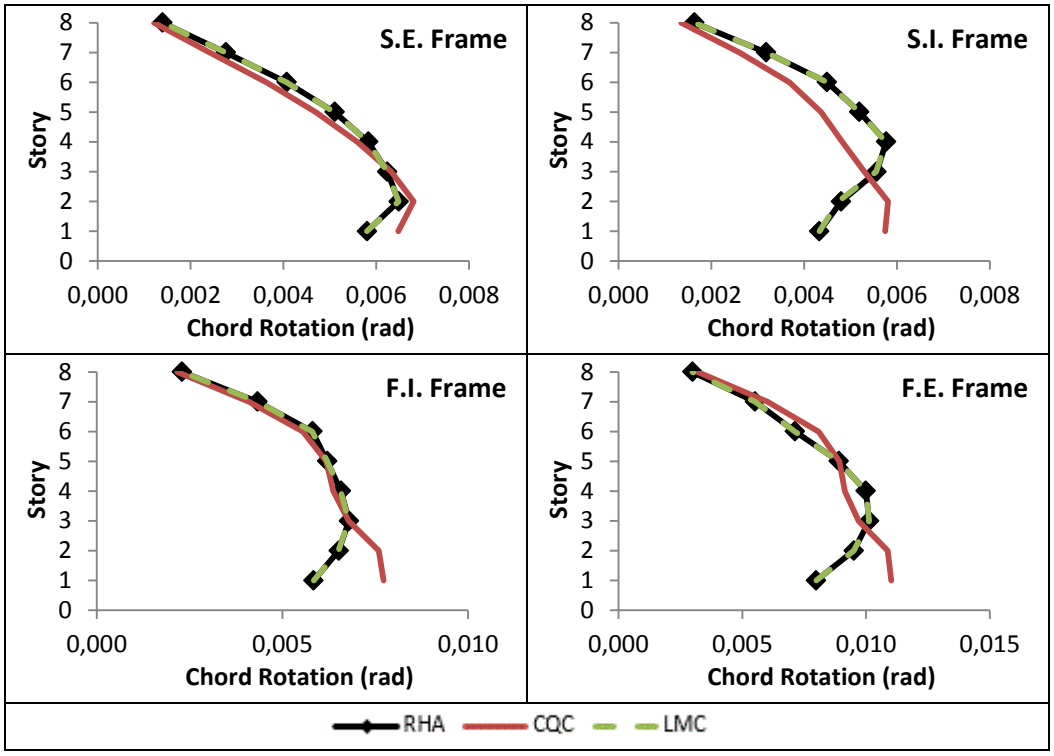

Figure 5.23: Mean beam chord rotation distributions under Loma Prieta 1989 CLS090

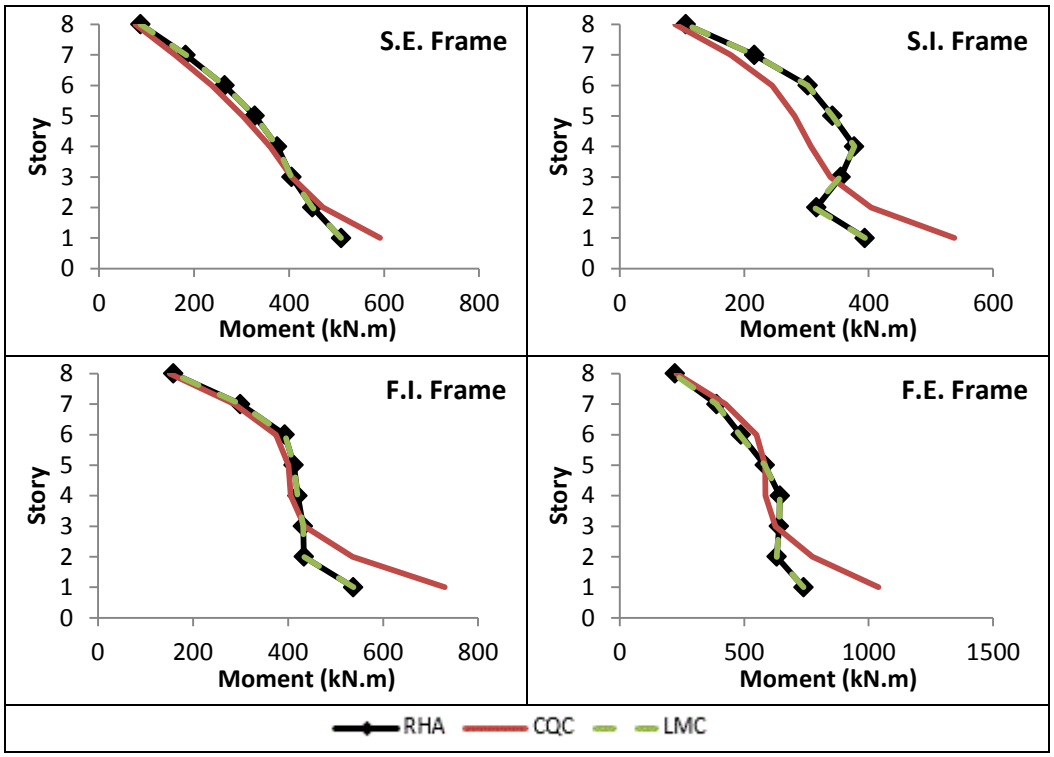

Figure 5.24: Interior column bottom end moment distr. under Loma Prieta 1989 CLS090

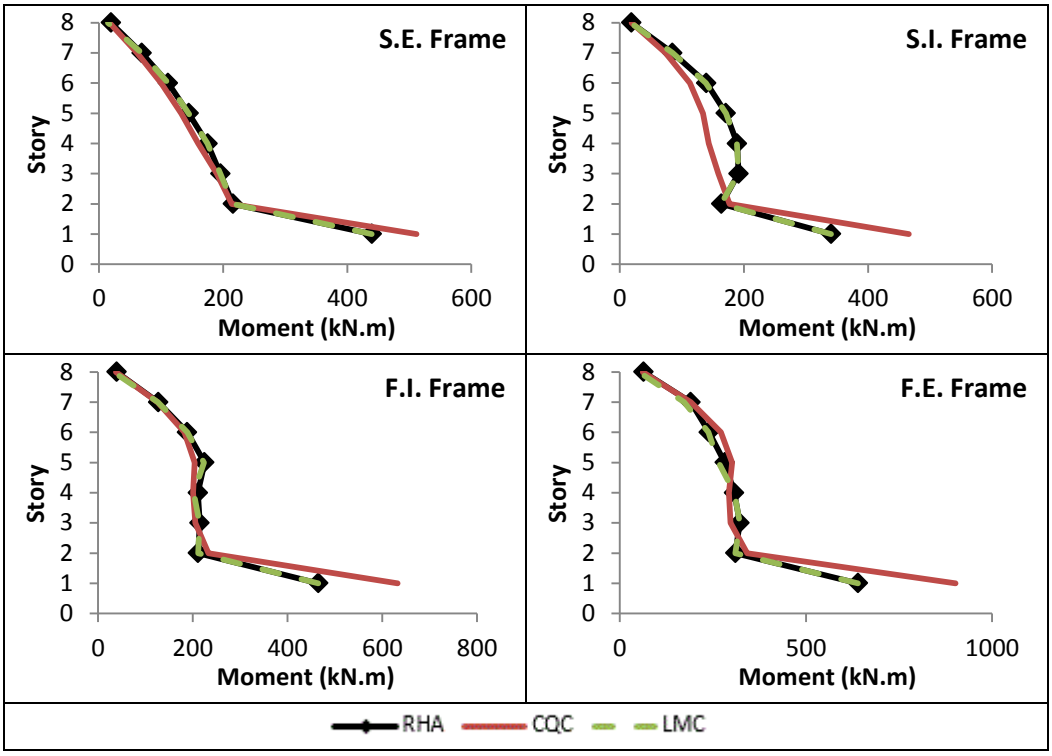

Figure 5.25: Exterior column bottom end moment distributions under Loma Prieta 1989 CLS090

Table 5.15: CQC errors (%) for several response parameters under Loma Prieta 1989 CLS090

Stiff Edge Exterior Frame					
Story	**Interstory Drift Ratio**	**Story Shear Force**	**Mean Beam End Rotation**	**Interior Column Moment**	**Exterior Column Moment**
1	14,55	18,14	11,57	16,07	16,43
2	7,60	6,05	4,97	4,92	1,02
3	2,68	0,87	1,36	0,07	2,84
4	0,59	1,19	4,00	4,11	8,67
5	6,35	6,28	7,94	7,75	8,36
6	9,34	8,79	10,66	10,10	10,31
7	11,95	11,80	12,63	12,47	10,27
8	13,45	12,61	13,24	12,35	12,54
Stiff Edge Interior Frame					
Story	**Interstory Drift Ratio**	**Story Shear Force**	**Mean Beam End Rotation**	**Interior Column Moment**	**Exterior Column Moment**
1	35,08	38,42	32,74	36,45	36,84
2	30,14	31,02	21,01	27,75	8,03
3	6,27	4,22	4,81	4,76	17,19
4	12,45	15,61	16,44	18,52	24,20
5	17,28	18,83	15,94	17,78	21,57
6	16,61	18,12	18,00	18,93	18,97
7	18,09	17,97	18,12	17,61	13,15
8	17,79	16,93	17,51	15,95	1,73
Flexible Edge Interior Frame					
Story	**Interstory Drift Ratio**	**Story Shear Force**	**Mean Beam End Rotation**	**Interior Column Moment**	**Exterior Column Moment**
1	34,36	37,64	32,11	35,71	36,07
2	28,00	30,42	16,50	23,66	10,14
3	6,30	6,24	0,08	0,68	4,39
4	3,29	3,50	3,18	3,54	5,03
5	0,10	1,11	0,49	2,74	9,15
6	3,15	4,36	4,45	4,80	3,16
7	4,69	4,24	5,22	4,21	1,10
8	5,54	5,40	5,53	4,70	3,75
Flexible Edge Exterior Frame					
Story	**Interstory Drift Ratio**	**Story Shear Force**	**Mean Beam End Rotation**	**Interior Column Moment**	**Exterior Column Moment**
1	39,60	42,29	37,84	40,69	40,98
2	26,45	32,10	14,33	22,75	10,16
3	3,25	4,25	4,24	2,28	7,72
4	8,27	8,68	8,51	8,98	4,64
5	5,41	4,44	0,29	0,07	6,88
6	7,73	12,12	13,21	12,82	13,33
7	11,10	10,75	9,07	9,35	0,07
8	7,62	6,73	7,23	2,93	3,00

Table 5.16: CQC errors (%) for beam end moments under Loma Prieta 1989 CLS090

Stiff Edge Exterior Frame						
Beam	**Left Exterior**		**Interior**		**Right Exterior**	
End	**i**	**j**	**i**	**j**	**i**	**j**
Story 1	11,67	11,47	11,56	11,56	11,47	11,67
Story 2	4,89	4,91	5,14	5,14	4,91	4,89
Story 3	1,37	1,36	1,34	1,34	1,36	1,37
Story 4	4,03	3,97	4,00	4,00	3,97	4,03
Story 5	7,89	7,84	8,11	8,11	7,84	7,89
Story 6	10,58	10,52	10,95	10,95	10,52	10,58
Story 7	12,50	12,45	13,06	13,06	12,45	12,50
Story 8	13,25	13,07	13,57	13,57	13,07	13,25
Stiff Edge Interior Frame						
Beam	**Left Exterior**		**Interior**		**Right Exterior**	
End	**i**	**j**	**i**	**j**	**i**	**j**
Story 1	32,74	32,62	32,88	32,88	32,62	32,74
Story 2	20,42	20,50	22,30	22,30	20,50	20,42
Story 3	4,97	4,96	4,45	4,45	4,96	4,97
Story 4	16,42	16,33	16,61	16,61	16,33	16,42
Story 5	15,87	15,85	16,15	16,15	15,85	15,87
Story 6	17,83	17,77	18,50	18,50	17,77	17,83
Story 7	18,00	17,98	18,44	18,44	17,98	18,00
Story 8	17,59	17,54	17,42	17,42	17,54	17,59
Flexible Edge Interior Frame						
Beam	**Left Exterior**		**Interior**		**Right Exterior**	
End	**i**	**j**	**i**	**j**	**i**	**j**
Story 1	32,10	31,97	32,28	32,28	31,97	32,10
Story 2	16,03	16,03	17,57	17,57	16,03	16,03
Story 3	0,20	0,22	0,22	0,22	0,22	0,20
Story 4	3,14	3,14	3,27	3,27	3,14	3,14
Story 5	0,33	0,21	1,01	1,01	0,21	0,33
Story 6	4,28	4,24	4,92	4,92	4,24	4,28
Story 7	5,16	5,14	5,40	5,40	5,14	5,16
Story 8	5,68	5,62	5,24	5,24	5,62	5,68
Flexible Edge Exterior Frame						
Beam	**Left Exterior**		**Interior**		**Right Exterior**	
End	**i**	**j**	**i**	**j**	**i**	**j**
Story 1	37,82	37,72	38,00	38,00	37,72	37,82
Story 2	13,87	13,80	15,49	15,49	13,80	13,87
Story 3	4,36	4,40	3,93	3,93	4,40	4,36
Story 4	8,47	8,46	8,62	8,62	8,46	8,47
Story 5	0,20	0,13	0,60	0,60	0,13	0,20
Story 6	13,51	13,62	12,36	12,36	13,62	13,51
Story 7	9,37	9,46	8,24	8,24	9,46	9,37
Story 8	7,41	7,75	6,14	6,14	7,75	7,41

CHAPTER 6

PRACTICAL IMPLEMENTATION OF LINEAR MODAL COMBINATION PROCEDURE

6.1 Reduced Linear Modal Combination Procedure

Linear modal combination procedure as presented in this study is based on the assumption that interstory drift ratio of any story and the response parameters of all members (member end rotations, moments, shears, etc.) at that story attain their maximum values simultaneously, or with very short time differences. Theoretically, the interstory drift ratios of each story reach their maximum values at different times, i.e. they are independent of each other. Alıcı (2012) investigated this phenomenon on a twelve story plane frame structure, which is also employed as the third case study of this thesis, under CHY006-E component of the 1999 Chi-Chi earthquake ground motion. He observed that possible combinations of significant modes result in the maximum values of interstory drift ratios at particular stories. There are $2^{(n-1)}$ number of possible combinations which yield maximum response envelope of the interstory drift ratios if n number of modes contribute significantly to the total response, where $n<N$. The number of possible combinations that yield the maximum response envelope is $2^{(n-1)}$ which corresponds to $2^{(n-1)}$ independent t_{max} for calculating the modal scaling coefficients. Figure 6.1 shows the mentioned combinations that yield maximum responses at different story ranges, extracted from Alıcı (2012).

In view of Alıcı (2012), a similar brief study is conducted in this chapter on t_{max} values obtained under three ground motion records that are used in the case studies. Table 6.1 presents the same t_{max} values that are obtained in Section 5.1 again for convenience. Table 6.1 indicates that some adjacent stories reach their maximum response synchronously during dynamic response. As it is inferred from Table 6.1, there is a grouping among the stories in terms of the maximum occurrence times of interstory drift ratios. According to $2^{(n-1)}$ different combinations for n significant modes, four different ranges are determined where the t_{max} values are very close. The ranges are presented in Table 6.2.

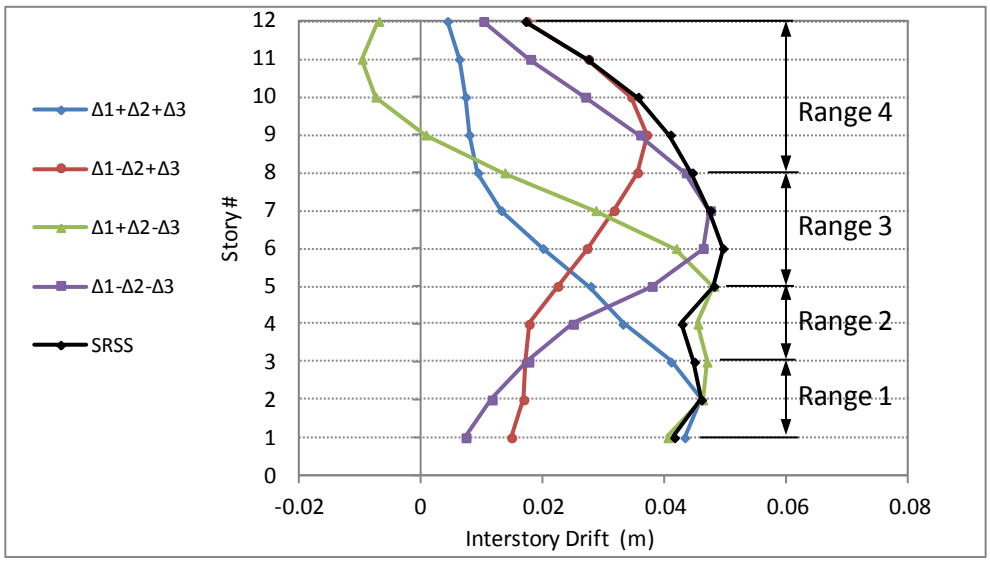

Figure 6.1: Comparison of SRSS drift profile and the combinations of the first three scaled modal drifts (Courtesy of F. S. Alıcı, 2012)

Table 6.1: t_{max} values of the twelve story plane frame under three different ground motions

Story	Northridge 1994 ORR090	El Centro 1979 H-E04140	Loma Prieta 1989 CLS090
1	9,300	8,180	4,355
2	9,300	8,185	4,370
3	9,340	7,000	4,390
4	9,400	7,020	4,415
5	9,460	7,170	4,455
6	8,420	7,255	3,880
7	8,460	7,275	4,780
8	8,480	7,280	4,735
9	8,480	7,280	4,730
10	9,680	7,270	4,740
11	9,700	7,250	4,755
12	9,700	7,235	4,760

Table 6.2: Ranges of t_{max} values under three ground motions

Range	Northridge 1994 ORR090	El Centro 1979 H-E04140	Loma Prieta 1989 CLS090
	Stories		
1	1-3	1-2	1-3
2	4-5	3-4	4-5
3	6-9	5	6
4	10-12	6-12	7-12

There should be four different story levels that represent four different ranges, and accordingly leading to four different modal scaling coefficients under each ground motion. A unified selection is pursued here, and the stories are selected as 1st, 4th, 7th, and 11th for all ground motions. Consequently, size of the modal scaling coefficient matrix is reduced to 4x3 when the linear modal combination procedure is reduced. The modal scaling coefficient matrix is 12x12 when the linear modal combination procedure is fully applied.

6.2 Presentation of Results

The reduced LMC (RLMC) procedure is applied to the same twelve story plane frame presented in Chapter 5. The same response parameters are observed in order to maintain consistency with the results presented in Section 5.1.3. The results of CQC method include the contributions from only the first three significant modes.

The distributions of story displacement, interstory drift ratio, mean beam end moments and rotations, and interior and exterior column bottom end moments are presented from Figure 6.2 to Figure 6.4. It can be observed from the results presented below that the RLMC results are very close to the benchmark RHA results for all response parameters under all three ground motions. Using four combinations instead of all 12 combinations yields reasonably good results. This behavior is especially seen in the results obtained under Northridge and El Centro ground motions. Higher mode contribution to the total response in Northridge ground motion is present at mid-level stories, while there is no contribution from higher modes in El Centro ground motion. The errors of RLMC at mid-level stories under Northridge ground motion diminishes as the first four modes are included in the RLMC procedure. This behavior shows that the primary source of errors in RLMC is the reduced number of modes included in the analysis. Other than that, RLMC with three modes and four combinations are considerably sufficient for the estimation of total maximum responses.

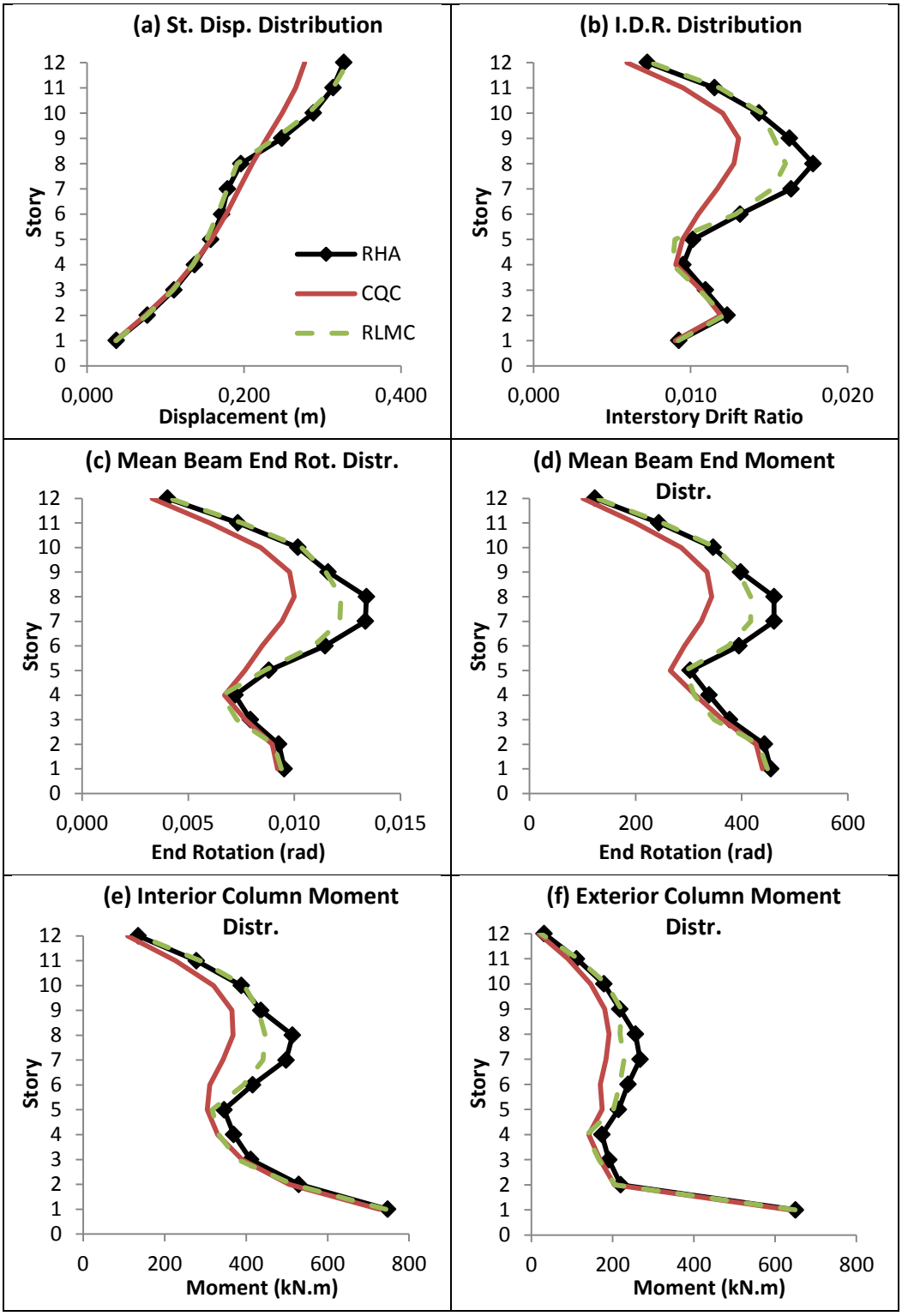

Figure 6.2: Distributions of several response parameters under Northridge 1994 ORR090 (a) Story displacement (b) Interstory drift ratio (c) Mean beam end rotation (d) Mean beam end moment (e) Interior column bottom end moment (f) Exterior column bottom end moment

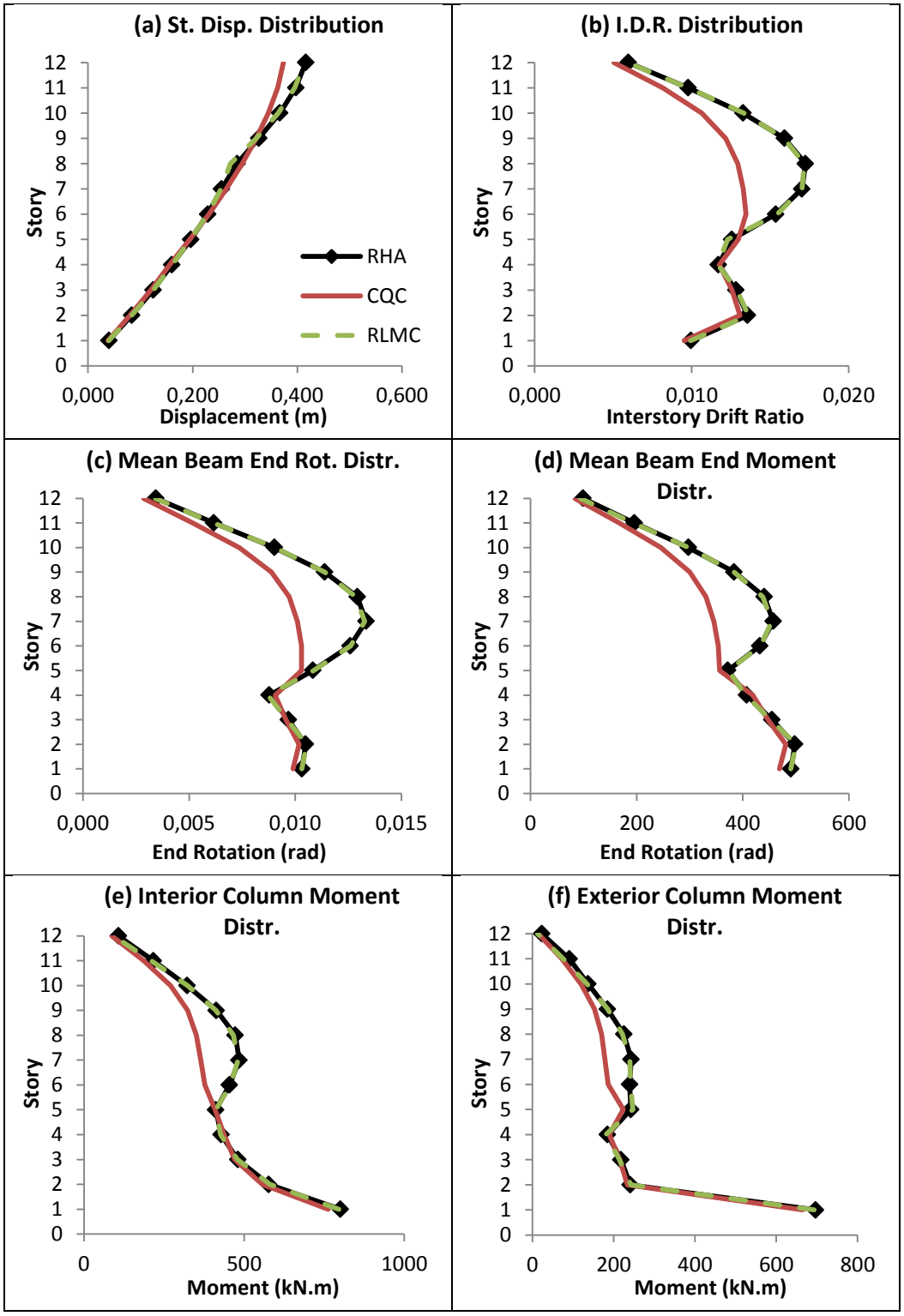

Figure 6.3: Distributions of several response parameters under El Centro 1979 H-E04140 (a) Story displacement (b) Interstory drift ratio (c) Mean beam end rotation (d) Mean beam end moment (e) Interior column bottom end moment (f) Exterior column bottom end moment

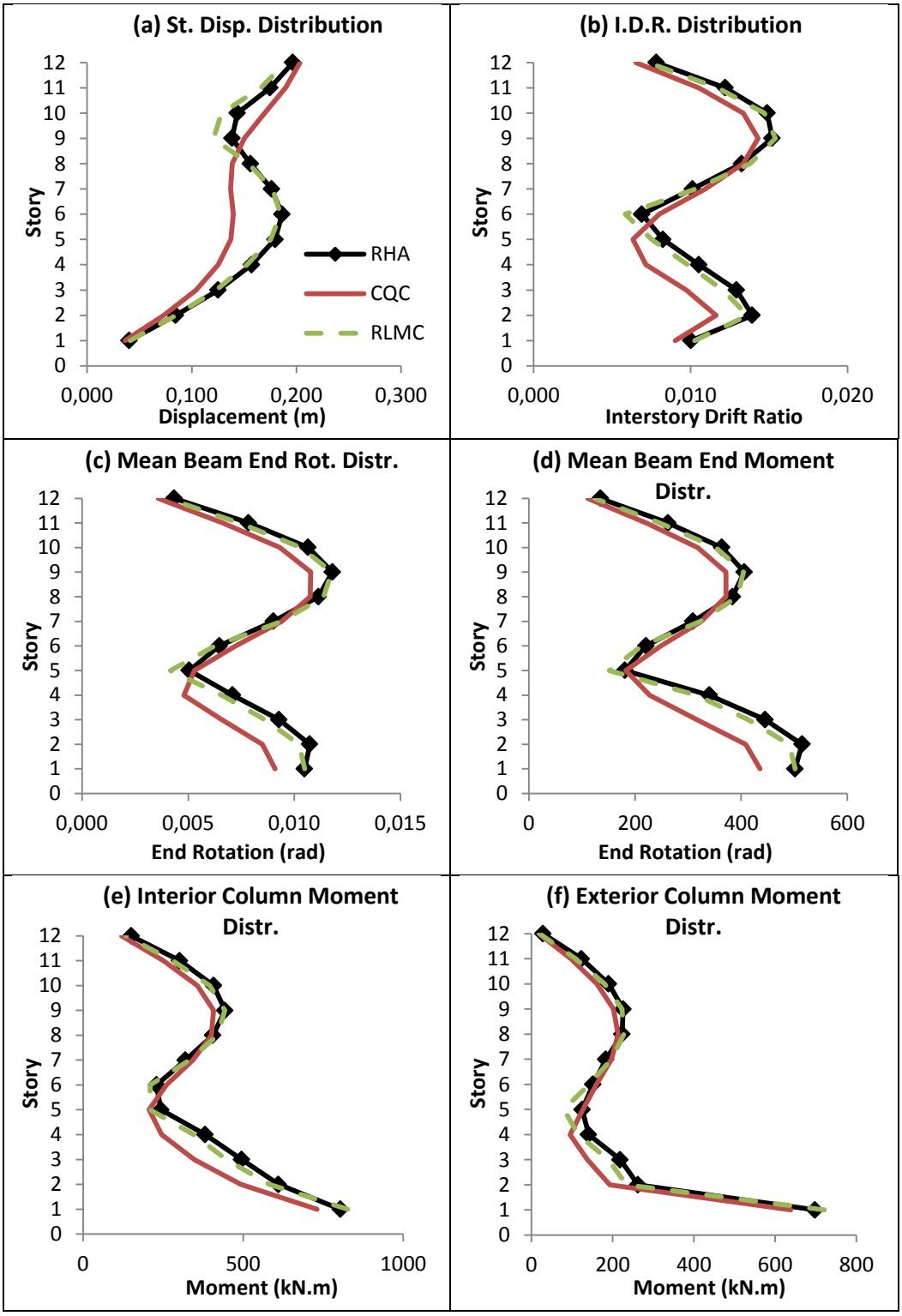

Figure 6.4: Distributions of several response parameters under Loma Prieta 1989 CLS090 (a) Story displacement (b) Interstory drift ratio (c) Mean beam end rotation (d) Mean beam end moment (e) Interior column bottom end moment (f) Exterior column bottom end moment

CHAPTER 7

SUMMARY AND CONCLUSIONS

7.1 Summary

The linear modal combination (LMC) procedure is developed in this study as a new deterministic analysis procedure for estimating the dynamic response of building structures. The suggested combination procedure is based on the participation level of vibration modes to the total maximum response of any specific response parameter. In order to express this participation level for each mode, modal scaling coefficients are introduced. By definition, the modal scaling coefficient of a mode n is the ratio of the response of n'th mode to the total maximum response of any parameter, at the time t_{max} when the total response of the specified parameter attains its maximum value. Therefore modal scaling coefficients depend on the occurrence time of the maximum response of a parameter. The principal response parameter is selected as the interstory drift ratio of the j'th story in the LMC procedure. While there is a different modal scaling coefficient corresponding to each mode, these modal scaling coefficients also change with each story j. Consequently, there are j x n modal scaling coefficients for a structure having j number of stories and n number of vibration modes. During the analysis of the structure with the LMC procedure, a specific response parameter at the j'th story is determined by multiplying (scaling) the maximum modal response of each mode n with the modal scaling coefficients corresponding to the j'th story, and then combining the modal responses linearly. The maximum modal response of a mode n is determined from the associated SDOF analysis. Modal scaling coefficients consider the direction of modal responses, i.e. they can be negative or positive. Since the scaled modal responses are linearly combined, LMC procedure is not affected from the drawbacks of any statistical combination rules such as SRSS or CQC.

The LMC procedure introduced herein is tested on two plane frame and two space frame structures, four case studies in total. The first two case studies are simple structures that are primarily used to investigate the effect of coupled modes on the LMC procedure. The third case study of the thesis is a twelve story plane frame structure where higher mode contributions are significant, and the fourth one is an eight story space frame structure with mass eccentricity. All four structures are analyzed under three different

ground motions. Linear response history analysis, linear modal combination procedure and response spectrum analysis with CQC method are carried out on the case studies. Several response parameters such as story displacement, interstory drift ratio, story shear force, and member end moments and end rotations are obtained for each analysis procedure and they are evaluated comparatively.

A brief study on the implementation of LMC procedure is also conducted in order to reduce the number of modal scaling coefficients in terms of both the number of modes and the story number. The reduction of the LMC procedure is based on the following criteria: There are $2^{(n-1)}$ number of combinations that result in the response envelope of the interstory drift ratios if there are n modes that significantly contribute to the total dynamic response. The stories are grouped according to the closeness of t_{max} values of adjacent stories. One specific story is selected in order to represent each story group. The modal scaling coefficients calculated for those specific stories are used for the entire group and the envelope of the results is obtained. The results are compared with the CQC method and RHA.

7.2 Conclusions

According to the results that are obtained in this thesis, the following conclusions are reached:

- LMC procedure either yields exact result or produce negligible errors in the estimation of all type of response parameters. This behavior is valid for all four case studies under all three ground motions used in the case studies. Interstory drift ratios are implicitly determined in the LMC procedure since the modal scaling coefficients used in the procedure are determined at the time when the IDR's reach their maximum value. The selection criterion of IDR as the principal response parameter was that any higher order response parameter at a specific story reaches its maximum value almost at the same time when IDR at that story attains its maximum response. Obtaining the exact (or almost exact) value of local parameters with the IDR-based modal scaling coefficients in the LMC procedure reinforces this criterion.

- CQC method results in sufficiently good estimations when the first mode is completely dominant in the total response. This is an expected behavior considering the more complex formulation compared to SRSS. However, the method, which is used over SRSS method in order to increase the accuracy of the response spectrum analysis especially when there is close coupling between vibration modes, produces larger errors when higher modes become effective. Besides, CQC method generally underestimates the exact values of the response parameters, which leads to an unsafe situation for the evaluation of structures.

- When the t_{max} values of each story are investigated, it is observed that some adjacent stories move synchronously during the ground motion response and attain their maximum IDR values at very close instants. This grouping of stories leads to the use of a reduced number of modes and modal scaling coefficients. Since there are a limited number of modes significantly contributing the total response, which is apparent in the modal analysis results of case studies, the number of coefficients is also reduced in terms of the number of significant modes. The results that are obtained from the reduced linear modal combination procedure (RLMC) procedure show that RLMC introduces the same accuracy compared with the full LMC procedure.

REFERENCES

F.S. Alıcı. “Generalized Pushover Analysis”. *M.Sc. Thesis, Middle East Technical University, Ankara*, 2012.

F.S. Alıcı, K. Kaatsız, and H. Sucuoğlu. “Genel Yük Vektörleri ile Çok Modlu İtme Analizi (Genel İtme Analizi)”. *Birinci Türkiye Deprem Mühendisliği ve Sismoloji Konferansı, Ankara, Turkey*, 2011.

A.K. Chopra. “Dynamics of Structures: Theory and Applications to Earthquake Engineering”. *2nd Edition*. Prentice Hall, Englewood Cliffs, N.J., 2001.

A.K. Chopra and R.K. Goel. “A Modal Pushover Analysis Procedure for Estimating Seismic Demands for Buildings”. *Earthquake Engineering and Structural Dynamics*, Volume 31 (No. 3): pp. 561-582, 2002.

A.K. Chopra and R.K. Goel. “A Modal Pushover Analysis Procedure for Estimating Seismic Demands for Unsymmetric-plan Buildings”. *Earthquake Engineering and Structural Dynamics*, Volume 33: pp. 903-927, 2004.

E. Heredia-Zavoni. “The Complete SRSS Modal Combination Rule”. *Earthquake Engineering and Structural Dynamics*, Volume 40: pp. 1181-1196, 2011.

T.S. Jan, M.W. Liu, and Y.C. Kao. “An Upper-Bound Pushover Analysis Procedure for Estimating the Seismic Demands of High-Rise Buildings”. *Engineering Structures*, Volume 26: pp. 117-128, 2004.

J.M. Kelly and J.L. Sackman. “Conservationism in Summation Rules for Closely Spaced Modes”. *Earthquake Engineering and Structural Dynamics*, Volume 8: pp. 63-74, 1980.

D. Lee, W. Choi, and J. Ahn. “Improved Distribution of Seismic Forces for Evaluation of Nonlinear Seismic Response of Building Structures”. *Journal of Earthquake Engineering*, Volume 5 (No. 2): pp. 33-47, 2002.

P. Leger and E.L. Wilson. “Modal Summation Methods for Structural Dynamic Computations”. *Earthquake Engineering and Structural Dynamics*, Volume 16: pp. 23-27, 1988.

Mathworks Inc. MATLAB – R2010b, 2010.

T. Matsumori, S. Otani, H. Shiohara, and T. Kabeyasawa. “Earthquake Member Deformation Demands in Reinforced Concrete Frame Structures”. *Proceedings of the U.S. – Japan Workshop on Performance-Based Earthquake Engineering Methodology for Reinforced Concrete Building Structures, Maui, Hawaii. PEER Center Rep.,* Univ. of California, Berkeley, 1999.

Ministry of Construction of Japan. “Building Standard Law Enforcement Order”. *Building Center of Japan,* 1981.

Ministry of Public Works and Settlement. “Turkish Earthquake Code: Specifications for the Buildings to be Constructed in Disaster Areas”, 2007.

OpenSees. “Open System for Earthquake Engineering Simulation”, from http://opensees.berkeley.edu, last accessed on 04.01.2013.

H. Park, T. Eom, and H. Lee. “Factored Modal Combination for Evaluation of Earthquake Load Profiles”. *Journal of Structural Engineering*, Volume 133 (No. 7), 2007.

PEER Strong Motion Database, from http://peer.berkeley.edu/smcat, last accessed on 25.09.2012.

M. Requena and A.G. Ayala. “Evaluation of a Simplified Method for the Determination of the Nonlinear Seismic Response of RC Frames”. *Proceedings of the 12th World Conference on Earthquake Engineering, Auckland, New Zealand*, 2000.

E. Rosenblueth. “A basis for a seismic design”. *Ph.D. Thesis*, University of Illinois, Urbana, 1951.

E. Rosenblueth and J. Elorduy. “Responses of Linear Systems to Certain Transient Disturbances”. *Proceedings of the Fourth World Conference on Earthquake Engineering, Santiago de Chile*, 1969; A1-185.

H. Sucuoğlu and M.S. Günay. “Generalized Force Vectors for Multi-mode Pushover Analysis”. *Earthquake Engineering and Structural Dynamics*, Volume 40 (No. 1): pp. 55-74, 2011.

M.D. Trifunac and A.G. Brady. “A Study on the Duration of Strong Earthquake Ground Motion”. *Bulletin of the Seismological Society of America*, Volume 65 (No. 3): pp. 581-626, 1975.

Turkish Standards Institute. “Design Loads for Buildings”, November 1997.

Turkish Standard Institute. “Requirements for Design and Construction of Reinforced Concrete Structures (TS-500)”, February 2000.

E.L. Wilson, A. Der Kiureghian, and E.P. Bayo. “A Replacement for the SRSS Method in Seismic Analysis”. *Earthquake Engineering and Structural Dynamics*, Volume 9: pp. 187-194, 1981.